Aus dem Institut für Immunologie im Biomedizinischen Centrum
Institut der Ludwig-Maximilians-Universität München
Medizinische Fakultät

Vorstand: Prof. Dr. rer. nat. Thomas Brocker

Antigen-exhausted CD4$^+$ T cells deviate towards multiple states of anergy

Dissertation

zum Erwerb des Doktorgrades der Naturwissenschaften
an der Medizinischen Fakultät
der Ludwigs-Maximilians-Universität zu München

Vorgelegt von
Anne Trefzer
aus Freiburg im Breisgau

2019

Mit Genehmigung der Medizinischen Fakultät
der Universität München

Betreuer:	PD Dr. Reinhard Obst
Zweitgutachterin:	Prof. Dr. rer. nat. Elfriede Nößner
Dekan:	Prof. Dr. med. dent. Reinhard Hickel
Tag der mündlichen Prüfung:	03.07.2020

In Erinnerung an meine Mutter

„Don't let anyone rob you of your imagination,
your creativity, or your curiosity.
It's your place in the world;
it's your life.
Go on and do all you can with it,
and make it the life you want to live."

Mae C. Jemison

Abstract

Persistent antigen presentation by tumor cells and during chronic infections functionally impairs T cells over time, limiting progress of adoptive T cell therapies for such diseases. To address how different kinetics and dosage of antigen presentation affect $CD4^+$ T cells in the absence of confounding pathologies of chronic infections, we followed TCR transgenic T cells transferred into antigen-transgenic recipients. There they received either transient or chronic TCR signals of varying strengths. We show that $CD4^+$ T cells exposed to different levels of persisting antigen presentation display phenotypes with varying kinetics and consequences. Chronically antigen-exposed $CD4^+$ T cells show impaired cytokine production upon re-stimulation, dose-dependent upregulation of exhaustion-, anergy-, and Tfh-associated markers and transcription factors. Continuous antigen presentation was sensed by the T cells, as indicated by Nur77-driven GFP-reporter expression and NFATc1 nuclear translocation, even at the highest dose where the TCR and LAT are chronically downregulated. When challenged, signaling pathways respond to strong TCR signals with Ca^{2+} fluxes being the most robust one while the MAPK and Akt pathways were more easily tuned by persisting antigen. The cells' transcriptional profiles reflected the qualitative and quantitative changes in antigen presentation by dose-dependent upregulation of exhaustion, anergy- and Tfh-associated, as well as downregulation of memory-associated genes. Comparisons with naturally occurring anergic and LCMV clone13-exhausted $CD4^+$ T cells highlighted a common transcriptomic signature describing antigen-induced T cell anergy and exhaustion. Despite upregulation of Tfh-associated markers, antigen-exhausted $CD4^+$ T cells lost their ability to provide help to B cells over time. Our results demonstrate that dose and timing of antigen presentation beyond the expansion phase reveal the plasticity of $CD4^+$ T cells and determine their range of dysfunctionalities within an otherwise sterile environment.

Zusammenfassung

Persistierende Antigenpräsentation durch chronische Virusinfektionen oder Tumorerkrankungen beeinträchtigt oft die Funktion von T-Zellen und führt zur sogenannten T-Zell-Erschöpfung und somit zur Minderung von adaptiven T-Zell-basierten Immuntherapien. Obwohl $CD8^+$ T-Zell-Erschöpfung bereits umfangreich charakterisiert wurde, sind ähnlich Zustände bei $CD4^+$ T-Zellen unter chronischen Konditionen unzureichend erforscht. In dieser Arbeit wurde untersucht, wie $CD4^+$ T-Zellen durch persistierendes Antigen beeinflusst werden. Mittels eines transgenen Mausmodells konnten wir TCR-transgene $CD4^+$ T-Zellen nach adaptivem T-Zell-Transfer in Antigen-transgene Rezipienten *in vivo* analysieren und dabei zusätzlich verkomplizierenden Pathologien, wie sie chronische Infektionsmodelle mit sich bringen, ausschließen. Transferierte T-Zellen wurden entweder transient oder persistent drei unterschiedlich starken Antigendosen (gering, mittel und stark) ausgesetzt und zu unterschiedlichen Zeitpunkten untersucht. Wir konnten zeigen, dass chronisch stimulierte $CD4^+$ T-Zellen unterschiedliche Antigendosen detektieren können und spezifisch darauf reagieren. So wiesen chronisch stimulierte T-Zellen dosisabhängige Phänotypen mit unterschiedlicher Kinetik und Konsequenzen auf. Neben einer deutlich verminderten Zytokin-Produktion wurden dosisabhängige Expressionsmuster der erschöpfungsassoziierten Checkpoint-Molekülen, Anergie-assoziierten und Tfh-assoziierten Markern, sowie Transkriptionsfaktoren induziert. T-Zellen, die mit der höchsten Dosis stimuliert wurden, zeigten eine dauerhafte Abnahme des Oberflächen-TCRs und der LAT Expression und konnten interessanterweise dennoch kontinuierlich Antigen detektieren. Identifizierte Transkriptionsprofile reflektieren die quantitativen und qualitativen Veränderungen der Antigenpräsentation. So fanden wir eine dosisabhängige Induktion von erschöpfungs-, anergie- und Tfh-assoziierten und eine Reduktion von gedächtnis-assoziierten Genen. Die aufschlussreichen Vergleiche unserer drei unterschiedlichen, antigenerschöpfter $CD4^+$ T-Zellen mit natürlich vorkommenden anergen und mit LCMV Klon13-erschöpften $CD4^+$ T-Zellen, verdeutlichten eine gemeinsame Signatur, die sowohl antigeninduzierte T-Zell-Erschöpfung als auch Anergie beschreibt. Zusätzlich verloren antigenerschöpfte $CD4^+$ T-Zellen ihre Fähigkeit, trotz deutlich erhöhter Expression von Tfh-assoziierten Markern, B-Zell-Hilfe zu leisten. Zusammenfassend verdeutlichen unsere Ergebnisse, dass die Antigendosis und die Präsentationsdauer nach der Expansionsphase für die Plastizität und den Grad der Dysfunktionalität von $CD4^+$ T-Zellen innerhalb eines (sonst) sterilen Milieus entscheidend sind.

Table of Contents

List of Abbreviations

Ag	antigen
AKT	protein kinase B
AP-1	activation protein 1
APC	antigen presenting cell
B10.BR	B10.BR/SgSnJ
B-ALL	B cell acute lymphoblastic leukemia
Bcl-6	B cell lymphoma 6
bio	biotinylated
bp	base pair
BSA	bovine serum albumin
CAR	chimeric antigen receptor
CD	cluster of differentiation
CLIP	class II-associated invariant chain peptide
CRs	co-stimulatory receptors
c-SMAC	central supramolecular activation cluster
CTLA-4	cytotoxic T-lymphocyte antigen 4
ctrl	control
CTV	Cell trace violet
DAG	Diacylglycerol
DAPI	4´,6-diaminidin-2-phenylindol
DC	dendritic cell
DMEM	Dulbeco's modified Eagle's medium
dNTP	deoxynucleioside triphosphate
dox	doxycycline
dpt	days post transfer
dtg	double transgenic
EAE	experimental autoimmune encephalomyelitis
EDTA	ethylenediaminetetraacetic acid
Egr2	Early growth response gene 2
EOMES	Extracellular signal-regulated
Erk1	kinase 1
FACS	fluorescence-activated cell sorting
FCS	fetal calf serum
FDA	US Food and Drug Administration
FR4	folate receptor 4
FSC-A	forward scatter area
FSC-H	forward scatter height
FoxP3	forkhead box P3
FVD	fixable viable dye
GFP	green fluorescent protein
gMFI	geometric mean fluorescence intensity
HBV	hepatitis B virus
HCV	hepatitis C virus
HIV	human immunodeficiency virus
i.p.	intra peritoneal
IC	isotype control
ICOS	inducible T cell co-stimulator
IFN-γ	Interferon gamma
Ig	immunoglobulin
Ii	invariant chain (CD74)
IL	interleukin
Immgen	The Immunological Genome Project
IP3	Inositol 1,4,5-trisphosphate
IRs	inhibitory receptors
IRF4	interferon regulatory factor 4
ITAM	immunoreceptor tyrosine-based activation motif
ITIM	immunoreceptor tyrosine-based inhibitory motif
ITSM	immunoreceptor tyrosine-based switch motif
kDa	kilodalton
Lag-3	Lymphocyte-activation gene 3
LAT	linker of activated T cells
Lck	lymphocyte-specific protein tyrosine kinase
LCMV	lymphocytic choriomeningitis virus
LPA	linear polyacrylamide
Ly6C	Lymphocyte antigen 6 complex
mAb	monoclonal antibody
MACS	magnetic-activated cell sorting
Maf	Musculoaponeurotic fibrosarcoma oncogene homolog
MAPK	mitogen-activated protein kinase
MCC	moth cytochrome c
MCMV	mouse cytomegalovirus
MEM	minimal essential medium
MFI	mean fluorescence intensity
MHC	Major Histocompatibility Complex
mL	Milligram
mM	Millimolar
MPEC	memory precursor effector cells
mRNA	messengerRNA
mTOR	Mammalian target of rapamycin
N	average division number
NFAT	Nuclear factor of activated T cells
NF-κB	nuclear factor kappa-light-chain-enhancer of activated B cells
ng	Nanogram
ns	not significant
PBS	phosphate buffered saline
PBMC	peripheral blood mononuclear
PCC	pigeon cytochrome c
PCR	cells polymerase chain reaction
PD-1	programmed cell death 1
PD-L1	programmed cell death ligand 1
PFA	paraformaldehyde
pfu	plaque forming units
PI3K	phosphoinostide 3-kinase
PKC	protein kinase C

PLC-γ	phospholipase C-gamma
pMHC	peptide-MHC-complex
p-SMAC	peripheral supramolecular activation cluster
pt	post transfer
RFU	relative fluorescent units
RPMI	Roswell Park Memorial Institute Medium
rTA	reverse tetracycline transactivator
Runx2	runt-related transcription factor 2
SA	Streptavidin
SLEC	sort-lived effector cells
SLP-76	SH2 domain-containing leukocyte phosphoprotein of 76 kDa
SSC	side scatter
T-bet	T cell-specific T-box transcription factor
Tcf-1	T-cell factor 1
TCR	T cell receptor
Teff	effector T cells
Tex	exhausted T cells
tg	transgenic
TGF-β	tumor growth factor beta
Th	T-helper
TIGIT	T cell immunoreceptor with Ig and ITIM domains
TILs	Tumor-infiltrating lymphocytes
TIM	tetracycline inducible invariant chain with MCC_{93-103}
Tim-3	T-cell immunoglobulin and mucin-domain containing-3
Treg	regulatory T cells
Trem	residential memory T cells
Tmem	memory T cells
TNF-α	tumor necrosis factor alpha
TOX	nuclear HML box protein
tTA	Tetracycline-controlled transcriptional activation
wt	wild type
ZAP-70	Zeta-chain-associated protein kinase 70 kDa
α	anti
β_2m	beta-2 microglobulin
*μ*g	Microgram
*μ*l	Microliter
*μ*M	Micromolar

1. Introduction

During our entire life, we encounter a variety of pathogens that put our health at risk and may lead to life-threatening conditions. To fight them, the immune system has evolved that employs innate immune and adaptive defense mechanisms. Effector T cells are the most important players of the adaptive immunity, the loss of which is associated with disease progression and compromised fitness and survival of the affected individual. Besides genetic or acquired immunodeficiencies and pathogenic mechanisms of immune evasion, it has been observed that immune responses to self and chronically persisting antigens are physiologically impaired. Understanding the mechanisms of such impaired immune responses potentially provides information to improve therapeutic strategies to treat chronic infections, autoimmune disorders, and cancer. Here, the current understanding of T cell dysfunctions is introduced, and the biology of T cells exhausted by antigen in terms of their phenotype, functionality, and transcriptional profile is investigated.

1.1 T cell activation and differentiation

During acute infections or upon vaccinations naïve T cells are activated and primed by mature antigen-presenting dendritic cells (DCs). Effective T cell activation requires three different signals. Signal one is transmitted by interactions of the T cell receptor (TCR) with peptide/major histocompatibility complex (pMHC) molecules, signal two via co-stimulatory receptors like CD28 binding to its ligands CD80 (B7-1) or CD86 (B7-2), and signal three by cytokines. Following antigen-specific activation, T cells undergo proliferation to expand and differentiate into short-lived effector cells (Teff). They directly control infections and kill target cells by producing effector cytokines and cytotoxic molecules (granzyme B and perforin) (Cui and Kaech, 2010; Zinkernagel, 1996). Upon successful antigen clearance the majority of Teff die via apoptosis and only a small subset of long-lived cells survive as memory cells with a down-modulated effector program (Cui and Kaech, 2010; O'Shea and Paul, 2010; Swain et al., 2012). Stem-like memory T cells acquire the ability of self-renewal (IL-7 and IL-15 driven slow homeostatic proliferation) and the potential to survive in an antigen-independent fashion (Cui and Kaech, 2010; O'Shea and Paul, 2010; Swain et al., 2012), and yet promote an effective immune response upon recall infections (Figure 1A).

In contrast, during chronic infections and cancer when pathogen or antigen persist over time, efficient protection by functional effector and memory T cells fails and so-called exhausted T cells (Tex) develop instead (Figure 1B). Tex cells represent a unique subset of T cells as they are phenotypically and functionally distinct from effector and memory T cells found during acute infections and vaccinations.

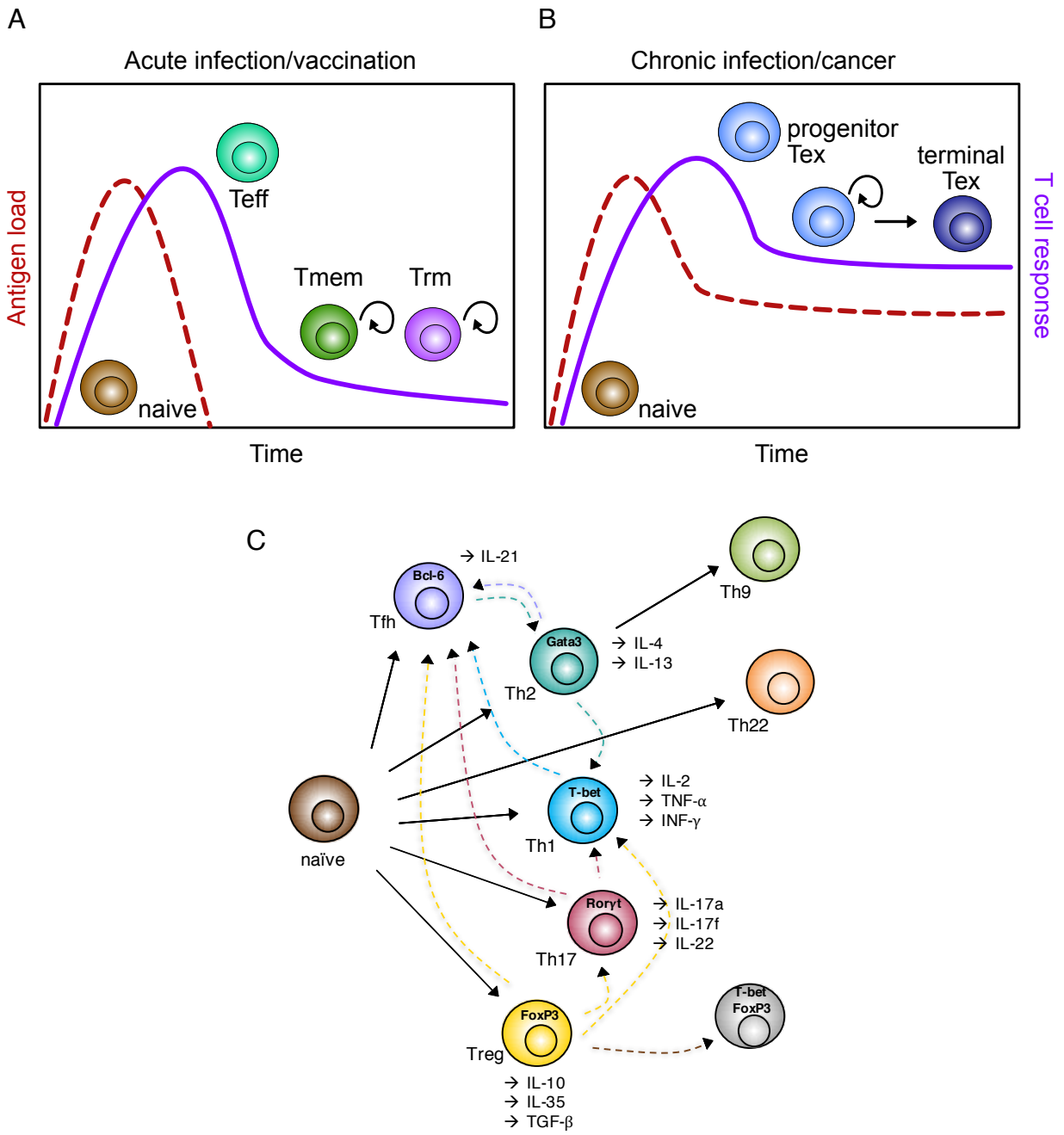

Figure 1: Model of T cell differentiation in response to acute or chronic infection/vaccination. A, B, and C was modified from McLane L. M. et al., 2019. Red lines represent antigen load over time, purple lines represent the T cell response over time, circled arrows indicate a stem-like, self-renewable capacity. Teff = effector T cells, Tmen = memory T cells, Trm = residential memory T cells, Tex = exhausted T cells. (A) Schematic outline representing an acute immune response. (B) Schematic outline representing a chronic immune response. (C) Schematic outline of Th cell differentiation and plasticity.

1.2 Lineage commitment and plasticity of helper CD4+ T cells

Upon antigen encounter naïve CD4+ T cells undergo extensive cell proliferation and differentiate, dependent on their stimulating milieu, into specific T helper (Th) cell subsets, such as T helper type 1 (Th1) cells, Th2, Th9, Th17, Th22, T follicular helper (Tfh), and T regulatory (Treg) cells, with unique phenotypes and functions (Bluestone et al., 2009; Caza and Landas, 2015; O'Shea and Paul, 2010) (Figure 1C). Th cell-linage commitment is influenced and determined by TCR stimulation (signal #1), co-receptor stimulation (signal #2), and cytokine milieu (signal #3) during the initial priming phase of a naïve CD4+ T cell. Activated professional antigen presenting cells (APCs) present pathogen-derived peptides on MHC II molecules, upregulate co-stimulatory molecules, such as CD80 and CD86, and secrete pro-inflammatory cytokines, such as type I interferons (IFN-I), tumor necrosis factors (TNF), interleukin 1 (IL-1), IL-4, IL-6, and IL-12, and thus influence Th cell differentiation. Th1 cells polarize during the response to viral infections by high levels of IL-12, IFN-I and IFN-γ within the priming milieu and produce large amounts of the Th1 effector-cytokines TNF-α, IFN-γ, and IL-2. In response to helminths, where high levels of IL-4 are found within the priming milieu, Th cells preferentially differentiate towards Th2 type cells, which produce large amounts of IL-4 and IL-13 (Figure 1C). However, T cell polarization has been shown to be plastic as polarized Th2 cells transferred into LCMV infected recipients acquired a Th1-like phenotype, producing high levels of IFN-γ and low amounts of IL-4 (Hegazy et al., 2010). The polarization of Tfh cells is driven by IL-21 and IL-6 within the priming microenvironment. They produce IL-21, provide help to B cells thereby driving germinal center (GC) development, promote antibody affinity maturation, and support long-lived plasma cell differentiation (Crawford et al., 2014; Crotty, 2015; Hale et al., 2013). However, whether Tfh cells represent a unique T helper cell subset or rather a state of the other Th cells is still unclear (Fazilleau et al., 2009; King et al., 2008; Zhou et al., 2009) (Figure 1C). Moreover, priming signals received chronically beyond the priming phase further influence CD4+ T cell differentiation and function (Vella et al., 2017).

1.3 Occurrence of exhausted T cells

T cell exhaustion was first described during chronic LCMV infection in mice (Ahmed et al., 1984; Gallimore et al., 1998; Moskophidis et al., 1993; Moskophidis and Zinkernagel, 1995; Zajac et al., 1998). Today, we know that Tex cells are also generated during chronic viral infections in man, such as hepatitis B virus (HBV) (Ye et al., 2015), hepatitis C virus (HCV) (Gruener et al., 2001; Lechner et al., 2000), and human immunodeficiency virus (HIV) (Day et al., 2006; Goepfert et al., 2000) infections. Tumor-specific CD8+ Tex cells are found in several human cancers including ovarian cancer (Matsuzaki et al., 2010), chronic lymphocytic leukemia

(Fraietta et al., 2018; Riches et al., 2013), chronic myeloid leukemia (Mumprecht et al., 2009), Hodgkin lymphoma (Gandhi et al., 2006), melanoma (Ahmadzadeh et al., 2009; Baitsch et al., 2011; Fourcade et al., 2010; Huang et al., 2017; Lee et al., 1999), non-small cell carcinoma (Bengsch et al., 2018; Zhang et al., 2010). Tumor-infiltrating lymphocytes (TILs) also show features of Tex cells (Ahmadzadeh et al., 2009; Baitsch et al., 2011; Bengsch et al., 2018; Bengsch et al., 2010; Fourcade et al., 2010; Lee et al., 1999; Matsuzaki et al., 2010; Radoja et al., 2001; Riches et al., 2013). Exhaustion has been widely studied focusing on $CD8^+$ T cells, yet it was also described for their $CD4^+$ T cell counterparts (Crawford et al., 2014) and other immune cell populations including B cells (Moir and Fauci, 2014) and NK cells (Bi and Tian, 2017). Thus, understanding the mechanisms underlying T cell exhaustion will help to improve immunotherapies targeting these cells in order to reinvigorate effector functions and thereby promote immunity to chronic infections and cancer.

1.4 Features of $CD8^+$ Tex cells

Tex cells are a unique population of immune cells that are characterized by impaired effector functions, sustained high surface expression of multiple inhibitory receptors (IRs), altered transcriptional and epigenetic profiles, as well as changes in cell metabolism. Additionally, heterogeneity was described within the Tex pool with stem-like progenitor Tex cells that give rise to more terminally exhausted T cells (for more details see section 1.4).

1.4.1 Loss of effector function

During chronic infections, $CD8^+$ Tex cells lose the ability to efficiently produce the cytokines IFN-γ (Gallimore et al., 1998; Zajac et al., 1998), IL-2, and TNF-α (Fuller and Zajac, 2003; Wherry et al., 2003a) as well as the cytotoxic molecules granzyme B and perforin. This loss was described to be a hierarchical and progressive process with IL-2 production being lost first, followed by TNF-α (Fuller and Zajac, 2003; Wherry et al., 2003a) and in more severe stages, correlating with more terminally differentiated Tex cells, defects in IFN-γ production occur (Agnellini et al., 2007; Fuller et al., 2004; Mackerness et al., 2010; Shin et al., 2009; Wherry et al., 2003a). Furthermore, it was reported that under certain conditions $CD8^+$ Tex cells gained the ability to skew cytokine production profile towards IL-10 production (Abel et al., 2006; Crawford et al., 2014; Ejrnaes et al., 2006; Zanussi et al., 1996) and in some situations with very high antigen stimulation physiological depletion of Tex cells was reported (Wherry et al., 2003b; Zajac et al., 1998). Thus, T cell exhaustion may consist of a variety of functional defects.

1.4.2 Surface expression of multiple IRs

A characteristic of exhausted T cells is the increased and sustained surface expression of multiple IRs. Up to now, numerous IRs have been identified that negatively influence the activation and function of the corresponding lymphocytes (Figure 3). Transient expression of IRs on Teff cells has an important role in restraining the immune response and attenuating T cell activation and function at the end of acute infections to prevent from autopathology destroying healthy cells and tissues. In contrast, sustained high expression level of multiple IRs, as found during chronic infections and cancer, results in a dysfunctional state of Tex cells (Bengsch et al., 2014; Bengsch et al., 2010; Blackburn et al., 2009; Day et al., 2006; Kaufmann et al., 2007; Petrovas et al., 2006; Radziewicz et al., 2007; Trautmann et al., 2006; Urbani et al., 2006; Wherry et al., 2007). Moreover, the abundance and the specific expression patterns of IRs directly correlate with the severity of T cell exhaustion (Blackburn et al., 2009). Thus, T cell exhaustion can occur with a variety of dysfunctional states that can be categorized by their phenotypic surface expression patterns.

1.4.3 Transcriptional and epigenetic profile

Not only IRs are differentially expressed and regulated by Tex cells. Another feature of Tex cells is their unique transcriptional and epigenetic profile. Transcriptional and epigenetic profiling of Tex cells has provided a better understanding of T cell exhaustion. Gene expression changes occur in genes encoding for IRs and co-stimulatory receptors (CRs), transcription factors, cytokines, TCR signaling molecules, and cell metabolism. Therefore, Tex cells have a distinct transcriptional profile in comparison to effector and memory T cells and thus make up a unique T cell subset (Alfei and Zehn, 2017; Crawford et al., 2014; Doering et al., 2012; Pauken et al., 2016; Sen et al., 2016; Wherry et al., 2007) (For more details see section 1.6.).

1.5 Development of T cell exhaustion

The exact mechanisms and pathways driving T cell exhaustion are incompletely understood. However, it is clear that the development of $CD8^+$ T cell exhaustion is a progressive and dynamic process caused by antigen persistence and/or prolonged inflammation (McLane et al., 2019). The signals received by T cells can be put into three categories. Signal 1 is mediated by TCR stimulation, signal 2 by co-stimulation, and signal 3 by soluble cytokines and inflammation. This three-signal model has been, with modifications, applied to the development of T cell exhaustion (McLane et al., 2019) and will be followed here. However, additional mediators are involved in Tex development as both early loss of $CD4^+$ T cell help during chronic viral infections

(Matloubian et al., 1994) and the presence of immunoregulatory cells, such as regulatory T cells (Treg) (Veiga-Parga et al., 2013) have been described to contribute to $CD8^+$ T cell exhaustion.

1.5.1 The three-signal model applied to T cell exhaustion

Persisting signal 1 transmitted via chronic antigen presentation by tumors, virally infected cells, and/or professional antigen-presenting cells (APCs) causes a hyperactive state of T cells that is followed by and eventually even drives the upregulation of multiple IRs. Their specific ligands are additionally presented by signal-1-providing cells thus, also providing an altered signal 2. Signal 2 mediated via IRs provides inhibitory signals and therefore, prevent optimal T cell activation and diminishes effector responses (more on IRs in section 1.2.2 and following). Additionally, chronically antigen-presenting cells as well as Treg cells provide an altered signal 3 by producing inhibitory cytokines such as IL-10 or TGF-β (Soyer et al., 2013).

1.5.2 Signal 1: Persistent antigenic TCR stimulation

What chronic infections and tumors have in common is the persistent antigen presentation to T cells (Blackburn et al., 2009; Bucks et al., 2009; Mueller and Ahmed, 2009; Shin et al., 2009; Streeck et al., 2008; Utzschneider et al., 2016a; Wherry et al., 2007). Both, high-dose antigen levels and prolonged exposure correlate with the severity of $CD8^+$ T cell exhaustion during LCMV cl13 infections in mice or HBV, HCV, and HIV infections in man (Boni et al., 2007; El-Far et al., 2008; Goepfert et al., 2000; Reignat et al., 2002; Shankar et al., 2000; Wherry and Kurachi, 2015; Wherry et al., 2003b; Zajac et al., 1998). Development of T cell exhaustion appears to be progressive, since $CD8^+$ T cells isolated during an early exhaustion phase (within the first two weeks post LCMV cl13 infection) are able to reverse the Tex phenotype and recover to Tmem cells when transferred back into acutely infected wild type mice (Angelosanto et al., 2012; Brooks et al., 2006a). However, extended priming by chronic antigenic stimulation resulted in un-rescuable T cell dysfunction and exhausted phenotype (Angelosanto et al., 2012; Brooks et al., 2006a; Utzschneider et al., 2016b). Thus, the severity of $CD8^+$ T cell exhaustion is dependent on antigen dose and the duration of antigen presentation.

1.5.2.1 TCR signal transduction pathways

Antigen presentation plays an important role already during T cell development in the thymus. Only T cells that are able to recognize self-pMHC complexes in the thymic cortex receive signals to survive, a process called positive selection (Hogquist et al., 1994, 2012; Starr et al., 2003). In contrast, during negative selection in the thymic medulla, all T cells that recognize self-pMHC complexes with a strong reactivity are depleted to prevent autoimmunity (Klein et al., 2014; Nossal, 1994; Starr et al., 2003).

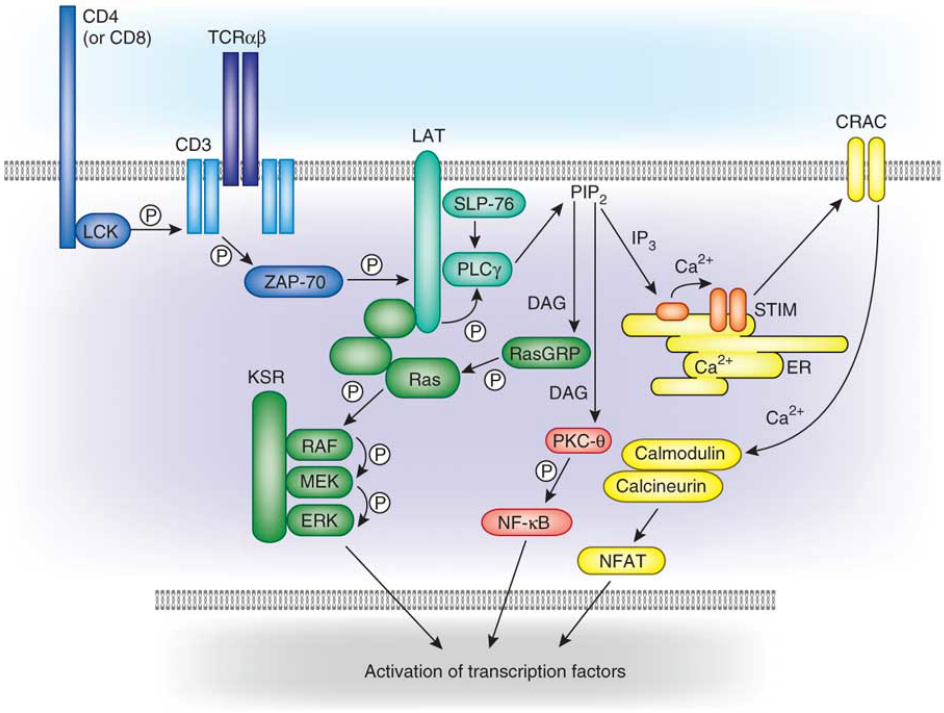

Figure 2: Model of TCR-mediated signaling pathways. Figure adapted from Morris and Allen, 2012. Upon TCR/pMHC interaction, the protein tyrosine kinase Lck bound to coreceptor (CD4 or CD8) is recruited and phosphorylates the immunoreceptor tyrosine-based activation motif (ITAM) domains of the CD3ζ subunit, generating the docking-site of zeta-chain-associated protein kinase 70 (ZAP-70), which in turn phosphorylates the transmembrane protein linker of activated T cells (LAT). Downstream of LAT several signaling pathways are involved. Mitogen-activated protein (MAP) kinase signaling results in activation protein 1 (AP-1) transcription factor generation (green cascade) and calcium signaling induces NFAT transcription factors (yellow cascade).

TCR/pMHC engagement triggers the formation of the so-called immunological synapse at the interface between the T cell and the APC, also known as supramolecular activation cluster (SMAC) (Monks et al., 1998). SMACs control T cell activation and polarized secretion of cytotoxic granules and cytokines and are divided into the central c-SMAC and the peripheral p-SMAC. Upon TCR/pMHC engagement and cluster formation, complex molecular mechanisms are induced. First, the corresponding co-receptors (CD4 or CD8) bind to agonistic pMHC (Li et

al., 2004; Turner et al., 1990) thus, recruiting the constitutively bound protein tyrosine kinase Lck (Barber et al., 1989; Turner et al., 1990) to the TCR/CD3 complex. In the proximity of CD3, Lck phosphorylates the immunoreceptor tyrosine-based activation motif (ITAM) domains of the CD3ζ subunit, probably following conformational changes in the cytoplasmic tail of the CD3ε and CD3ζ (Aivazian and Stern, 2000; Nika et al., 2010; Xu et al., 2008), and thus generates the docking-site of zeta-chain-associated protein kinase 70 (ZAP-70). Subsequently, ZAP-70 is recruited to its docking-site where it is now able to phosphorylate the transmembrane protein linker of activated T cells (LAT) (Paz et al., 2001). Phosphorylated LAT serves as an adaptor protein for several signaling molecules, such as the scaffold protein SLP-76 and PLCγ-1. These proteins then control Ca^{2+} influx and the production of second messengers diacylglycerol (DAG) and IP_3, which leads to gene transcription driven by AP-1, NFAT, and NFκB. Thus, mediating TCR downstream signaling with the final outcome of productive T cell activation, proliferation, differentiation, and cytokine production (Figure 2).

1.5.3 Signal 2: Inhibitory receptors

Inhibitory signaling via IRs is mediated after IR engagement with its cognate ligand. Cognate ligands are expressed on professional APCs, virally infected cells during chronic infections, and tumor cells (Keir et al., 2008; Virgin et al., 2009). Several mechanisms have been described by which IRs modulate T cell functions (Odorizzi and Wherry, 2012; Schietinger and Greenberg, 2014).

In 2018 two scientists, James P. Allison, then at the University of California, now at the University of Texas MD Anderson Cancer Center and Tasuku Honjo at the Kyoto University have won the Nobel Prize for medicine for developing blocking monoclonal antibodies (mABs) targeting cytotoxic T-lymphocyte-associated protein 4 (CTLA-4) and programmed cell death 1 (PD-1) respectively. These are probably the best-studied IRs. Using blocking mABs are promising treatment strategies referred to as *immune checkpoint therapy* to combat cancer in human with a fundamentally change in outcome for patients with advanced cancer (Sharma and Allison, 2015). Therefore, it is important to understand the underlying molecular mechanisms.

1.5.3.1 PD-1

PD-1 is a marker for early T cell activation as it is transiently expressed on functional Teff cells and is reduced to baseline expression levels after activation. However, during chronic situations sustained high PD-1 surface expression-levels are established on Tex cells (Barber et al., 2006; Boni et al., 2007; Day et al., 2006; Iwai et al., 2002; Urbani et al., 2006; Wherry et al., 2007).

There are two ligands described, PD-L1 (B7.H1) and PD-L2 (B7.DC) (Araki et al., 2013; Odorizzi and Wherry, 2012; Okazaki et al., 2013). PD-L1 is found on immune and non-immune cells, such as tumor cells, whereas PD-L2 is found on germinal center B cells, DCs, and macrophages (Keir et al., 2008; Liang et al., 2003).

The cytoplasmic tail of PD-1 harbors an immunoreceptor tyrosine-based inhibitory motif (ITIM) and an immunoreceptor tyrosine-based switch motif (ITSM) (Riley, 2009) that recruit adapter proteins, such as tyrosine-protein phosphatases SHP1 (PTPN6) and SHP2 (PTPN11) (Chemnitz et al., 2004; Yokosuka et al., 2012) proteins and thus, inhibits positive signaling events mediated by both, T cell receptor (TCR) and co-stimulation via CD28 (Hui et al., 2017; Kamphorst et al., 2017; Yokosuka et al., 2012) (Figure 3a). Particularly, the phosphoinositide 3-kinase (PI3K)/AKT pathway is impaired by PD-1 signaling (Riley, 2009), which links PD-1 also to cell cycle control (Patsoukis et al., 2012). Finally, downstream signaling of PD-1 induces the expression of inhibitory genes that in turn negatively regulate the expression of the transcription factor BATF (Quigley et al., 2010). BATF was shown to control T cell differentiation by binding to AP-1 binding sites after forming heterodimers with the AP-1 transcription factor family member JUN (Dorsey et al., 1995; Schraml et al., 2009). However, PD-1 expression is not necessarily required for T cell exhaustion as Tex cell can also develop in a PD-1-independent fashion shown by PD-1$^{-/-}$ CD8^{+} T cells (Odorizzi et al., 2015). These cells are more terminally exhausted meaning PD-1 *protects* some functions. Furthermore, PD-1 is also expressed by Tfh cells (Schmitt and Ueno, 2013).

1.5.3.2 CTLA-4

Another mechanism of inhibition is evolved by CTLA-4 that competes with the co-stimulatory receptor CD28 for ligand binding. During normal T cell activation CD28 binds to its ligand B7-1 (CD80) and B7-2 (CD86) and in concert with TCR signal transduction activates PI3K/AKT pathways driving T cell proliferation and effector cytokine production. During chronic situations CTLA-4 expression is elevated, binds the same ligands as CD28 (Pentcheva-Hoang et al., 2004), induces intercellular transfer of its ligands (Qureshi et al., 2011), and thus hinders proper T cell activation (Figure 3b). Furthermore, CTLA-4-knockout mice develop a severe phenotype as their T cells are activated in the periphery, proliferate spontaneously, infiltrate organs, and cause tissue damage (Tivol et al., 1995). These mice suffer from pancreatitis and myocarditis (Tivol et al., 1995).

1.5.3.3 Lag-3

The IR Lymphocyte-activation gene 3 (Lag-3) is expressed on activated T cells during acute infections (Huard et al., 1994a). Lag-3 binds its main ligand MHC class II with higher affinity than CD4 and thus, oust CD4/MHC class II interactions (Baixeras et al., 1992; Huard et al., 1995). This way, Lag-3 interferes with the positive-signaling cascade and provides inhibitory signals (Figure 3c). Furthermore, the DC-SIGN family member LSECtin, which is highly expressed on many tumors, is suggested to be a further ligand for Lag-3 (Xu et al., 2014). As Lag-3 is highly expressed on Tex cells (Blackburn et al., 2009; Richter et al., 2010) and TILs (Matsuzaki et al., 2010) the interaction also with this ligand might contribute to diminished T cell proliferation, activation, and cytokine production within this tissues (Anderson et al., 2016; Blackburn et al., 2009; Hannier et al., 1998; Huard et al., 1994b). Lag-3-deficient T cells revealed per se no phenotype but Lag-3-knockout T cells exhibit reduced expansion and increased cell death thus, suggesting that Lag-3 regulates T cell expansion (Workman and Vignali, 2003). There are more IRs that work in a similar way, such as Tim-3.

1.5.3.4 Tim-3

T-cell immunoglobulin and mucin-domain containing-3 (Tim-3) is an IR that interacts with multiple components of the TCR complex (Lee et al., 2011; van de Weyer et al., 2006). Engagement of Tim-3 with its ligand galectin-9 (Wada and Kanwar, 1997) induces Ca^{2+} flux and drives apoptosis (Zhu et al., 2005) thus, providing inhibitory signals and negatively regulate T cell functions (Tomkowicz et al., 2015) (Figure 3c). Tim-3 is highly expressed on $CD8^+$ Tex cells during chronic viral infections (Jin et al., 2010) and cancer (Fourcade et al., 2010; Gao et al., 2012; Lu et al., 2017; Shayan et al., 2017; Yang et al., 2012) and is described to drive T cell exhaustion in concert with Lag-3 and PD-1 (Blackburn et al., 2009). Moreover, during experimental autoimmune encephalomyelitis (EAE) in mice, Tim-3 expression is induced on $CD4^+$ Th1 cells and correlates with the severity of the disease (Monney et al., 2002). Therefore, Tim-3 inhibition is also a promising candidate for immunotherapy.

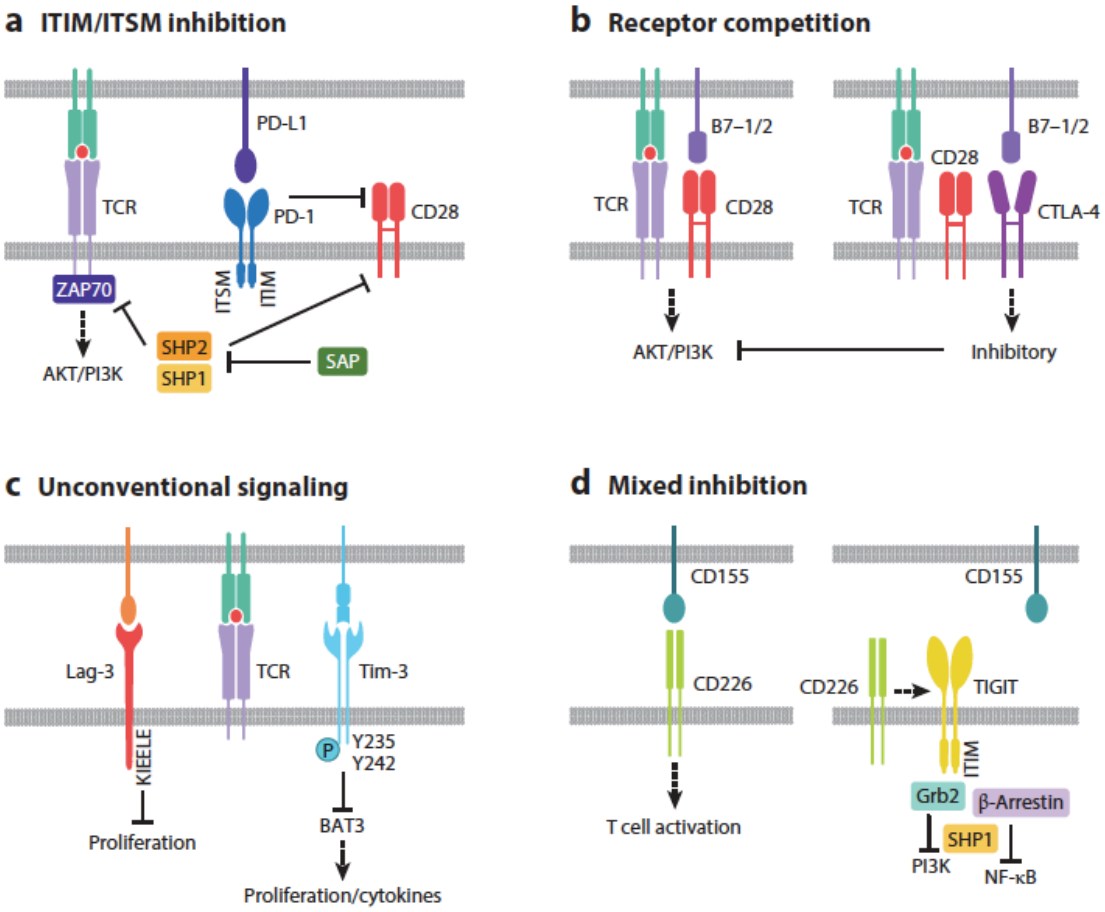

Figure 3: Collection of selected inhibitory receptors (IRs). Figure modified from McLane L. M. et al., 2019. (a – d) Schematic illustration of different mechanisms of IRs mediating inhibitory signals to impair T cell activation and effector function. IRs such as PD-1 signal via intracellular ITIM/ITSM domains interfere with co-stimulatory signals (a), other IRs, such as CTLA-4 directly compete with co-stimulatory receptors (b). Another group of IRs, including Lag-3 and Tim-3, induce unconventional signaling (c) or use a combination of both, such as TIGIT (d).

1.5.3.5 TIGIT

T cell immunoreceptor with Ig and ITIM domains (TIGIT) is an IR that mechanistically combines the inhibition pathways of other IRs, such as receptor competition (e.g. CTLA-4) and unconventional signaling (e.g. Lag-3, Tim-3). It competes with CD226 for ligand (CD155) binding (Yu et al., 2009b) and additionally contains an ITIM domain via which unconventional signaling inhibits PI3K and nuclear factor kappa-light-chain-enhancer of activated B cells (NF-κB) pathways and thus, T cell activation (Ho et al., 1998). TIGIT expression is elevated and sustained on $CD8^+$ T cells during chronic viral infections, as HIV infections (Chew et al., 2016) as well on $CD8^+$ T cells and $CD8^+$ TILs in cancer patients (Chauvin et al., 2015). Blocking TIGIT-mediated signaling using mABs was shown to rejuvenate the effector function of HIV-specific $CD8^+$ T cells regarding cell proliferation and cytokine production (Chew et al., 2016) and enhanced tumor rejection in mice (Chauvin et al., 2015).

1.5.4 Signal 3: Inhibitory cytokines

Signal 3 provides positive signals during acute viral infections via soluble mediators, such as interleukin 2 (IL-2). Positive signal 3 is required for T cell activation and survival (Vella et al., 1998). In contrast, during chronic infections the inflammatory milieu has changed. Anti-inflammatory cytokines, such as IL-10 (Wilson and Brooks, 2011; Yi et al., 2010) and TGF-β (Derynck and Zhang, 2003; Li et al., 2006; Tinoco et al., 2009), promote the development of T cell exhaustion. Today, a number of proinflammatory cytokines are known to influence the development of Tex cells even though, signal 3 alone is not sufficient to induce Tex phenotype in absence signal 1 and/or signal 2 (Stelekati et al., 2014). Indeed, IL-10 production is increased in many chronic viral infections in mice and man, such as LCMV cl13, HBV, HCV, and HIV (Yi et al., 2010), where Tex cells are found. Blocking IL-10-mediated negative signal 3 using neutralizing IL-10 mABs in combination with other checkpoint blockades, such as anti-PD-1, reduced the Tex development and reverted Tex cells into functional Teff and Tmem cells during chronic LCMV infections (Brooks et al., 2008; Brooks et al., 2006b; Ejrnaes et al., 2006). Similar approaches are currently being tested for cancer treatment (Ni et al., 2015; Zarour, 2016) (more on immunotherapies in section 1.9).

1.6 Heterogeneity within the Tex pool

Tex cells represent a unique cell lineage that is distinct from Teff and Tmem cells regarding their phenotype and functionality (McLane et al., 2019). Within the $CD8^+$ Tex pool heterogeneity exists. Tex cells arise from MPEC precursor cells (Figure 1) that give also rise to Teff and Tmem cells (Angelosanto et al., 2012). Progenitor Tex cells are stem-like as they have the potential of self-renewal and give rise to the more terminal differentiated exhausted T cells (Paley et al., 2012). Terminal Tex cells represent the majority of all Tex cells; these cells lost their ability to proliferate and finally enter cell death if high-dose antigen stimulation continues to persist (Paley et al., 2012) (Figure 4). Progenitor $CD8^+$ Tex cells isolated during an early phase of LCMV cl13-induced exhaustion (up to two weeks post infection) and transferred into antigen-free hosts where able to establish effector functions nevertheless, terminal Tex cells failed to do so. Recently, Bengsch et al. identified approximately nine different subsets of Tex cells based on their surface marker expression characteristics using high-dimensional cytometry (Bengsch et al., 2018). Progenitor Tex cells are characterized by T-bet^{hi}, PD-1^{int}, and $CD44^{hi}$ expression and are responsive to checkpoint blockades. In contrast, the more terminal Tex cells are rather unresponsive and are defined by an $EOMES^{hi}$, PD-1^{hi}, and $CD44^{int}$ surface expression profile (Figure 4).

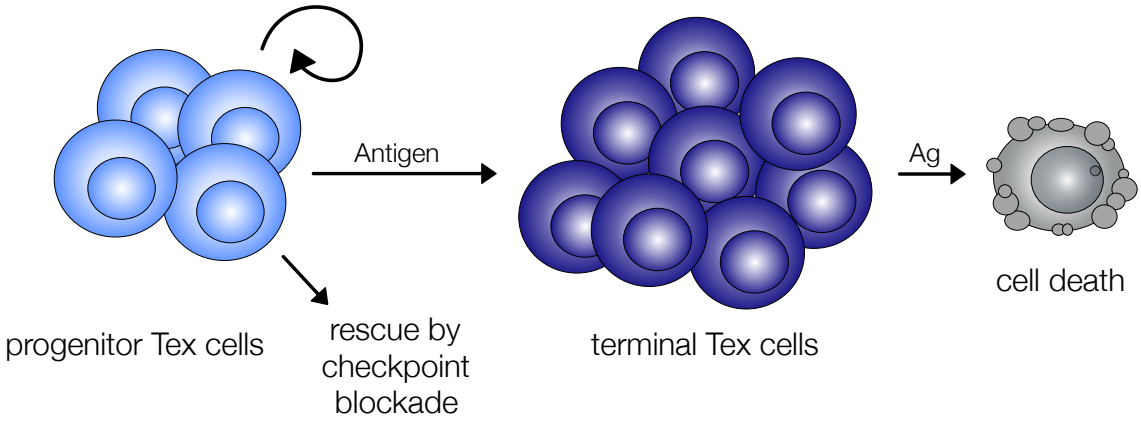

Figure 4: Model of progressive Tex development. Graphic illustration of the progression of T cell exhaustion over time and dependent on antigen load. Progenitor Tex cells have a self-renewable capacity and are rescuable by checkpoint blockades and differentiate into terminal Tex cells that finally enter cell death when antigen continuous to persist.

1.7 Transcriptional control and epigenetic landscape of Tex cells

As mentioned above (section 1.3.3) one of the features of Tex cells are significant changes in gene-expression. Transcription factor expression and their transcriptional connectivity play a major role in T cell exhaustion (Doering et al., 2012; Paley et al., 2012). Network analysis revealed that Tex cells are able to reuse transcription factors expressed by Teff or Tmem cells in a new, context-specific way within another network connectivity (Doering et al., 2012). Context-specific activity of transcription factors may be on the basis of binding-partners, co-factors, differently regulated localization within the cellular compartments, and dose-dependent binding potential. Additionally, chromatin accessibility of Tex cells has a major function in controlling gene-expression patterns (Pauken et al., 2016; Philip et al., 2017; Scott-Browne et al., 2016). Therefore both, context-specific activity of transcription factors and chromatin accessibility modulate T cell activation, differentiation, and fate commitment. Here, the function and role of some exhaustion-associated transcription factors are highlighted.

1.7.1 NFAT

The nuclear factor of activated T-cells (NFAT) family member transcription factors play an important role during T cell activation (Crabtree and Olson, 2002; Rao et al., 1997) and is also involved in T cell exhaustion (Martinez et al., 2015; Schietinger and Greenberg, 2014; Wherry, 2011) and anergy (Macian et al., 2002) (more on T cell anergy in section 1.9). Upon acute TCR stimulation Ca^{2+} flux is induced, which in turn results in nuclear NFAT translocation. Once

located in the nucleus, NFATs form heterodimers with AP-1 (a heterodimer built by Fos and Jun) and together, drive T cell activation and effector function (Macian et al., 2000; McHenry et al., 1998). By contrast, during chronic viral infections nuclear NFAT abundance is increased in absence of AP-1 family members (Wherry, 2011; Wherry et al., 2007). A constitutive nuclear/active mutant of NFAT1, which is unable to form heterodimers together with AP-1, so-called “partnerless” NFAT, provides negative signals attenuating activation and effector signaling (Martinez et al., 2015), probably by binding to different exhaustion-associated genes, such as genes encoding for the IRs PD-1, Lag-3, and Tim-3 (Martinez et al., 2015; Oestreich et al., 2008; Quigley et al., 2010).

1.7.2 Tcf-1

T-cell factor 1 (Tcf-1) is a transcription factor that is required during thymic and peripheral T cell development, associated with memory formation (Verbeek et al., 1995; Yu et al., 2009a), and functions as a “gatekeeper” of T-cell fate during early T cell activation (Germar et al., 2011). Tcf-1 is expressed by functional Tmem cells as well as by a subpopulation of Tex cells. In both T cell populations Tcf-1 maintains the stemness and promotes the progenitor capacity (Man et al., 2017; Utzschneider et al., 2016b; Wu et al., 2016).

1.7.3 c-Maf

Musculoaponeurotic fibrosarcoma oncogene homolog (Maf) expression is significantly induced in $CD8^+$ TILs in melanoma patients as well as in virus-induced Tex cells and is reported to mechanistically drive $CD8^+$ T cell exhaustion (Verdeil, 2016) but, in $CD4^+$ T cells, is associated with Th2 and Tfh differentiation (Ho et al., 1998; Kroenke et al., 2012; Xu et al., 2009).

1.7.4 TOX

The transcription factor nuclear HMG-box protein TOX is transiently expressed during positive selection and thus, is associated with thymic T cell development and linage commitment (Huang et al., 2014; Wilkinson et al., 2002). Moreover, it is also found significantly upregulated on $CD8^+$ T cells during many cancers including breast, lung, and gastric cancer, leukemia, and lymphoma (Yu and Li, 2015). Nowadays, TOX expression is used as a biomarker for cancer progression and prognosis (Huang et al., 2014).

1.8 CD4+ T cells during acute vs. chronic viral infections

In acute viral infections, antigen-specific CD4+ T cells preferentially differentiate into functional Th1 cells producing IFN-γ (Hale et al., 2013; Sallusto, 2016) or into Tfh cells providing help to B cell-mediated immunity by driving germinal center (GC) development, promoting antibody affinity maturation, and supporting long-lived plasma cell differentiation (Crawford et al., 2014; Crotty, 2015; Hale et al., 2013). In contrast, during chronic viral infections the differentiation profile and functions of antigen-specific CD4+ T cells can differ from that generated during acute infections (Crawford et al., 2014) as they show a compromised ability to produce regular Th1-specific cytokines. This defect is probably driven by persistently high levels of antigen beyond the priming phase (Han et al., 2010). However, since chronically LCMV-cl13-infected mice only established a lifelong unresolving viremia upon CD4+ T cell depletion during infection (Matloubian et al., 1994), CD4+ T cells are not entirely dysfunctional during chronic viral infections, but display another phenotype (Aubert et al., 2011). Indeed, the cytokine production profile of chronic CD4+ T cells is changed, as the production of IFN-γ, TNF-α, and IL-2 is significantly reduced (Crawford et al., 2014; Han et al., 2010) whereas the expression of IL-21 is elevated (Crawford et al., 2014; Elsaesser et al., 2009; Fahey et al., 2011; Fröhlich et al., 2009; Vella et al., 2017). It was also reported that chronic CD4+ T cells skew towards a Tfh phenotype as they express the key Tfh-driving transcription factor B cell lymphoma 6 (BCL-6) as well as Tfh-specific surface markers as ICOS, CXCR5, and PD-1(Fahey et al., 2011). Moreover, significant amounts of virus-specific T-cell-dependent antibodies are found during chronic LCMV cl13 infections in mice as well as HCV infections in man (Bartosch et al., 2003) indicating that at least some features of T cell help to B cells are still intact. In agreement with these findings is the fact that broadly-neutralizing antibodies rarely occur in HIV patients (Caskey et al., 2019). Together, these findings support the hypothesis that at least some antigen-specific CD4+ T cells differentiate towards Tfh cells during chronic infections. However, it was also shown that chronic CD4+ T cells up-regulate the surface expression of multiple IRs such as PD-1, CTLA-4, TIM-3, and Lag-3 like their CD8+ counterparts and genome-wide transcriptional profiling of chronic CD4+ T cells revealed no obvious skewing towards one of the T helper subsets mentioned above, including the Tfh phenotype (Vella et al., 2017). Additionally, similar to CD8+ Tex cells, chronic CD4+ cells have their unique gene-expression profile and both, CD8+ Tex and chronic CD4+ T cells, share a certain gene-expression signature of exhaustion but still being different cell types (Vella et al., 2017). Thus, whether chronic CD4+ T cells differentiate into Tfh or other cells or whether they become exhausted as their CD8+ counterparts still remain unclear. To improve CD4+ T cell effector functions it is important to gain further insights into the mechanisms and pathways involved in CD4+ T cell dysfunction.

1.9 T cell anergy

T cell anergy is an acquired dysfunctional state of cells. The term *anergy* has been introduced by Pirquet who reported that children infected with measles are transiently unresponsive to tuberculin prick tests and called it the anergic phase (Pirquet, 1908). About 80 years later, such a hyporesponsive state was described for antigen-specific $CD4^+$ Th1 cells that had been first stimulated *in vitro* by fixed APCs exclusively providing signal 1 and subsequently by live APCs providing full activating conditions (signal 1, 2, and 3). As these T cells failed to proliferate and to produce IL-2, this unresponsive state was termed *clonal anergy* (Jenkins and Schwartz, 1987; Schwartz et al., 1989). T cell anergy has also been shown in a number of mouse models. It was observed in mice treated with the protein staphylococcal enterotoxin B (SEB), a superantigen. In this model, *in vivo* stimulated T cells exhibited a proliferative defect and failed to produce IL-2 in response to *in vitro* re-stimulation with SEB or exogenous IL-2, respectively (Rellahan et al., 1990). However, *in vivo* induced clonal anergy was reversible upon antigen removal (Rocha et al., 1993). And it was shown that *in vitro* T cell stimulation using anti-CD3/TCR antibodies alone (signal 1) induced an anergic phenotype, while using anti-CD3/TCR together with anti-CD28 (signal 2) was sufficient to fully activate the T cells (Jenkins and Johnson, 1993). In 1994, the induction of T cell anergy was reported to be dependent on the levels of presented pMHC complexes *in vivo* (Ferber et al., 1994). High levels of pMHC caused TCR downregulation and rapidly induced an hyporesponsive state (Taams et al., 1999). Later, TCR tg mouse models have allowed further *in vivo* studies, which revealed that *in vivo* induced anergy is different from *in vitro* induced clonal anergy. Thus, *in vivo* also other effector cytokines, such as IL-4 and IFN-γ were downregulated. Furthermore, the anergic phenotype depended on antigen persistence, and *in vivo* anergized T cells failed to proliferate in response to exogenous IL-2 (Chiodetti et al., 2006). Therefore, it was suggested to name the *in vivo*-anergic state adaptive tolerance (Schwartz, 2003).

Anergy is thought to play a role for peripheral tolerance induction and to protect the hosts from autoimmune disorders (Kalekar et al., 2016; Schwartz, 1990; Wells, 2009) and immunopathology (Knoechel et al., 2005; Martinez et al., 2012). Anergic T cells are also found in cancer patients where positive signal 2/co-stimulation is missing or is overwritten by a negative signal 2 mediated by IRs (Blank et al., 2004; Curiel et al., 2003; Zou and Chen, 2008). In mice, *in vivo* anergized T cells are characterized by high CD73 and FR4 surface expression (Martinez et al., 2012) and are associated with low IL-2 production, cell cycle arrest, improper mTOR and MAPK signaling (Zheng et al., 2012), and surface expression of IRs such as PD-1, CTLA-4, and Lag-3. Early growth response gene 2 (Egr2) and NFAT as homodimers are central transcription factors regulating the anergy-inducing gene-transcription profile (Anandasabapathy et al., 2003; Soto-Nieves et al., 2009; Zheng et al., 2012). Furthermore,

anergic CD4+ T cells are described to be precursors for peripheral FoxP3-expressing Treg cells (Kalekar and Mueller, 2017; Kalekar et al., 2016). Notably, the anergic state is reversible as loss of FoxP3 expression leads to the conversion of anergic CD4+ T cells towards functional Teff and Tmem cells (Zhou et al., 2009). However, the exact molecular and cellular mechanisms driving T cell anergy are still poorly understood.

1.10 Immunotherapy: Reinvigoration of effector functions in Tex cells

As mentioned above, immunotherapies have become very promising and revolutionizing strategies to combat cancer (Pardoll, 2012), chronic viral infections (Blackburn et al., 2009), as well as autoimmune diseases (Feldmann and Steinman, 2005). Currently, there are more than 864 antibody-based clinical stage (phase I/II/III) candidates for immunotherapies, including antibody-based molecules, such as antibodies targeting checkpoint molecules (discussed above, section 1.4.3 and following), T-cell-attracting bispecific antibodies, BiTes, and chimeric antigen receptor (CAR) T cell-based approaches (Strohl, 2018). Up to date, 74 antibody-based molecules have already been approved by the US Food and Drug Administration (FDA) and are being in clinical use. Probably, the most promising immunotherapeutic approach are antibody-based checkpoint blockades; mAbs inhibiting IR-mediated pathways, such as pembrolizumab and nivolumab targeting PD-1, atezolizumab, avelumab, and durvalumab targeting PD-L1, and ipilimumab targeting CTLA-4. These checkpoint-blocking mAbs are approved to treat melanoma, non-Hodgkin lymphoma, lung carcinoma, and several other types of cancer and are either being used as monotherapy or in combination (Balachandran et al., 2017; Ribas and Wolchok, 2018; Topalian et al., 2012, 2015; Wolchok et al., 2013) to reinvigorate effector functions of Tex cells, representing the key responding cells to checkpoint blockades (Huang et al., 2017; Kamphorst et al., 2017; Twyman-Saint Victor et al., 2015). Additionally, targeting CRs or cytokine receptors in combination with checkpoint blockades are also currently in clinical trials to improve Tex rejuvenation. Recently, the first two CAR-T-cell-based immunotherapies to treat B cell lymphoma patients targeting CD19-expressing B cells have been approved by the FDA. Since CAR T cells are supposed to act within the exhaustion-promoting microenvironment of solid tumors, checkpoint inhibitor treatment might have to be administered in combination to prevent exhaustion of CAR T cells upon administration.

What do all these immunotherapeutic strategies have in common? They collectively rely on the understanding of the biology of T cell exhaustion. Therefore, it is necessary to deepen our understanding of the molecular mechanisms and pathways involved in the development and control of exhaustion.

1.11 The iMCC and cMCC antigen-presenting mouse models

T cell exhaustion has been mainly studied using the LCMV cl13 infectious model. Since a LCMV cl13 infection typifies a chronic viral infection with continuously high productive replication (Virgin et al., 2009) complex immune responses are initiated, including innate and adaptive immunity. Besides the complexity of the induced immune response, the LCMV cl13 infection model brings with it confounding factors that affect the animal´s immune system more generally. It causes permanent splenocytic lymphopenia (Ejrnaes et al., 2006) and immunosuppression (Borrow et al., 1995), as infected hosts fail to establish an efficient immune response against unrelated Vaccinia virus for at least one month (Althage et al., 1992). It has also been shown that unspecific (bystander) T cells become unresponsive during a LCMV cl13 infection (Barnstorf et al., 2019; Mothe et al., 2007). Additionally, LCMV cl13 infected mice are actually able to clear the pathogen within 40 to 80 days (Matloubian et al., 1994). However, the contributions of the LCMV cl13 model are very important for our understanding of T cell mediated immunity.

To avoid complex immune responses that are hard to dissect, a minimalistic system without the induction of responses where innate and adaptive immunity can be triggered independently would be an ideal tool to investigate T cell exhaustion. Here we have used a dtg mouse model for the manipulation of specific antigen presentation by DC which has been used already to investigate DC activation and maturation (Obst et al., 2007), $CD4^+$ T cell priming (Obst et al., 2005; Rabenstein et al., 2014), and to address questions regarding antigen persistence *in vivo* (Han et al., 2010).

This minimalistic antigen-presenting mouse model is based on Bujard´s tetracycline system (Figure 5) and consists of two genetically modified antigen-presenting recipient mouse lines of the B10.BR background (iMCC and cMCC) as well as an MCC-specific TCR-transgenic $CD4^+$ T cell donor mouse line (AND). In the inducible iMCC model, antigen presentation of moth cytochrome C (MCC) by H-$2E^k$ can be induced in DCs by doxycycline-induced expression of the reverse tetracycline transactivator transgene (rTA-S2) driven by invariant chain (Ii, CD74) promoter and MHC class II enhancer elements. Ii-rTA tg expression then drives the expression of the second tg (TIM) encoding for a modified Ii cDNA where the CLIP region is replaced by $MCC_{93\text{-}103}$ (Figure 5). In the constitutive cMCC model, a fusion protein of the invariant chain (Ii) of MHC class II and the $MCC_{88\text{-}103}$ peptide is constitutively expressed under the control of H-2Eα promoter elements (Figure 5) thus presenting high dose antigen. Adoptively transferred AND TCR transgenic $CD4^+$ T cells specifically recognize $MCC_{93\text{-}103}$ and $MCC_{88\text{-}108}$ in the context of H-$2E^k$ (Han et al., 2010; Kaye et al., 1989) (Figure 6) (more on the mouse models see section 4.2.3).

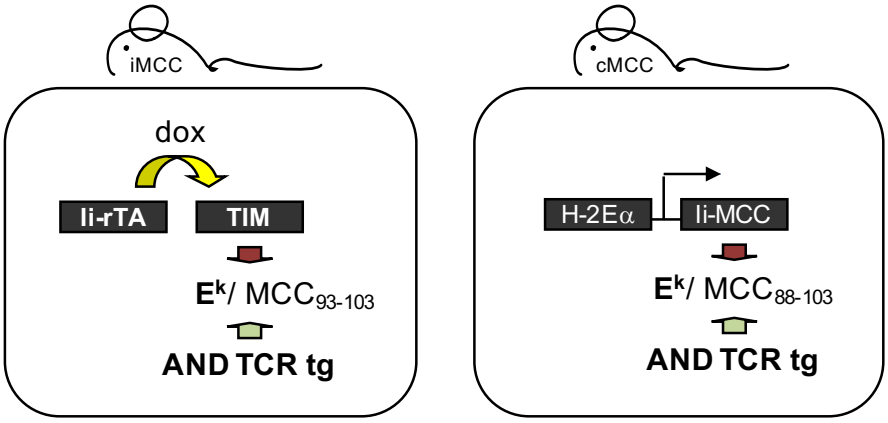

Fig. 5: Transgenic systems for manipulated antigen MCC expression *in vivo*. Genetically modified antigen-presenting recipient mice of the B10.BR genetic background present moth cytochrome C (MCC) by H-2Ek (MHC class II) either in an inducible (left: iMCC) or constitutive (right: cMCC) manner. In the iMCC model (on the left), MCC expression can be induced in DCs by doxycycline-induced expression of the reverse tetracycline transactivator transgene (rTA-S2) driven by invariant chain (Ii, CD74) promoter. In presence of doxycycline (dox) Ii-rTA transgene expression drives the expression of the second transgene (TIM) encoding for a modified invariant chain (Ii) cDNA where the class II-associated invariant chain peptide (CLIP) region is replaced by MCC_{93-103}. In the constitutive cMCC model (on the right), a fusion protein of the invariant chain of MHC class II and the MCC_{88-103} peptide is constitutively expressed under the control of H-2Eα promoter elements. In both mouse models, MCC on $H\text{-}2E^k$ can be specifically recognize by MCC-specific TCR-transgenic $CD4^+$ T cells (AND).

Thus, this minimalistic mouse model offers the opportunity to investigate T cell plasticity for several reasons. First, antigen presentation in the iMCC strain can be rapidly induced and terminated at any given time point e.g. after T cell priming on day three to generate memory T cells, or after 10 or even 30 days post transfer to generate early and late antigen-exhausted T cells, respectively (Han et al., 2010). Second, antigen dose is tunable depending on the amount of dox, which is fed with the drinking water (section 4.2.6). This allows us to analyze different T cell behaviors in response to varying amounts of presented antigen. In this regard, low or intermediate levels of antigen using the iMCC model and high-level antigen using the cMCC model. Third, antigen presentation is reversible, meaning we can study secondary responses as we reapply dox at a given time point. Most importantly, chronic antigen presentation can be investigated in the absence of potentially distracting innate, $CD8^+$ T cell, or B cell responses, without complicating inflammation, permanent splenocytic lymphopenia, and immunosuppression (Han et al., 2010). Thus, whether and how $CD4^+$ T cells become exhausted or dysfunctional by persistent antigen presentation can be studied within an otherwise sterile environment.

2. Motivation and Aim of the Thesis

During our entire life, we encounter a large variety of pathogens. On average, we are chronically infected with eight to 12 different viruses (Virgin et al., 2009). Some of them are so common that we consider them as part of our normal microbial flora, our metagenome (Virgin et al., 2009). However, chronic infections are considered as one of the biggest global health threats (Frebel et al., 2010). This raises the questions how our immune system deals with chronic pathogens and how it copes with persistent non-self-antigen presentation. During chronic viral infections e.g. with HBV, HCV, or HIV, as well as during cancer, T cells enter a progressively dysfunctional state and become “exhausted”. The same phenomenon was reported for about 40% of cancer patients treated with CAR-T-cell-based immunotherapy targeting $CD19^+$ B cell acute lymphoblastic leukemia (B-ALL) (McLane et al., 2019; Wang et al., 2017). Furthermore, it has been reported that for a maximal antitumor CAR-T-cell-based response, the ratio of used naïve $CD4^+$ to central memory $CD8^+$ T cells plays a crucial role, thus implying the importance of functional $CD4^+$ T cells. In the context of T cell exhaustion, $CD8^+$ T cell responses have been extensively studied in mice primarily using chronic LCMV cl13 infections. Even though the importance of $CD4^+$ T cells during such chronic viral infections has been demonstrated some time ago (Matloubian et al., 1994), the role and function of $CD4^+$ T cells during chronic viral infections and cancer is still unclear.

Therefore, the aim of this study was to investigate the role of persisting antigen presentation beyond the priming phase of $CD4^+$ T cells and to analyze their differentiation profile and functionality in response to increasing antigen-dose and -timing. Understanding the underlying molecular mechanisms involved in $CD4^+$ T cell exhaustion may allow to improve immunological approaches, such as immunotherapies, to rejuvenate functional effector T cell responses in endogenous $CD4^+$ and CAR T cells.

3. Materials and Methods

3.1 Materials

3.1.1 Chemicals and solutions

Product	Supplier
2-Mercaptoethanol	Carl Roth, Arlesheim, Switzerland
Agarose	Peqlab, Erlangen, Germany
Antibiotic/antimycotic	GE Healthcare, Chalfont St Giles, UK
BD Cytofix Buffer	BD, Franklin Lakes, NJ, USA
BD PermBuffer III	BD, Franklin Lakes, NJ, USA
Bovine serum albumin (BSA), Fraction V	Fisher Scientific, Schwerte, Germany
Brefeldin A	Sigma-Aldrich, Steinheim, Germany
Casy ton	Roche, Basel, Switzerland
CellTraceTM Violet	Invitrogen, Carlsbad, CA, USA
CFDA-SE Cell Tracer Kit	Invitrogen, Carlsbad, CA, USA
Chloroform	Carl Roth, Arlesheim, Switzerland
DAPI (4´,6-diamidino-2-phenylindole)	Invitrogen, Carlsbad, CA, USA
Dimethyl sulfoxide (DMSO)	Fischer Scientific, Schwerte, Germany
DMEM (powder)	AppliChem, Darmstadt, Germany
dNTPs	Peqlab, Erlangen, Germany
Doxycycline	AppliChem, Darmstadt, Germany
EDTA (Gibco)	Life Technologies, Carlsbad, CA, USA
Ethanol	Diagonal, Münster, Germany
Ethidium bromide (1% solution)	AppliChem, Darmstadt, Germany
FCS (Gibco)	Life Technologies, Carlsbad, CA, USA
Foxp3/ Transcription Factor staining buffer set Fixation/Permeabilization Concentrate Fixation/Permeabilization Diluent Permeabilization buffer (10x)	eBioscience, San Diego, CA, USA
FVD (eFlour450 and eFlour660)	eBioscience, San Diego, CA, USA
Gelatin	Sigma-Aldrich, St. Louis, MO, USA
Gene ruler (Fermentas)	Thermo Fisher Scientific, Waltham, MA, USA
GenEluteTM-LPA	Sigma-Aldrich, St. Louis, MO, USA
Glycerin	AppliChem, Darmstadt, Germany
H2O	AppliChem, Darmstadt, Germany
Hen egg lysozyme (HEL)	Sigma-Aldrich, St. Louis, MO, USA
HEPES (PAA)	GE Healthcare, Chalfont St Giles, UK
IC Fixation Buffer	eBioscience, San Diego, CA, USA
Imject® Alum	Thermo Fisher Scientific, Waltham, MA, USA
Ionomycin (IM)	Diagonal, Münster, Germany
Isopropanol	Diagonal, Münster, Germany
L-Glutamine (PAA)	GE Healthcare, Chalfont St Giles, UK

Linear Polyacrylamide (LPA)	Sigma-Aldrich, St. Louis, MO, USA
MACS anti-biotin MicroBeads	Miltenyi Biotec, Bergisch Gladbach,Germany
MEM non-essential amino acids (PAA)	GE Healthcare, Chalfont St Giles, UK
Moth cytochrome C (MCC) peptide CGG-88-103	Peptides & Elephants, Potsdam, Germany
Orange G	Sigma-Aldrich, St. Louis, MO, USA
Pancoll human	PAN Biotech GmbH, Aidenbach, Germany
Paraformaldehyde	Diagonal, Münster, Germany
PCR Buffer	Peqlab, Erlangen, Germany
PCR Enhancer	Peqlab, Erlangen, Germany
PCR Water	AppliChem, Darmstadt, Germany
Phorbol myristate acetate (PMA)	Sigma-Aldrich, Steinheim, Germany
Pigeon cytochrome C (PCC) peptide 93-103	Sigma-Aldrich, Steinheim, Germany
Polymycin B	AppliChem, Darmstadt, Germany
Proteinase K	Diagonal, Münster, Germany
RCB Lysis Buffer	Biolegend, San Diego, CA, USA
RPMI 1640 + GlutaMAX Supplement	Life Technologies, Carlsbad, CA, USA
Streptavidin (PE, PeCy7, BV450)	Biolegend, San Diego, CA, USA
Taq all inclusive (peqGOLD Taq DNA polymerase, reaction buffer, enhancer solution P, dNTP-mix)	Peqlab, Erlangen, Germany
TRIS	AppliChem, Darmstadt, Germany
Triton X-100 (Fluka)	Sigma-Aldrich, St. Louis, MO, USA
Trizol LS reagent	Life Technologies, Carlsbad, CA, USA
Trypan Blue	Carl Roth, Arlesheim, Switzerland
Volvic, Water	Danone Waters, Frankfurt, Germany

3.1.2 Buffers and media

Buffers or Media	Ingredients
Agarose gel (1%)	1.5 g Agarose 150 mL TAE (1 x)
Cell transfer buffer	DMEM 10 mM HEPES
CFSE/CTV medium	PBS (1 x) 0.1% BSA (w/v)
Culture medium	RPMI + GlutamaxTM 10% BSA 5 mM HEPES 5 mM nonessential amino acids 2 μL β-Mercaptoethanol

DMEM (pH 7.0)	DMEM (w/v) 3.7 g $NaHCO_3$ 10 mL HEPES 50 mL BSA add up to 1 L H_2O
DNA isolation buffer (10 x)	H_2O 670 mM TRIS, pH8.8 166 M $(NH_4)2SO_4$ 65 mM $MgCl_2$ 0.1% Gelatin
Doxycycline (20 mg/mL)	1 g Doxycycline add up to 50 mL H_2O (Volvic)
Ethidiumbromid	7.44 mL H_2O 650 µL Ethidium bromide (1%)
FACS medium	DMEM HyCloneTM HEPES solution 1% bovine serum albumin (BSA)
FACS medium ø BSA	DMEM w/ HEPES
Gene ruler	100 µL Marker 700 µL TAE 200 µL Loading buffer
Loading buffer (6 x)	250 mg Orange G 30 mL Glycerol 30% 70 mL H_2O
MACS buffer degassed	PBS (1 x) 0.5% BSA (w/v) 1 mM EDTA
Paraformaldehyde buffer (2%) pH 7.4	PBS 2% Paraformaldehyde
PCR mastermix	H_2O 1 x PCR buffer 0.5x PCR enhancer 0.5 µM Oligonucleotide 1 0.5 µM Oligonucleotide 2 0.2 mM dNTPs 0.026 U/µL Taq polymerase

Phosphate buffered saline (PBS) (10 x)	90 g NaCl 14.33 g $Na_2HPO_4x2H_2O$ 2.17 g KH_2PO_4 add up to 1 L H_2O
Phosphate buffered saline (PBS) (1 x)	100 mL PBS (10 x) add up to 1L H_2O
Proteinase K buffer	DNA isolation buffer (1 x) 0.3 mg/mL Proteinase K 0.5% Triton X-100 1% β-Mercaptoethanol
T cell medium	RMPI 1680 10 % FCS (v/v) 2 mM Glutamine MEM non-essential amino acids 5 µM β-Mercaptoethanol
TAE (50 x)	242 g TRIS 57.1 mL acetic acid 99% 100 mL EDTA 0.5 M, pH8 add up to 1 L with H_2O
TAE (1 x)	20 mL TAE (50 x) add up to 1L H_2O
TE	H_2O 1 M TRIS, pH 7.6 0.5 M EDTA
Tissue digestion buffer	PCR H_2O DNA isolation buffer (1 x) 0.3 mg/mL Proteinase K 0.5% Triton X-100
Tris-EDTA	10 mM Tris, pH 7.6 1 mM EDTA
Trypan Blue solution (10 x)	PBS 0.05% Trypan Blue (w/v)

3.1.3 Kits

Product	Supplier
Agilent RNA 6000 Pico	Agilent, Böblingen, Germany
CTV Cell Tracer Kit	Invitrogen, Carlsbad, CA, USA
NucleoSpin® RNA Clean-up XS	Macherey-Nagel, Düren, Germany

3.1.4 Oligonucleotides

Target gene/construct	Primer name	Sequence (5'-3')
CD45.1	RO489	CATGGGGTTTAGATGCAGGA
	RO490	GCAAGGCAGGATGCTAGAAA
CD45.2	RO484	GAGCCTGTATCTAAACCTGAGT
	RO487	GGCAACATGCCCCTTAACT
li-rTA	RO281	GTCTCAGAAGTGGGGGCATA
	RO282	GGACAGGCATCATACCCACT
NR4	RO445	CGGGTCAGAAAGAATGGTGT
	RO446	CAGTTTCAGTCCCCATCCTC
SWHEL HC	RO373	GTCTCTGCAGGTGAGTCCTAACTTCT
	RO374	CAACTATCCCTCCTCCAGCCATAGGAT
SWHEL LC	RO375	CAGGGCCAGCCAAAGTATTG
	RO376	TCCAACCTCTTGTGGGACAGTT
TIM	RO235	CTCATCTCAAACAAGAGCCA
	RO236	CACTGCTTACTTCCTGTACC
EAMCC	RO295	CAGGCCACCACTGCTTACTT
	RO296	ATCTTCCAGTTCACGCCATC

3.1.5 Enzymes

Enzyme	Supplier
rDNAse	Macherey-Nagel, Düren, Germany
Proteinase K	Diagonal, Münster, Germany
Peg Gold Tag DNA Polymerase	Peqlab, Erlangen, Germany

3.1.6 Antibodies

3.1.6.1 Antibodies for flow cytometry and cell sorting

Specificity	Conjugate(s)	Clone	Reactivity	Company
CD4	PerCP-Cy5.5, Al647	RM4-5	rat anti-mouse	Biolegend, San Diego, CA, USA
CD4	PE, PE/Cy7	Gk1.5	rat anti-mouse	eBioscience, San Diego, CA, USA
CD5	bio, PE	53-7.3	rat anti-mouse	Biolegend, San Diego, CA, USA
CD8α	bio	53-6.7	rat anti-mouse	Biolegend, San Diego, CA, USA
CD11b	bio	M1/70	rat anti-mouse	Biolegend, San Diego, CA, USA
CD11c	bio	N418	armenian hamster α-mouse	Biolegend, San Diego, CA, USA
CD19	Al647	6D5	rat anti-mouse	Biolegend, San Diego, CA, USA
CD44	FITC, PE/Cy7	IM7	rat anti-mouse/human	Biolegend, San Diego, CA, USA

CD45.1	Al488, Al647, PerCP, BV510	A20	mouse anti-mouse	Biolegend, San Diego, CA, USA
CD45.2	PE, Al647	104	mouse anti-mouse	Biolegend, San Diego, CA, USA
CD45R	PeCy7, BV510	RA3-6B2	rat anti-mouse	Biolegend, San Diego, CA, USA
CD49b	bio	DX5	rat anti-mouse	Biolegend, San Diego, CA, USA
CD62L	PE	MEL-14	rat anti-mouse	Biolegend, San Diego, CA, USA
CD69	PE	H1.2F3	armenian hamster α-mouse	Biolegend, San Diego, CA, USA
CD73	PE	TY/11.8	rat anti-mouse	Biolegend, San Diego, CA, USA
CD90.1	Fitc	HIS51	mouse anti-mouse	eBioscience, San Diego, CA, USA
CD90.1	PE	KW322	mouse anti-mouse/rat	Biolegend, San Diego, CA, USA
CD90.1	Al647, PerCP	OX7	rat anti-mouse	Biolegend, San Diego, CA, USA
CD127	PE	A7R34	rat anti-mouse	eBioscience, San Diego, CA, USA
CD134 (Ox40)	PE	Ox-86	rat anti-mouse	Biolegend, San Diego, CA, USA
CD137L	PE	TKS-1	rat anti-mouse	Biolegend, San Diego, CA, USA
CD154 (CD40L)	PE	MR1	armenian hamster α-mouse	Biolegend, San Diego, CA, USA
CD200 (Ox2)	PE	OX-90	rat anti-mouse	Biolegend, San Diego, CA, USA
CD218a (IL-18Ra)	PE	P3TUNYA	rat anti-mouse	eBioscience, San Diego, CA, USA
CD223 (LAG-3)	bio	C9B7W	rat anti-mouse	Biolegend, San Diego, CA, USA
CD244.2 (2B4)	FITC	m2B4 (B6)458.1	mouse anti-mouse	Biolegend, San Diego, CA, USA
CD278 (ICOS)	FITC	C398.4A	armenian hamster α-mouse	Biolegend, San Diego, CA, USA
CD279 (PD-1)	PE/Cy7	RMP1-30	rat anti-mouse	Biolegend, San Diego, CA, USA
CD366 (Tim-3)	PE	RMT3-23	rat anti-mouse	Biolegend, San Diego, CA, USA
cMaf	PE	symOF1	mouse anti-mouse/human	Invitrogen, USA
FC-receptor	unconjugated	2.4G2	rat anti-mouse	BioXcell, West Lebanon, NH, USA
Foxp3	eFluor® 660	FJK-16s	rat anti-mouse	eBioscience, San Diego, CA, USA
FR4	PE/Cy7	eBio12A5	rat anti-mouse	eBioscience, San Diego, CA, USA
IFN-γ	APC	XMG1.2	rat anti-mouse	Biolegend, San Diego, CA, USA
IL-2	PE/Cy7	JES6-5A4	rat anti-mouse	eBioscience, San Diego, CA, USA
IRF4	PE	IRF4.3E4	mouse anti-mouse/human	Biolegend, San Diego, CA, USA
LAT	unconjugated		rabbit anti-mouse	Cell Signaling, Cambridge, UK
Ly-6C	FITC	HK1.4	rat anti-mouse	Biolegend, San Diego, CA, USA
NFATc1	Al488	7A6	mouse anti-mouse/human	Biolegend, San Diego, CA, USA
TCR β	FITC, AL647	H57-597	armenian hamster α-mouse	Biolegend, San Diego, CA, USA
Ter119	bio	TER-119	rat anti-mouse	Biolegend, San Diego, CA, USA
TIGIT	PE	1G9	mouse anti-mouse	Biolegend, San Diego, CA, USA
TNF-α	FITC	MP6-XT22	rat anti-mouse	Biolegend, San Diego, CA, USA

TOX	PE	TXRX10	rat anti-mouse	Invitrogen, USA
Vα11	APC	RR8-1	rat anti-mouse	eBioscience, San Diego, CA, USA
Vβ3	FITC	Kj25		Kindly provided by N. Asinovski, C. Benoist and D. Mathis (Harvard Medical School, Boston, MA, USA)

3.1.6.2 Secondary antibodies

Specificity	Conjugate(s)	Clone	Reactivity	Company
Anti-Rabbit IgG	FITC	Poly4055	Goat	BD, Franklin Lakes, NJ, USA

3.1.6.3 Isotype control antibodies

Specificity	Conjugate(s)	Clone	Reactivity	Company
IgG	unconjugated	DA1E	Rabbit	Cell Signaling, Cambridge, UK
IgG1, κ	AI488, PE	MOPC-21	Mouse	Biolegend, San Diego, CA, USA
IgG1, κ	FITC, APC	RTK2071	Mouse	Biolegend, San Diego, CA, USA
IgG2a, κ	AI488, PE, PE/Cy7	RTK2758	Mouse	Biolegend, San Diego, CA, USA

3.1.6.4 Antibodies used *in vivo* or *in vitro*

Specificity	Clone	Company
CD40	FGK45.5	BioXcell, West Lebanon, NH, USA
CD3	145-2C11	BioXcell, West Lebanon, NH, USA
CD28	37.51	BioXcell, West Lebanon, NH, USA

3.1.7 Consumables

Product	Supplier
Cannulas 23G blue	Carl Roth, Arlesheim, Switzerland
Casy cups	Roche, Basel, Switzerland
Cell culture plate, 6-well	Sarstedt, Nümbrecht, Germany
Cell culture plate, 96-well round bottom	Sarstedt, Nümbrecht, Germany
Cell strainer (100 μm, sterile)	BD, Franklin Lakes, NJ, USA
Cover slides (glass)	Diagonal, Münster, Germany
Dissecting scissors	WPI-europe, Hertfordshire, UK
Ear punch, 10 cm, 2 mm diameter	WPI-europe, Hertfordshire, UK
FACS tubes	Sarstedt, Nümbrecht, Germany
Filter tips OneTip, 1-10 μL	Starlab, Hamburg, Germany
Filter tips OneTip, 2-20 μL	Starlab, Hamburg, Germany
Filter tips, 1000 μL	Diagonal, Münster, Germany
Glaspipette 5 mL	Diagonal, Münster, Germany
Gloves small	Diagonal, Münster, Germany

Insulin syringes 0.5 mL 0.30 x 8 mm	Diagonal, Münster, Germany
Insulin syringes 1 mL 0.33(29G) x 12.7 mm	Diagonal, Münster, Germany
MACS LS columns	Miltenyi, Bergisch-Gladbach, Germany
Microfine Syringes for i.p and i.v. injections	BD, Franklin Lakes, NJ, USA
Non-Stick Rnase-Free 1.5 mL Microfuge Tubes	Thermo Fisher Scientific, Waltham, MA, USA
Omnifix 1 mL syringes	Diagonal, Münster, Germany
Omnifix 20 mL syringes	Diagonal, Münster, Germany
Operating scissors	WPI-europe, Hertfordshire, UK
PCR reaction tubes stripes	Diagonal, Münster, Germany
PCR-plates, 96-well	Diagonal, Münster, Germany
Petri dish 60 mm x 15 mm	Diagonal, Münster, Germany
Pipette tips 20-200 μL, yellow	Brand, Wertheim, Germany
Pipette tips 50-1000 μL, blue	Brand, Wertheim, Germany
Polyamide-mesh, pore size 150 μm	RCT, Heidelberg, Germany
Polyamide-mesh, pore size 80 μm	RCT, Heidelberg, Germany
Reaction tube rack	Carl Roth, Arlesheim, Switzerland
Reaction tubes 50 mL	Greiner, Kremsmünster, Austria
Reaction tubes round-bottom 4 mL and 14 mL	BD, Franklin Lakes, NJ, USA
Reaction tubes Safeseal 1.5 mL	Sarstedt, Nümbrecht, Germany
Rotilabo-Abdeckfolien für PCR-Platten	Carl Roth, Arlesheim, Switzerland
Serological pipettes 5 mL, 10 mL, 25 mL	Sarstedt, Nümbrecht, Germany
Steril filter Milex-GP 0.22 μm	Diagonal, Münster, Germany
TPP Bottle-Top-Filter 500 mL, 0.22 μm	Sigma-Aldrich, ST. Louis, MO, USA

3.1.8 Laboratory equipment

Device	Manufacturer
Affymetrix Mouse Gene ST 2.0 arrays	Thermo Scientific, Rockford, IL, USA
BD FACSCalibur Flow Cytometer	BD Bioscience, Franklin Lakes, NJ, USA
BD FACSCanto II Flow Cytometer	BD Bioscience, Franklin Lakes, NJ, USA
Bioanalyzer	Agilent, Böblingen, Germany
CASY Cell Counter & Analyzer	Omni Life Science, Bremen, Germany
Centrifuge 5417R	Eppendorf, Hamburg, Germany
Centrifuge 5424	Eppendorf, Hamburg, Germany
Centrifuge Rotanta 460 R	Hettich, Tuttlingen, Germany
Electrophoresis Power supply (EPS200)	Pharmacia Biotech, Upsalla, Sweden
Encore® Biotin Module	NuGEN Technologies, San Carlos, CA, USA
Fridge, Freezer	Liebherr, Bulle, Switzerland
Gamma-cell 40	AECL, Chalk River Laboratories, Canada
Gel-documentation system	Intas, Göttingen, Germany
GeneChip Scanner 3000 7G	Thermo Scientific, Rockford, IL, USA
Heatblock Thermomixer 5436	Eppendorf, Hamburg, Germany
HeraeusTM MultifugeTM X3R	Thermo Scientific, Rockford, IL, USA
Ice machine	Scotsman, Radevormwald, Germany
ImageStream®X Imaging Flow Cytometer	EMD Millipore Seattle, WA, USA

Incubator 5 % CO2	Heraeus, Hanau, Germany
Incubator 5% CO2, 3% O2	Heraeus, Hanau, Germany
Laminar airflow cabinet HeraSafe	Heraeus, Hanau, Germany
Microscope Labovert FS	Leitz, Wetzlar, Germany
Microscope Leica	Leica Microsystems GmbH, Wetzlar, Germany
Microwave	DAEWOO, Seoul, South Korea
MoFlo XDP Sorter	Beckman Coulter, Indianapolis, IN, USA
Multichannel pipette	Brandt, Wertheim, Germany
Multifuge X3R	Heraeus, Hanau, Germany
Ovation Pico WTA System V2	NuGEN Technologies, San Carlos, CA, USA
Pipette 12-channel, 20-200 μL	Eppendorf, Hamburg, Germany
Pipette 8-channel, 0.1-10 μL	Eppendorf, Hamburg, Germany
Pipettes	Brandt, Wertheim, Germany
Thermocycler TADVANCED	Biometra, Göttingen, Germany
Thermocyler T1	Biometra, Göttingen, Germany
Vortex Genie 2	Bender & Hobein, Zürich, Switzerland
Water bath	Lauda, Lauda-Köningshofen, Germany

3.1.9 Software

Software	Company
BD cell quest	BD, Franklin Lakes, NJ, USA
FACSDiva 6.1.2	BD, Franklin Lakes, NJ, USA
Flowjo 10.4.2 for Mac	Treestar Ashland, OR, USA
Gel Documentation System	Intas, Göttingen, Germany
GenePattern 3.7.0	Broad Institute, Cambridge, MA, USA
Graph Pad Prism 7.0c for Mac	GraphPad, La Jolla, CA, USA
IDEAS Application Version 6.2	Merck KGaA, Darmstadt, Germany
Microsoft Office for Mac 2011	Microsoft, Redmond, WA, USA

3.2 Mice and treatment of mice

3.2.1 Wild type (wt) mice

Mice with the B10.BR-H2^{k2}H2-T18^{a}/SgSnJ background were used as wild type mice and were originally received from the Jackson Laboratory (stock number 004804).

3.2.2 Congenic markers

For identification of adoptively transferred cells the congenic markers CD45.1 (Ly5.1) and CD90.1 (Thy-1.1) were used. Both markers were originally derived from B6.SJL-Ptprc^{a} Pepc^{b}/BoyJ and B6.PL-Thy1^{a}/CyJ mice, respectively and provided by Diane Mathis and Christophe Benoist at Harvard Medical School in Boston, MA, USA.

3.2.3 Genetically modified mice

3.2.3.1 T cell receptor transgenic mice

AND T cell receptor (TCR) transgenic (tg) mice (B10.BR-Tg(TcrAND)53Hed) harbor T cells with predominant expression of a MHC II-restricted TCR consisting of productively rearranged Vα11.1-Jα84 and Vβ3-Jβ1.2 chains that recognize a core epitope derived from moth cytochrome c (MCC_{93-103}) or pigeon cytochrome c (PCC_{94-104}) in the context of H-2E^{k} (Kaye et al., 1989). AND-tg mice were kindly provided by Diane Mathis and Christophe Benoist at Harvard Medical School in Boston, MA, USA. The Vα11 and Vβ3 transgenic constructs were obtained from the CD4^{+} T cell clones AN6.2 and 5C.C7, respectively and contain endogenous promotor and enhancer elements. To generate AND-tg mice both constructs were co-injected into male pronuclei of (B6xSJL) F2 zygotes (Kaye et al., 1989). For some experiments, RAG1 deficient AND TCR-tg mice were used. They produce > 90% TCR-tg CD4^{+} T cells in the lymph nodes. Such ANDxRAG$^{o/o}$ mice lack endogenous B and T cell pool and exclusively harbor T cells that express the AND TCR. For TCR signal transduction experiments, double transgenic (dtg) AND^{+}Nur77-EGFP-reporter mice were used. To generate such reporter mice AND TCR-tg animals were crossed to Nur77-EGFP-reporter mice (Tg(Nr4a1-EGFP/cre)820Khog) which were generated by inserting an enhanced green fluorescent protein (eGFP) reporter gene at the ATG start site of a Nr4a1 BAC transgene (Moran et al., 2011). Nur77-EGFP-reporter mice were purchased from Jackson Laboratory. All mice were maintained on the B10.BR background with one of the congenic markers mentioned above.

3.2.3.2 Tet-inducible antigen-expressing double transgenic (dtg) mice

Dtg iMCC mice expressing the cognate antigen of AND TCR-tg CD4+ T cells, MCC_{93-103} in the context of H-2E^k on MHC II positive cells in a doxycycline-dependent manner (Obst et al., 2005) were generated by crossing Ii-rTA tg mice (Tg(Cd74-rtA)#Doi) (Obst et al., 2005) to mice carrying the tetracycline (tet)-inducible invariant chain (Ii) with MCC_{93-103} (TIM) transgene Tg(tetO-Cd74/MCC)#Doi (van Santen et al., 2000; van Santen et al., 2004). Since MCC_{93-103} replaces the CLIP region of the invariant chain, it is efficiently delivered to the H-2E^k binding groove. Dtg iMCC mice were received from Diane Mathis and Christophe Benoist from Harvard Medical School in Boston, MA, USA. All mice were maintained on the B10.BR background.

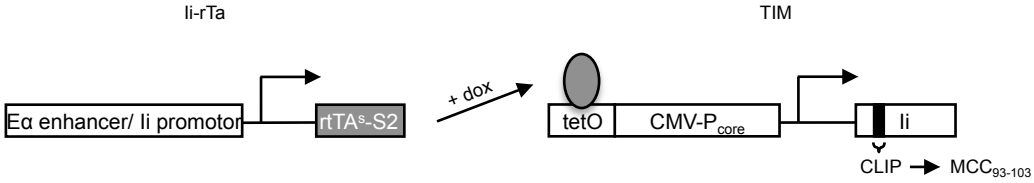

3.2.3.3 Constitutive antigen-expressing transgenic mice

The cMCC mice (Tg(H2-Ea-Cd74/MCC)37Gnnak) constitutively express a fusion protein that consists of the invariant chain of MHC II and the MCC_{88-103} peptide under the control of H-2Eα promotor and enhancer elements. Thus, cMCC mice present the cognate antigen MCC_{88-103} on H-2E^k constitutively at a high abundance to AND TCR-tg CD4+ T cells. The cMCC mice were kindly provided by Naoko Nakano, Science University of Tokio, Japan and Diane Mathis and Christophe Benoist at Harvard Medical School, Boston, MA, USA. All mice were maintained on the B10.BR background.

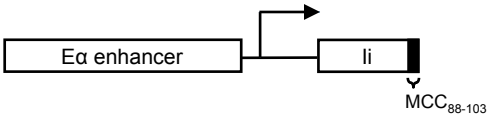

3.2.3.4 B cell receptor (BCR) transgenic cMCCxSW$_{HEL}$ mice

Most B cells of the SW$_{HEL}$ mice (Tg(H2-Ea-Cd74/MCC)37GNnak-Ightm1Rbr Tg(IgkHyHEL10) 1Rbr-Ptprca) express an anti-hen egg lysozyme (HEL) light chain transgene. SW$_{HEL}$ mice were generated by a knock-in of a rearranged V_HDJ_H gene at its physiological position at the 5' end of the IgH locus (Phan et al., 2003) and are able to undergo class switch recombination to all Immunoglobulin (Ig) classes. SW$_{HEL}$ mice were kindly received from Martin Turner, Babraham Institute of Cambridge, UK. SW$_{HEL}$ mice were crossed to cMCC mice to generate HEL-specific

B cells presenting MCC_{88-103} on H-2E^k constitutively. These mice were maintained on the B10.BR background with the congenic marker CD45.1.

3.2.4 Breeding and housing of mice

All animals were bred and maintained at the animal facility of the Institute for Immunology, Ludwig-Maximilians-University of Munich, Munich, Germany. All experiments were approved by the Government of Upper Bavaria and conducted in compliance with German federal guidelines.

3.2.5 Genotyping of mice

AND TCR-tg mice were typed by surface staining of peripheral blood lymphocytes for the AND specific β-chain Vβ3, CD4, and the congenic marker CD45.1 or CD90.1. To do so, 2-3 drops of blood from the tail vail were collected and processed and flow cytometric analysis was performed as described in section 3.3.3.3.
All other mice were genotyped by polymerase chain reaction (PCR). For primers and protocols see section 3.1.4 and 3.3.1.2.

3.2.6 Doxycycline treatment

To induce antigen presentation in iMCC mice, animals were treated with doxycycline (dox) diluted in drinking water low in divalent cations (Volvic, Danone Waters, Frankfurt, Germany) to prevent formation of precipitates that form in the presence of Mg^{2+} and Ca^{2+} and might reduce bioactivity of dox. Mice were fed with either low dose (10 µg/ml) or high dose (100 µg/ml) of dox in the drinking water, resulting in a “low” and “intermediate” expression on antigen, respectively. Dox treatment started usually one day before adoptive T cell transfer and was continued according to the experimental set up as indicated within the experimental schemes.

3.2.7 Intra-peritoneal application of monoclonal antibodies

DCs were activated *in vivo* for optimal T cell priming and memory differentiation with a stimulatory mAB against CD40 (Hawiger et al., 2001; Obst et al., 2007). Sterile dilution of monoclonal antibody α-mouse CD40 (clone FGK45.5) were prepared using 1 x PBS. 20 µg α-mouse CD40 were injected intraperitoneal (i.p.) per mouse in a volume of 100 µl.

3.3 Methods

3.3.1 Molecular biology

3.3.1.1 Tissue digest

Tail biopsies (approximately 2 mm) were removed from mice to be typed and subsequently digested in 100 µl proteinase K buffer at 56 °C for at least 6 hours. After digestion proteins were denatured by incubation at 90 °C for 10 minutes.

3.3.1.2 Polymerase chain reaction (PCR)

For genotyping of transgenic mice, the digested tissue samples were diluted 1:10 in H_2O. One µL of each dilution was mixed on ice with 24 µL of PCR master mix solution, prepared as described in Tab.1. The final PCR reaction mixture was covered with a drop of mineral oil and run in the thermo cycler using a standard PCR program, described in Tab. 2.

PCR master mix	
PCR H_2O	
PCR buffer	1 x
PCR enhancer	0.5 x
Oligonucleotide 1	0.5 µM
Oligonucleotide 2	0.5 µM
dNTPs	0.2 mM
Taq polymerase	0.026 U/µL

Table 1: PCR master mix components.

Step	Cycle #	Repeats	Time	Heat
Initial denaturation	1	1	5 min	95 °C
Denaturation	2 - 36	35	30 sec	95 °C
Primer annealing	2 - 36	35	30 sec	55 °C
DNA elongation	2 - 36	35	45 sec	72 °C
Final elongation	37	1	5 min	72 °C
Cooling period	38	1	10 sec	20 °C

Table 2: Standard PCR program.

3.3.1.3 Agarose gel electrophoresis

PCR-amplified DNA fragments were analyzed by agarose gel electrophoresis. DNA samples were mixed with sample buffer and loaded side by side with a 100 bp marker ladder on a 1,5% agarose gel and run at 120 V for 25 min in 1 x TAE running buffer. To visualize the results, the gels were exposed to UV light within a gel documentation system and pictures were taken.

3.3.1.4 RNA isolation and clean-up

To isolate total RNA from samples that were FACS sorted in Trizol LS and stored at -80 °C (protocol described in section 3.3.3.5) samples were thawed on ice. 300 μL chloroform was added and subsequently handshaked 15 times. Samples were incubated for 3 min at RT and centrifuged for 15 min (12,000 x g, 4 °C). The upper aqueous phase containing the RNA was transferred into new tubes and 1 volume of isopropanol + 1 μL linear polyacrylamide (LPA) was added. RNA samples were incubated o/n at -20 °C to increase the precipitation yield. Samples were centrifuged for 10 min (12,000 x g, 4 °C), supernatants were removed, and RNA pellets were washed with 1 mL of 70% EtOH. Final RNA pellets were dissolved in 100 μL RNAse-free water. The NucleoSpin® RNA Clean-up XS kit (Macherey-Nagel) was used to purify RNA according to manufacturer´s instructions. Finally, RNAs were eluted in 12 μL supplied RNAse-free H_2O and stored at -80 °C.

3.3.1.5 RNA quality check

To assess RNA quality the Agilent RNA 6000 Pico kit was used according to manufacturer´s instructions. RNA integrity number (RIN) was measured for each sample using a 2100 Bioanalyzer and all samples with high quality RNA (RIN > 8) were used for microarray analysis.

3.3.1.6 Gene expression analysis

RNA amplification, labeling, and hybridization was done by Martin Irmler and Johannes Beckers, Institute of Experimental Genetics, Helmholtz Zentrum München, Neuherberg. For RNA amplification the Ovation Pico WTA System V2 together with the Encore Biotin Module (Nugen) were used. Amplified cDNA was hybridized on Affymetrix Mouse Gene ST 2.0 arrays containing 35,000 probe sets. According to the Affymetrix expression protocol, including minor modifications as suggested in the Encore Biotin protocol, staining and scanning were performed using a GeneChip Scanner 3000 7G.

3.3.2 Cellular methods

3.3.2.1 Organ removal and generation of single cell suspensions

Mice were sacrificed by carbon dioxide (CO_2) asphyxiation and fixed in a supine position on a dissection trey and disinfected with 70% ethanol. The skin was opened medially and laterally. Axillary, brachial, and inguinal lymph nodes (LN) were dissected and pooled in 5 mL FACS buffer (Van den Broeck et al., 2006). The abdominal wall was opened, the spleen was removed and stored in 5 mL FACS buffer kept on ice. Single cell suspensions from lymph nodes and spleens were generated by two methods. Organs were ground using the rough side of two microscope glass slides and filtered through a mesh with 150 μm pores when cells were intended for flow cytometric analysis. For adoptive transfers sterile cell strainers were used. Lymph node cell suspensions were centrifuged for 5 min (1,500 x rpm, 4 °C) and the pellets were resuspended in 1 mL FACS buffer. Spleen cell suspensions were underlaied with 3 mL Pancoll and centrifuged 10 min (2,000 x rpm, 4 °C, deceleration ramp 5 of 9) for separation. The lymphocyte layer between Pancoll and FACS buffer was carefully removed, transferred into new tubes, and washed with FACS buffer. Pellets were resuspended in 3 mL FACS buffer.

3.3.2.2 Magnetic-activated cell sorting (MACS) of $CD4^+$ T cells

Enrichment of polyclonal $CD4^+$ T cells was achieved by negative selection by magnetic-activated cell sorting (MACS). This technique allows for separation of a certain cell population based on characteristic surface marker expression. Cells to be depleted were stained with biotinylated antibodies specific for such characteristic surface molecules and subsequently incubated with paramagnetic anti-biotin-beads. Thus, allowing separation of labeled and unlabeled cells within MACS columns placed in a strong magnet. Magnetically labeled, unwanted cells stick to the MACS columns while unlabeled cells can be collected in the flow through. $CD4^+$ T cells to be sorted for microarray analysis were thus selected before FACS-sorting (described in section 3.3.3.5), LN and spleen single cell suspensions were generated as described in 3.3.2.1 and pooled from the same mouse. Cell suspensions were centrifuged for 5 min (1,500 x rpm, 4 °C), incubated in 200 μL FACS buffer containing biotinylated mAbs as listed in tab.3 for 15 min on ice. Cells were washed three times with 3 mL FACS buffer and two small aliquots from each sample were taken, one for a pre-MACS purity check using flow cytometry analysis and the other (10 μL) to count cell numbers before MACS purification. After the last washing step pellets were resuspended in 90 μL FACS buffer and 10 μL anti-biotin-beads were added per mouse. Samples were incubated for 20 min at 4 °C and swirled gently for 10 min. Samples were washed twice with MACS buffer and resuspended in 2 mL MACS

buffer. For negative selection cell suspensions were loaded onto equilibrated MACS columns. Columns were washed twice with 3 mL MACS buffer. Eluted cells were collected, centrifuged for 5 min (1,300 x rpm, 4 °C) and resuspended in 1 mL FACS buffer. Two aliquots were taken, one for post-MACS purity check and the other one (10 μL) to count cells post MACS enrichment.

Volume / mouse	mAb specificity	Target cells
5 μL	CD8	T cells, DCs
5 μL	CD45R	B cells
3 μL	CD11b	DCs, Macrophages
3 μL	CD11c	DCs
3 μL	CD49	NK cells
3 μL	Gr-1	Granulocytes
3 μL	TER119	Erythrocytes

Table 3: Biotinylated mAbs for MACS purification of $CD4^+$ T cells.

3.3.2.3 Counting live cells in single cell suspension

Live cells were either counted manually using a Neubauer counting chamber (depth 0.1 mm, 0.0025 mm^2) or automatically, using a CASY Cell Counter & Analyzer.

For manual cell counting, 10 μL single cell suspension was diluted twice 1:10 in Tryptan blue buffer. Under the light microscope live and dead cells could be distinguished by the fact that only dead cells take up Tryptan blue. Round unstained cells of two quarters of the counting chamber were counted, averaged, and multiplied by 1 x 10^6 to obtain the cell number per mL.

For automatic cell counting, 10 μL of a single cell suspension were diluted 1:1000 in CASY buffer (10 mL) and measured using CASY Cell Counter & Analyzer. The read with this dilution factor equaled to the cell number per 1 mL.

3.3.2.4 Cell trace violet (CTV) labeling

Cell trace violet (CTV) is a proliferation indicator dye that binds proteins in the cell and thus gets diluted by half per cell division. Therefore, this dye is used for flow cytometric visualization of cell proliferation indicated by the reduction of CTV intensity. Using this dye, 1 to 8 cell divisions can be detected (Quah and Parish, 2012). To calculate the average number of divisions (N) even if peaks were indistinguishable, the MFI values of whole populations were used (Rabenstein et al., 2014):

$$N = \log_2(\text{CTV MFI}_{ctr}/\text{CTV MFI}_{sample})$$

To label cells of interest, single cell suspensions were adjusted to 20 x 10^6 cells per mL of pre-warmed (37 °C) PBS supplemented with 0.1% BSA. 2 μL 5 mM CTV stock were added per 20 x 10^6 cells while gently vortexing. Samples were incubated for 10 min at 37 °C in the dark and swirled after 5 min of incubation. After incubation 1 mL pre-warmed PBS + 0.1% BSA was added and 1 mL pre-warmed heat-inactivated FCS was underlaid. Samples were centrifuged for 5 min (1,500 x rpm, 4 °C) and washed twice with transfer buffer. Cells were counted as described in 3.3.2.3 and adjusted to 1 x 10^6 cells/100 μL transfer buffer.

3.3.2.5 Adoptive T cell transfer

For adoptive T cell transfer lymph node single cell suspensions from donor LNs were generated according to the protocol in section 3.3.2.3. For phenotypic characterization of lymphocytes from donor mice, small aliquots of cells were taken and stained for surface markers as listed in Tab. 4, depending on the congenic markers of these mice. Flow cytometric analysis was used for marker visualization (protocol in 3.3.3.1/3.3.3.3). Transgenic TCR expression was confirmed by positive Vβ3 staining on $CD4^+$ T cells, congenic marker expression was confirmed by CD45.1 or CD90.1 surface expression, and lacking CD45R expression verified the ANDxRAG$^{o/o}$ phenotype. CD62L and CD44 surface expression determined the activation status of donor lymphocytes as naïve $CD4^+$ T cells are $CD44^{lo/int}CD62L^{hi}$. Only samples with more than 90% naïve cells were used for transfers. Also, the percentage of transgenic $CD4^+$ T cells was analyzed. Data were acquired on a Canto II flow cytometer.

Staining	FITC	PE	PerCP	PeCy7	Al647	PB	BV510
A	Vβ3	CD62L	CD4	CD44	CD45.1	Dapi	
B	Vβ3	CD62L	CD4	CD44	CD90.1	Dapi	
C	Vβ3	CD62L	CD4	CD44	CD45.1	Dapi	CD45R

Table 4: Antibody-staining strategies for phenotypic characterization of AND T cells

Upon successfully characterizing donor $CD4^+$ T cells, cell numbers were measured (see 3.3.2.3) and absolute transgenic $CD4^+$ T cell numbers were calculated.
Lymphocytes were washed with 1 mL transfer buffer and adjusted to 1 x 10^6 transgenic $CD4^+$ T cells/100 μL transfer buffer. Cells were always kept on ice. The tails of recipient animals were heated briefly and disinfected with 70% ethanol, and 100 μL buffer containing 1 x 10^6 cells were injected intravenously (i.v.).

3.3.2.6 Secondary adoptive T cell transfer

For secondary adoptive T cell transfers recipient mice were sacrificed, organs were removed, and single cell suspensions were generated as described in 3.3.2.1. $CD4^+$ T cells were MACS purified according to 3.3.2.2 and prepared and adoptively transferred as described in 3.3.2.5.

3.3.2.7 Adoptive B cell transfer

For adoptive B cell transfers single cell suspensions from donor spleens were generated as described in 3.3.2.1. Upon Pancoll based separation of splenocytes the percentage of B cells was determined by FACS analysis. Antibody staining strategy was used as indicated below. Cells were counted and labeled with CTV following the protocol in section 3.3.2.4. The amount of CTV labeled B cells was set to 5 x 10^6 B cells in 100 μL transfer buffer and injected i.v.

Staining	FITC	PE	PerCP	PeCy7	Al647	PB
A	HEL-Ig	CD62L	CD45.1	CD44	CD19	Dapi

Table 5: Antibody staining strategy for phenotypic characterization of B cells

3.3.2.8 T cell re-stimulation using phorbol myristate acetate and ionomycin

To investigate $CD4^+$ T cell functionality upon chronic antigen exposure *in vivo*, cytokine production was quantified using flow cytometry upon re-stimulation with PMA and ionomycin *in vitro*. Therefore, splenocyte single cell suspensions were generated as described in section 3.3.2.3. 4 x 10^6 cells/well were transferred into a 96-well round-bottom plate and stimulated in 200 mL RPMI Full media with 20 ng/mL PMA in conjunction with 1 μg/mL Ionomycin. PMA stimulates protein kinase C and the Calcium ionophore Ionomycin facilitates the flux of Ca^{2+} ions into cells, thus inducing a very strong TCR-independent stimulation of T cells (Truneh et al., 1985). Plates were cultured for 4 h at 37 °C and 5% CO_2. 10 μg/mL Brefeldin A, inhibiting secretory vesicle formation and transport at the Golgi apparatus and thus preventing cytokine release, was included during the last 2 h of incubation (Rabenstein et al., 2014).

3.3.3 Flow cytometry

3.3.3.1 Fluorescence-activated cell sorting (FACS)

The technique of modern high-throughput flow cytometry is used to simultaneously detect, measure, and distinguish multiple characteristics of several cell populations within a single cell suspension. Cell-specific surface and intracellular markers are usually stained with mAbs either

directly or secondarily labeled with a fluorochrome or are genetically modified to be linked to a certain fluorescent protein like the enhanced green fluorescent protein (eGFP). To accurately measure the fluorescently labeled markers and optical characteristics for identification, labeled cells pass uniformly, one cell at the time, through focused laser beams. Also, relative cell size and granularity can be estimated by detecting forward-scattered light (FSC) and side-scattered light (SSC), respectively. Nowadays, flow cytometers have multiple lasers and detectors allowing for multiple mAb labeling and thus enable a precisely identification of target cells and their phenotypic characteristics. Using the droplet technology certain cell populations can be sorted based on several parameters including cell size and morphology, as well as marker expression. Sorted cells and can be later used for other experimental purpose.
For experimental data acquisition the BD FACSCanto II and for blood-genotyping data acquisition the BD FACSCalibur flow cytometers were used. Data analysis was performed using FlowJo 10.4 for Mac.

3.3.3.2 Imaging Flow Cytometry (IFC)

The technology of imaging flow cytometry combines the common high-throughput single-cell identification of conventional flow cytometry with single cell imaging properties of microscopy. The advantage of imaging flow cytometry is clearly the production of extraordinarily detailed fluorescent single cell images.
For experimental data acquisition the Millipore ImageStream®^{X} and for data analysis the IDEAS Application Version 6.2 were used.

3.3.3.3 Surface staining of lymphocytes

To stain surface markers of interest, single cell suspensions were transferred into 96-well plates with 3-5 x 10^6 cells per well, centrifuged for 5 min (1,500 x rpm, 4 °C), and resuspended in 50 μL mAb solution where Dapi was added to discriminate live and dead cells. Samples were incubated for 30 min at 4 °C in the dark and washed twice before flow-cytometric analysis. Antibodies were usually diluted 1:400, streptavidin and Dapi were diluted 1:1000. All staining and washing steps were performed using FACS buffer.

3.3.3.4 Intracellular staining of lymphocytes

For intracellular staining of cytokines PMA/IM stimulated lymphocytes were surface stained as describes in 3.3.3.3 but either Dapi (1:1000 in FACS buffer) or fixable viability dye (FVD) eFlour450 or eFlour660 (1:1000 in PBS) were used. Cells were fixed in 100 μL IC fixation buffer for 20-30 min at RT in the dark, incubated for 5 min at RT in 100 μL BD Perm Buffer III to

permeabilize the cell membrane, and washed twice with PBS. Fcγ-receptors were blocked using 100 µL 2.4G2 mAb diluted 1:400 in PBS (10 min at RT in the dark) and cytokines were stained intracellularly in 100 µL mAb solutions under the conditions described in Tab. 6.
For intracellular staining of molecules and transcription factors lymphocytes were transferred into 96-well plates with 4 x 10^6 cells/well, stained for 10 min at 4 °C in the dark within 100 µL FVD-eFlour450 or -eFlour660 (live/dead discrimination dye) diluted 1:1000 in PBS, washed, and subsequently surface stained as describes in 3.3.3.3. Cells were fixed and permeabilized using the FoxP3 staining kit following the manufacturer's protocol. After permeabilization the Fcγ-receptors were blocked and intracellular staining was performed as described above but instead of PBS, 1 x Permeabilization Buffer was used.

Specificity or dye	Dilution	Staining condition
2.4G2	1:400	10 min, RT
Anti-Rabbit Ig	1:400	30 min, 4°C
cMaf	1:400	30 min, 4°C
Draq5	1:1000	1 h, RT or o/n, 4 °C
FoxP3	1:400	30 min, 4°C
IFNγ	1:200	30 min, 4°C
IL-2	1:400	30 min, 4°C
IRF4	1:400	30 min, 4°C
LAT	1:100	1 h, 4 °C
NFATc1	1:100	1 h, RT or o/n, 4 °C
TCF-1	1:400	30 min, 4°C
TCR β	1:400	30 min, 4°C
TNFα	1:100	30 min, 4°C
Tox	50 µg/well	30 min, 4°C

Table 6: Antibody and dye staining conditions

3.3.3.5 Cell sorting by flow cytometry for microarray analysis

Single cell suspensions from LNs and Spleen were pooled and subsequently, $CD4^+$ T cells were MACS purified as described in section 3.3.2.2. After a test-surface staining with a small aliquot of cells to characterize the adoptively transferred $CD4^+$ T cells via flow cytometry, enriched $CD4^+$ T cells were surface stained with α-TCR-Fitc, α-CD90.2-PE, α-CD4-PerCP-Cy5.5, Streptavidin-PeCy7, α-CD45.1-Al647, and Dapi to identify AND TCR-tg T cells. Surface stained, enriched $CD4^+$ T cells were sorted using a Beckman Coulter MoFlo XDC Sorter operated by Lynette Henkel (AG Schieman, Institute for Medical Microbiology, Immunology and Hygiene, Technical University of Munich, Germany). To achieve high purity two doublet exclusion gates were included in the sorting strategy and all samples were sorted twice (see Figure 19). After the first

round all cells were sorted into tubes containing 250 µL FACS buffer with Dapi (1:1000) and a small fraction of cells were sorted into tubes containing 250 µL FACS buffer for purity check #1. During the second round a second small fraction of cells were sorted into tubes containing 250 µL FACS buffer for purity check #2 and all remaining cells were sorted into tubes containing 500 µL Trizol LS. Trizol samples were mixed and stored at -80 °C until further processing. Control samples were analyzed using flow cytometry (see Figure 20) and found > 99% pure.

3.3.3.6 Statistical analysis

Statistical analysis of FACS data was performed using GraphPad Prism® 7.0c and on Microarray data using the R 3.5.1 Software. If not indicated otherwise, geometric means, standard deviation and p values from unpaired two-tailed Student´s t-test are shown. P values < 0.05 were considered as statistically significant. Microarray analyses were done by Dr. Tobias Straub, LMU München.

4. Results

4.1 Identification of transgenic (tg) mice and prove of concept

4.1.1 Identification of AND TCR transgenic (tg) mice

To identify AND $CD4^+$ TCR-tg mice, blood genotyping was performed using flow cytometry. Blood lymphocytes were tested for the expression of AND specific TCR beta chain Vβ3, lineage marker CD4, and congenic marker, either CD90.1 (Figure 6A) or CD45.1 (Figure 6B, upper row: $RAG^{wt/wt}$ mice, lower row: $RAG^{0/0}$ mice).

To test for TCR transgenes it was sufficient to test for either Vβ3 or Vα11 expression since both chains are integrated at the same gene locus. Thus, the positivity of one of both chains, in this case Vβ3, indicated the expression of the AND TCR-transgene. For flow cytometric analyses, doublets were excluded based on forward scatter area (FSC-A) vs. height (FSC-H), lymphocyte gates were set according to the cell´s characteristics on FSC-A vs. side scatter (SSC-A), and dead cells were omitted by gating on Dapi negative cells. AND TCR-tg $CD4^+$ T cells were identified by $CD4^+CD45.1^+$ or $CD4^+CD90.1^+$ and Vβ3 surface expression, respectively.

All AND donor mice were re-typed using flow cytometry before being used for adoptive T cell transfer in all experiments. To this purpose both, transgenic TCR expression and activation status based on CD44 and CD62L surface expression were tested (Figure 6C). Naïve $CD4^+$ T cells express low levels of the activation marker CD44 (Curtsinger et al., 1999) and show a high expression of the homing receptor CD62L (Smalley and Ley, 2005). Upon T cell activation CD44 gets up- and CD62L downregulated (Smalley and Ley, 2005). Only animals with less than eight percent activated AND TCR-tg $CD4^+$ T cells were used for transfer experiments.

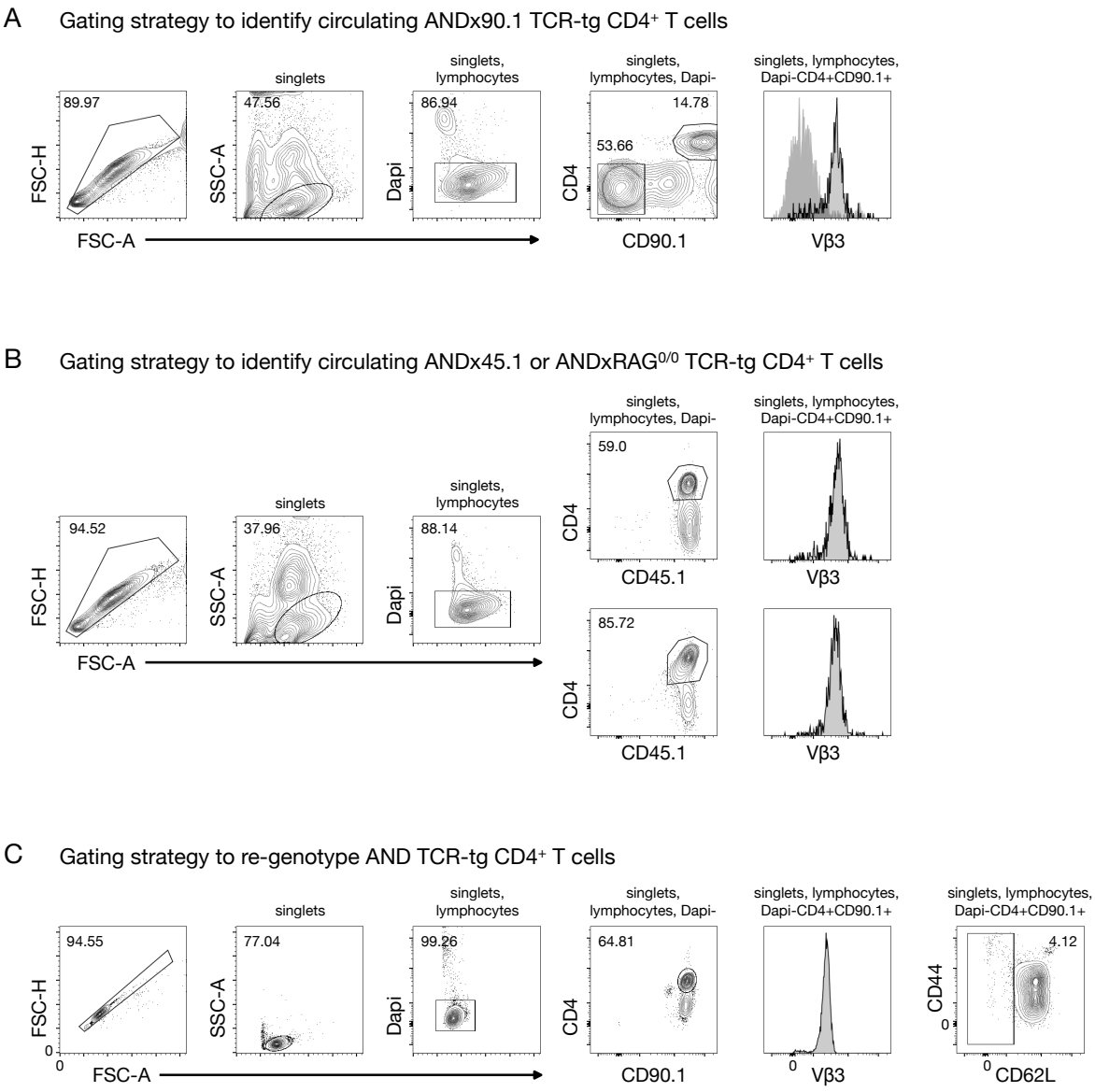

Figure 6: Blood genotyping and identification of AND TCR-tg mice. Flow cytometric identification of AND TCR-tg mice. All animals were tested for the expression of the AND specific Vβ3 chain and co-expression of the congenic marker (A) CD90.1 or (B) CD45.1, according to tested mouse lines. Within the ANDxCD45.1 line we used either $RAG^{wt/wt}$ (upper row) or $RAG^{0/0}$ (lower row) TCR-tg animals. (C) Before mice were used for adoptive T cell transfer lymphocytes were re-genotyped. Surface expression of CD4, specific congenic marker CD45.1 or CD90.1, Vβ3 chain, and activation markers CD44 and CD62L was analyzed. Mice with less than 8% of activated $CD4^{+}CD44^{hi}CD62L^{lo}$ T cells were used for experiments.

4.1.2 PCR genotyping of antigen-presenting recipient mice

Antigen-presenting recipient mice were typed by polymerase chain reaction (PCR) according to section 3.3.1.2. Here, dtg iMCC mice expressing $MCC_{93\text{-}103}$ in the context of H-$2E^k$ were PCR typed for the tetracycline (tet)-inducible invariant chain (Ii) (Figure 7, upper part) and the $MCC_{93\text{-}103}$ (TIM) transgene (Figure 7, lower part). To exclude genotyping mistakes each transgene was tested by two different sets of primer pairs. Double positive animals with matching PCR results were used for the following experiments.

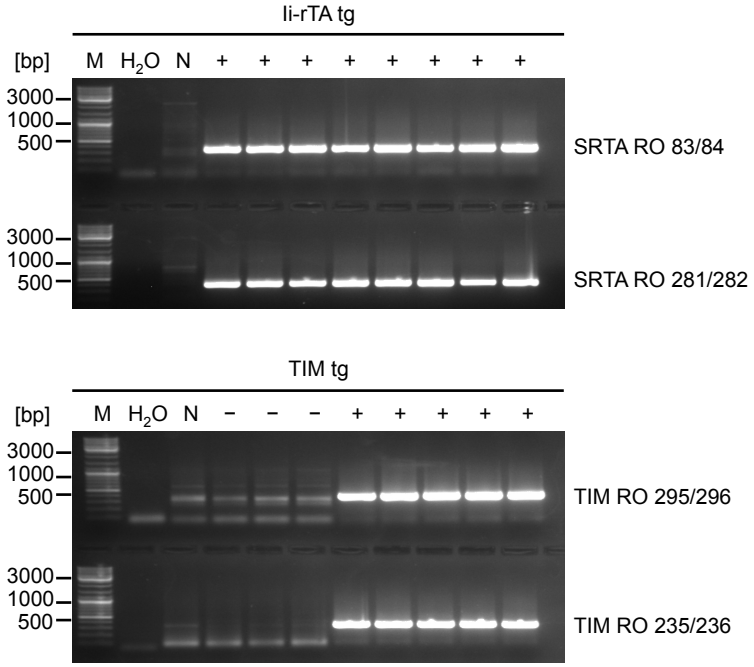

Figure 7: PCR genotyping of genetically modified recipient mice. Representative PCR products from iMCC transgenic mice analyzed by agarose gel electrophoresis. Double transgenic mice were tested for the transactivator Ii-rTA (upper gel) and the Ii-$MCC_{93\text{-}103}$ fusion protein (lower gel). Two sets of primer pairs were used for reliable identification of the two transgenes. From left to right: DNA marker (M) indicating DNA fragment size, water control (H_2O), negative control (N), PCR-amplified DNA of individual samples (+ or -).

4.1.3 Basic gating strategies to identify adoptively transferred cells

Adoptively transferred AND TCR-tg $CD4^+$ T cells are identified by surface expression of congenic markers (CD45.1 or CD90.1) since the recipients carry the .2 allelic variants of each. Using this advantage, we were able to follow and analyze adoptively transferred ANDs by flow cytometry. Depending on the experimental nature we either characterized the cell´s surface marker expression using the gating strategy described in Figure 8A or identified intracellular markers such as transcription factors or cytokines according to the gating strategy shown in Figure 8B. Doublets were excluded based on forward scatter area (FSC-A) versus height (FSC-

H). Next, we gated on lymphocytes according to the cell´s characteristics on FSC-A versus side scatter (SSC-A) and omit dead cells by gating on either Dapi negative viable cells or FVD negative fixed cells. This gating strategy was used for all experiments.

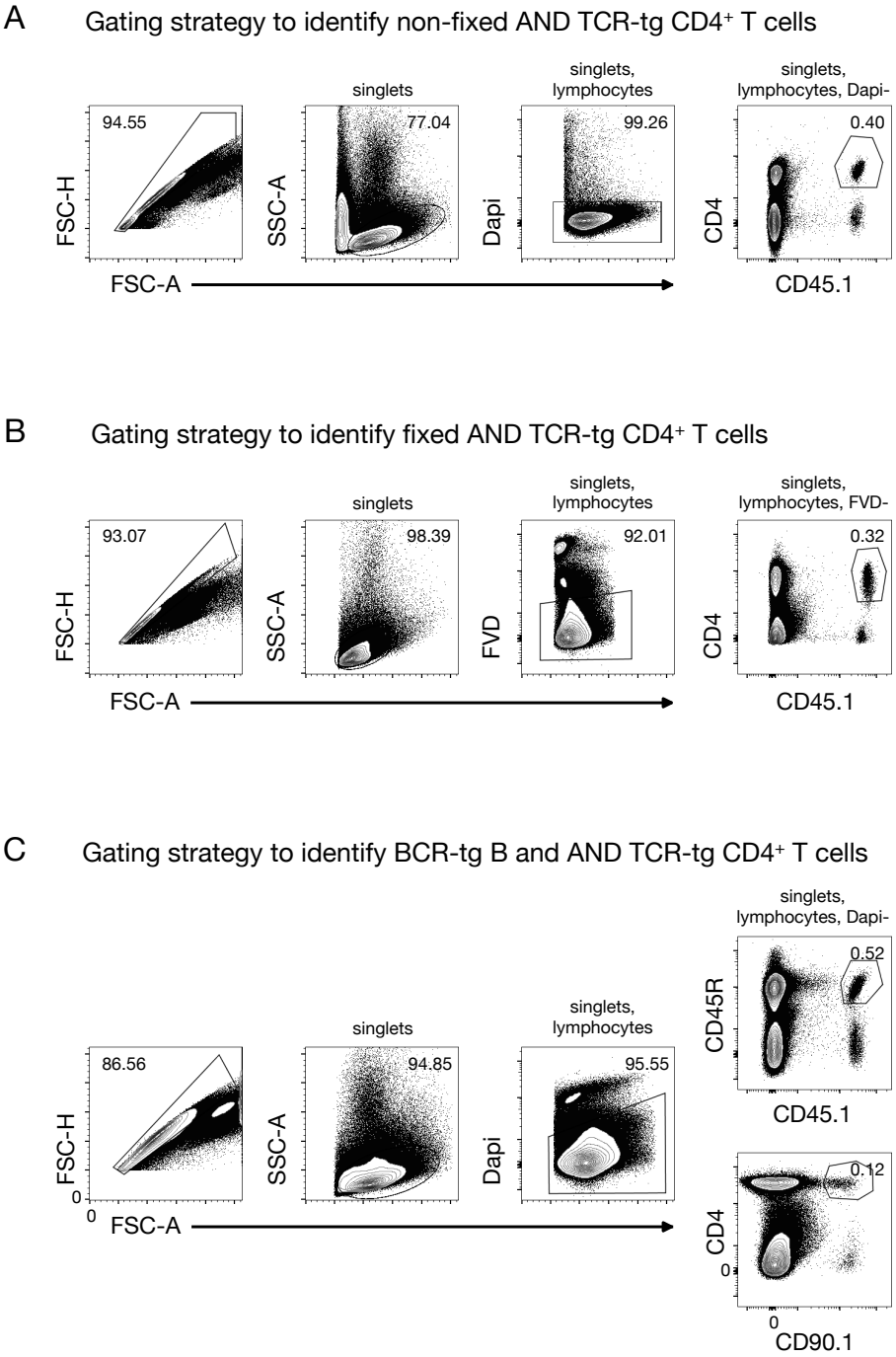

Figure 8: General flow cytometric gating strategies to identify cells of interest. Representative gating scheme to identify (A) viable or (B) fixed AND TCR-tg CD4+ T cells and (C) to identify viable HEL-specific BCR-tg B cells and AND T cells upon consecutively adoptive cell transfer. (A, B) Depicted are splenocytes 10 days post transfer (dpt) (C) and 15 dpt.

To follow and distinguish two different cell types consecutively transferred into the same recipients we took advantage of two congenic markers CD45.1 and CD90.1 to identify BCR tg B and TCR tg CD4+ T cells respectively, according to the gating strategy in Figure 8C. Thus, HEL-specific BCR tg B cells expressing CD45.1 and AND CD4+ T cells expressing CD90.1 were identified by their congenic and cell type specific markers CD45R (B220) and CD4, respectively. This gating strategy was also used to distinguish co-transferred AND T cells, which were either GFP reporter positive or negative.

4.1.4 CD4+ T cells encounter three different doses of antigen in MCC recipients

Having observed that AND CD4+ T cells recognize and respond to cognate antigen presented by dendritic cells (DCs) in iMCC and cMCC transgenic recipient mice (Han et al., 2010), we asked how AND cells respond to cognate antigen presentation in a dose-dependent fashion. We labeled AND T cells with Cell Trace Violet (CTV) and adoptively transferred them into different hosts. To induce antigen presentation recipient iMCC mice were treated with doxycycline (dox) in the drinking water starting the day before transfer (Obst et al., 2005) as described in Figure 9A. The dose of dox positively correlates with the amount of $MCC_{93\text{-}103}$ in context of $H2E^k$ on DCs in iMCC-recipient mice (Obst et al., 2005), indicated by a higher T cell proliferation rate ($N \geq 4$) in mice treated with high amount (100 μg/mL) of dox compared to the one in mice treated with low amount (10 μg/mL) of dox ($N \geq 3$) (Figure 9B and C). In cMCC-recipient mice, constitutively expressing very high amounts of the agonistic peptide $MCC_{88\text{-}103}$ in context of $H2\text{-}E^K$ (Han et al., 2010), we found the highest proliferation rate ($N \geq 6$). We found TCR downregulation in iMCC recipients, indicating high TCR stimulation as shown by reduced Vβ3 surface expression in Figure 9B and C. TCR downregulation is reported to be induced by T cell activation via TCR engagement with high affinity peptide MHC (pMHC) (Valitutti et al., 1995a; Valitutti et al., 1996; Zanders et al., 1983) and is seen as a control mechanism to prevent from hyper-activation.

Next, we used ANDxNur77-GFP reporter mice (Moran et al., 2011) to measure TCR signal strength by the three different priming conditions with increasing antigen dose 16 hours post transfer (hpt). ANDxNur77-GFP reporter cells were always co-transferred with reporter-negative AND T cells to assess specific GFP-reporter expression as opposed to mere changes of autofluorescence. TCR stimulation in iMCC treated with high amount (100 μg/mL) of dox and cMCC recipients induced high Nur77-GFP-reporter expression, indicating functional TCR stimulation and thus, T cell activation by intermediate and high-level of presented antigen.

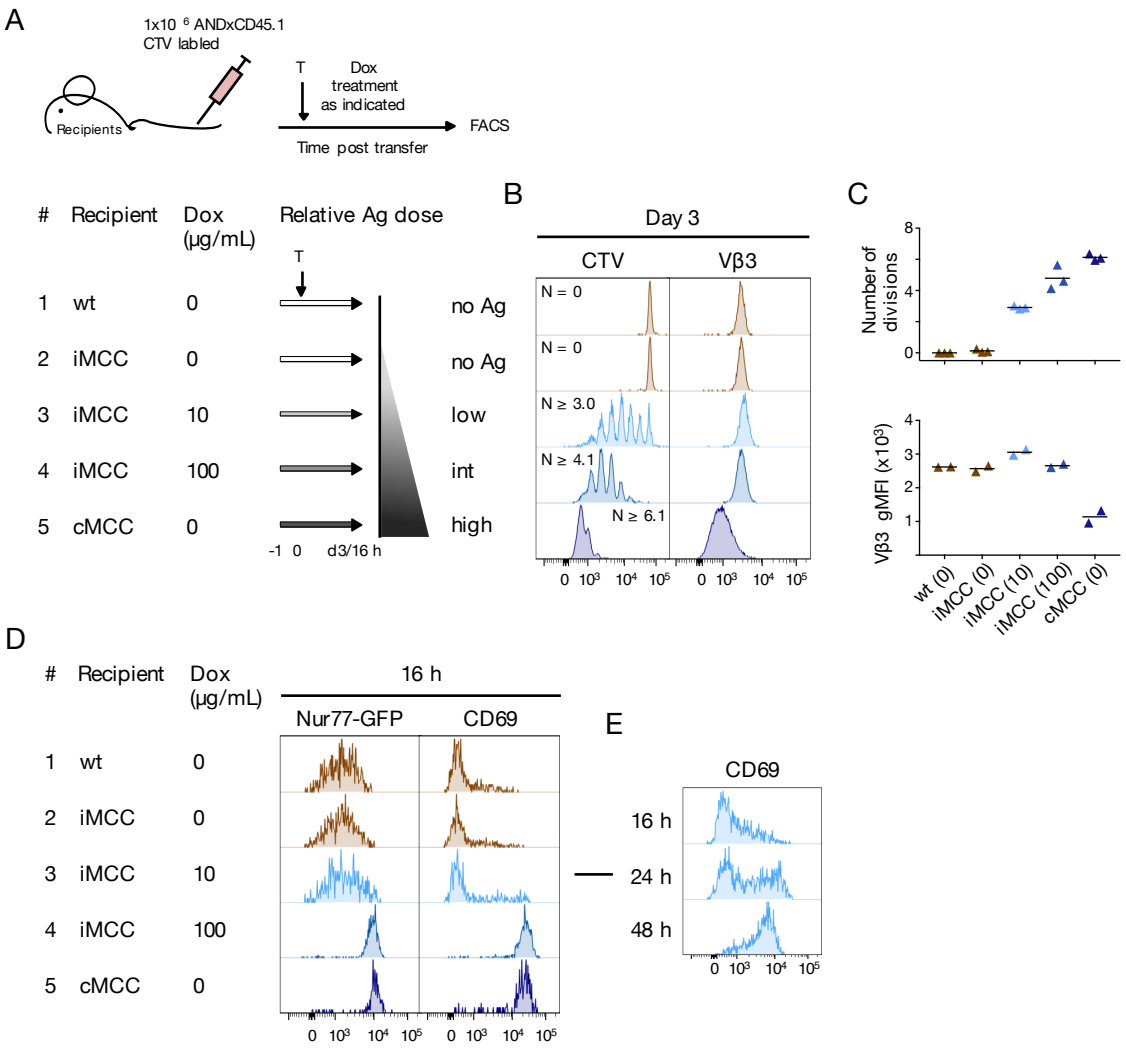

Figure 9: Specific CD4+ T cells respond to three different doses of antigen and respond dose-dependently to increasing amount of cognate antigen presented in MCC-transgenic recipients. (A) Schematic outline of the experimental approach, adoptive T-cell transfer and treatment strategy of recipient mice. The dose of doxycycline (dox) positively correlates with the amount of MCC_{93-103} in the context of H-$2E^k$ on dendritic cells in iMCC-recipient mice. cMCC-recipient mice constitutively express high amounts of the agonistic peptide MCC_{88-103} in context of H-$2E^K$. Thus, different AND T cell priming conditions with increasing antigen load could be generated. (B-E) CTV dilution and TCR expression of 1 x 10^6 adoptively transferred AND T cells isolated from recipient spleens using flow cytometry. All T cells shown were identified using the gating strategy described in Figure 8A. (B) T cell proliferation was used as readout for antigen presentation. Histograms show CellTrace Violet (CTV) dilution of AND T cells in response to increasing amounts of cognate antigen three days post transfer. Average numbers of AND T cell divisions were calculated with N = $\log_2(gMFI_{ctrl}/gMFI_{sample})$. The data are representative of three independent experiments. (C) Compilation of CTV dilution (upper panel) and TCR (Vβ3) surface expression (lower panel) of AND T cells in different recipients three dpt. Data from at least two independent experiments are shown. (D) Histograms show the expression profile of the early T cell activation markers Nur77-GFP and CD69 16 h post T cell transfer. Results are representative of two independent experiments. (E) CD69 surface expression in low-dose hosts, analyzed 16, 24, and 48 h post T cell transfer. The data are representative of two independent experiments. Antigen (Ag), doxycycline (dox).

However, low TCR stimulation (iMCC recipients treated with low amount of dox) was insufficient to induce Nur77-GFP and surface expression of the early activation marker CD69 (Figure 9D). Therefore, we followed AND T cells exposed to low-level antigen presentation over time (16, 24, and 48 hpt) and found a time-dependent upregulation of CD69 surface expression (Figure 9E). These data indicate that T cell activation by low-level antigen presentation require more time of interaction and accumulate over time to overcome the activation threshold to divide (Faroudi et al., 2003). Our results demonstrate that AND TCR-tg CD4$^+$ T cells encounter antigen of three different doses *in vivo* in these recipients at a constant level.

4.2 Characterization of AND T cells exposed to antigen for 10 days

4.2.1 Experimental setup and survival of antigen exposed CD4$^+$ T cells

The transgenic mouse models described enabled us to address the role of persisting antigen presentation beyond the priming phase on CD4$^+$ T cells in a dose- and time-dependent manner within an otherwise sterile environment (Han et al., 2010; Obst et al., 2005). We compared naïve and memory AND T cells with those that were exposed to low, intermediate (int), or high antigen levels beyond the priming phase. To do so, we generated the above-mentioned conditions according to the treatment scheme depicted in Figure 10A.

iMCC and cMCC recipient mice were injected with 20 μg/mL α-CD40 mAb i.p. on day -1 to induce DC maturation as described before (Bonifaz et al., 2004; Hawiger et al., 2001; Kerksiek et al., 2005; Obst et al., 2007; Shakhar et al., 2005). Dox treatment of iMCC recipient mice was started on the same day. Mice were fed with high dose dox (100 μg/mL) in the drinking water to establish antigen presentation in recipient mice. 1 x 10^6 naïve AND T cells were adoptively transferred on the next day (day 0). High dose dox was administered until three dpt to ensure that all AND T cells were primed the same way. Memory AND TCR-tg CD4$^+$ T cells were generated by switching off antigen presentation by dox removal three dpt (Obst et al., 2007). The same day dox was either changed to the low dose (10 μg/mL) or was maintained on the high dose (100 μg/mL) to present low and intermediate antigen levels beyond the priming phase, respectively. Dox water was changed every three to five days. In the cMCC model there is constitutive high presentation of antigen and thus no dox treatment required. For the “naïve” condition 1 x 10^6 naïve AND T cells were transferred into wild type (wt) mice three days before analysis. This was necessary as AND T cells disappear from recipients in the absence of antigen (Obst et al., 2007), a phenomenon described for other TCRs as well (Hataye et al., 2006). Recipient spleens and lymph nodes (LNs) were harvested and analyzed 10 dpt. In the following work I refer to AND T cells generated in the above described way as “naïve”, “memory

(mem)", "low", "intermediate (int)", and "high" AND T cells, actually describing the amount of antigen they were exposed to beyond the priming phase.

Naïve, memory, low, intermediate, and high AND T cells were isolated and analyzed from the spleen (Figure 10B, C) and LNs (data not shown) of recipient mice, demonstrating the survival of AND CD4+ T cells chronically stimulated by cognate antigen of varying dose and time. In general LN cells showed similar marker expression compared to splenocytes.

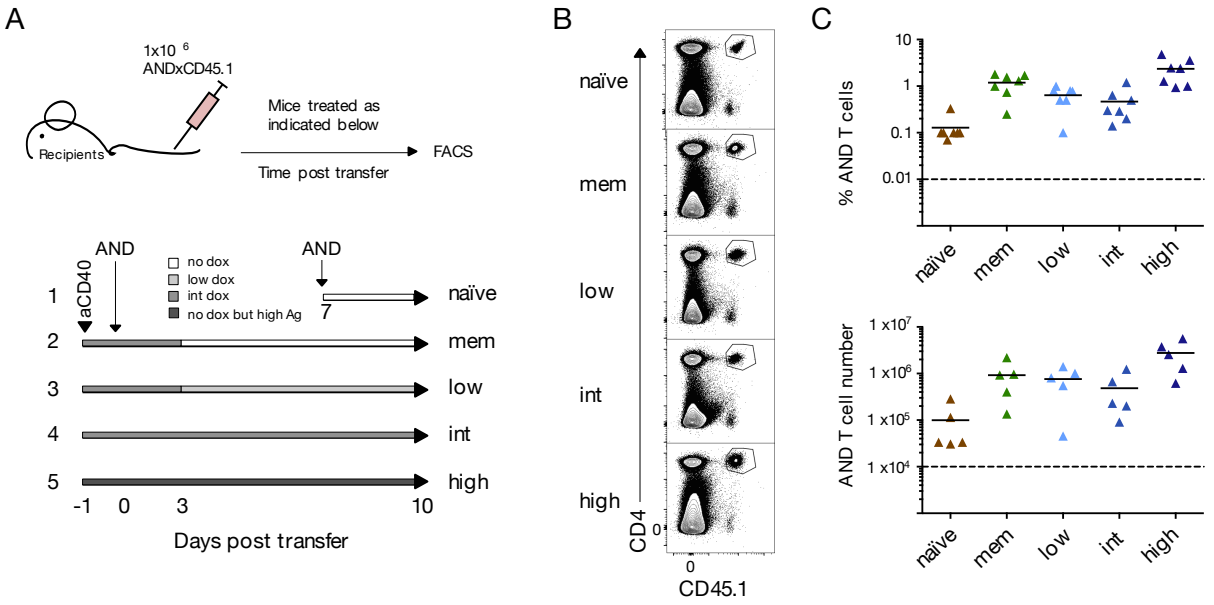

Figure 10: AND T cell survival in MCC-transgenic recipients with persistent antigen presentation of different quantity analyzed on day 10. (A) Schematic outline of the general treatment strategy to generate naïve, memory, low, intermediate (int), and high AND T cells. Recipient mice were injected with 20 μg α-CD40 antibody to induce DC maturation and were treated with dox in the drinking water as indicated to induce antigen presentation one day before adoptive cell transfer of 1 x 10^6 AND T cells. Dox treatment was continued as indicated and changed every three to five days. Spleens were harvested 10 dpt. (B, C) Quantification of adoptively transferred AND T cells using flow cytometry following the gating strategy described in Figure 8A. (B) Representative cytometric plots identifying AND T cells. (C) Graphs show percentage and absolute numbers of AND T cells. Data are shown of five independent experiments; each data point represents one mouse. Memory (mem), low, intermediate (int), and high represents the dose of antigen AND T cells have seen beyond the priming phase as schemed in Figure 10A.

4.2.2 CD4+ Tmem phenotype is hampered early by persisting antigen

We determined surface marker expression by flow cytometry to phenotype AND CD4+ T cells upon encountering low, intermediate, and high levels of cognate antigen chronically (Figure 11). We found the TCR being downregulated exclusively by very high TCR stimulation. CD44 expression was significantly upregulated in all four antigen-presenting conditions indicating AND T cells have seen their cognate antigen and have been activated. CD62L and the memory markers CD127 and Ly6C were expressed on memory ANDs but were significantly downregulated by antigen persistence. Especially, Ly6C surface expression, a marker of Tmem

cells (Tokoyoda et al., 2009) was reduced in a dose-dependent manner (Figure 11A and B). These results show that CD4+ T cells are able to sense and respond differently to increasing amount of antigen after the priming phase.

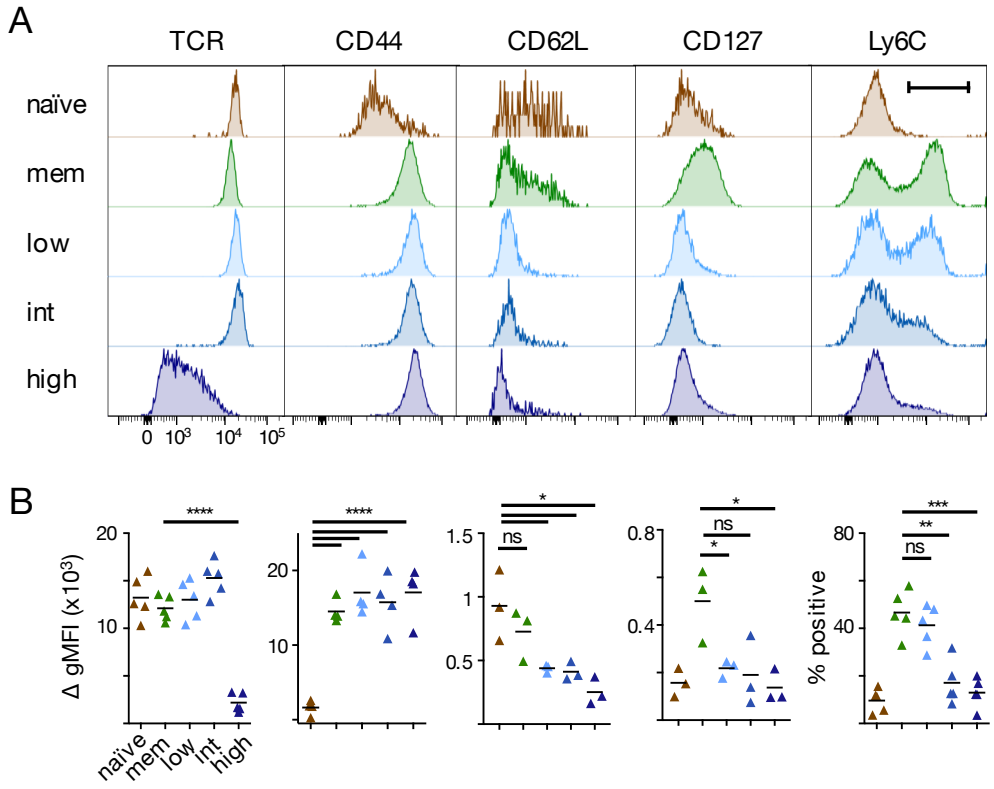

Figure 11: Persisting antigen induces phenotypic changes in specific CD4+ T cells that indicate a dose-dependent loss of memory phenotype. (A, B) Quantification of 1 x 10^6 adaptively transferred AND T cells using flow cytometry. Spleens and LNs were harvested 10 days post transfer. AND T cells shown were identified using the gating strategy described in Figure 8A. (A) Representative histograms showing surface marker expression of AND T cells exposed to increasing amounts of antigen isolated from the spleen. (B) Statistical quantification of surface marker expression. Delta geometrical means were calculated by $gMFI_{Sample}$ - $gMFI_{isotype\ control}$. Data were pooled from at least three independently performed experiments, each data point represents one mouse. *$p < 0.05$, **$p < 0.001$, ***$p < 0.0001$, ns = not significant (parametric unpaired two-tailed t-test). Memory (mem), low, intermediate (int), and high represents the dose of antigen AND T cells have seen beyond the priming phase as depicted in Figure 10A.

4.2.3 Persisting high-dose antigen stimulation causes TCR downregulation

TCR downregulation is an aspect of *in-vitro* T cell activation (Salio et al., 1997; Valitutti et al., 1995b; Viola and Lanzavecchia, 1996) and is induced by TCR/pMHC engagement (Valitutti et al., 1995a; Valitutti et al., 1996; Zanders et al., 1983), especially by high affinity peptides (Cai et al., 1997). Degradation of TCR-CD3 complex is seen as a control mechanism to down-regulate TCR surface expression, though the biological relevance is still unclear (Alcover et al., 2018; Valitutti, 2012).

We have shown that TCR down-modulation is induced *in vivo* by very high antigenic stimulation only (Figure 9B, 11A). We then asked whether TCR downregulation in cMCC recipients (Figure

11A) is caused by TCR degradation or whether the TCR complexes are internalized and maintained intracellularly. We measured intracellular TCR abundance of memory, intermediate and high AND T cells by flow cytometry. To this end we fixed, permeabilized, and stained the cells for intra- and extracellular TCR β-chains and compared total (extracellular (EC) + intracellular (IC)) with surface (extracellular) TCR abundance. An eight-fold increase of TCR was found in the spleen and a 23-fold increase in the LNs of cMCC recipient mice (Figure 12A). Total TCR levels of high AND T cells were similar to that of memory and intermediate AND T cells, indicating that TCR complexes are not degraded but maintained in intracellular compartments. These findings have been reproduced by Shu-Hung Wang, a master student in our laboratory. He could also show that TCR surface expression was recovered after an overnight rest in the absence of antigen *in vitro* (data not shown).

In cMCC animals, the MCC/E^k epitope is expressed not only in DCs but also in B cells (data not shown). To exclude that TCR downregulation is induced by antigen presenting B cells in these mice, we crossed them to the $RAG^{0/0}$ background. These $cMCC^+RAG^{0/0}$ mice lack the recombination-activating gene (RAG) enzyme RAG-2 and, therefore, lack the endogenous B and T cell pools and thus exhibit lymphopenia. We performed adoptive AND T cell transfer into such $cMCC^+RAG^{0/0}$ recipients and harvested the spleens 10 dpt. The T cells downregulated the TCR surface expression to a similar extent under lymphopenic conditions (Figure 12B). To exclude that lymphopenia itself caused the downregulation we took advantage of $cMCC^+CD3^{0/0}$ animals that exclusively lack the endogenous T cell pool and do harbor antigen presenting B cells. Also, under such T lymphopenic conditions TCR/CD3 complexes are comparably downregulated (Figure 12B). These results indicate that TCR downregulation is B-cell- as well as lymphopenia-independent and is rather induced by chronic antigen presentation at a high level. We tried to trigger TCR complex downregulation in AND T cells persistently exposed to intermediate amount of antigen in iMCC recipient mice by increasing the likelihood of AND T cells to interact with mature antigen presenting DCs. To this end, iMCC recipients were crossed to $RAG^{0/0}$ background. Within dox treated (100 μg/mL) and with anti-CD40 mAb injected (20 μg) $iMCC^+RAG^{0/0}$ lymphopenic recipients transferred ($1x10^6$) AND T cells encounter continuously mature DCs presenting cognate antigen in absence of any endogenous T cells competing for DC interactions. Such increased frequency of MCC-presenting cells failed to trigger the downregulation of surface TCRs on intermediate AND T cells (Figure 12 right part, bottom row). Memory and intermediate AND T cells served as positive and high AND T cells served as negative controls. These data demonstrate that lymphopenia itself does not affect TCR complex downregulation. Taken together, these findings reveal that AND $CD4^+$ T cells down-regulate their TCR surface expression in response to a high antigen stimulation in a B cell-independent manner.

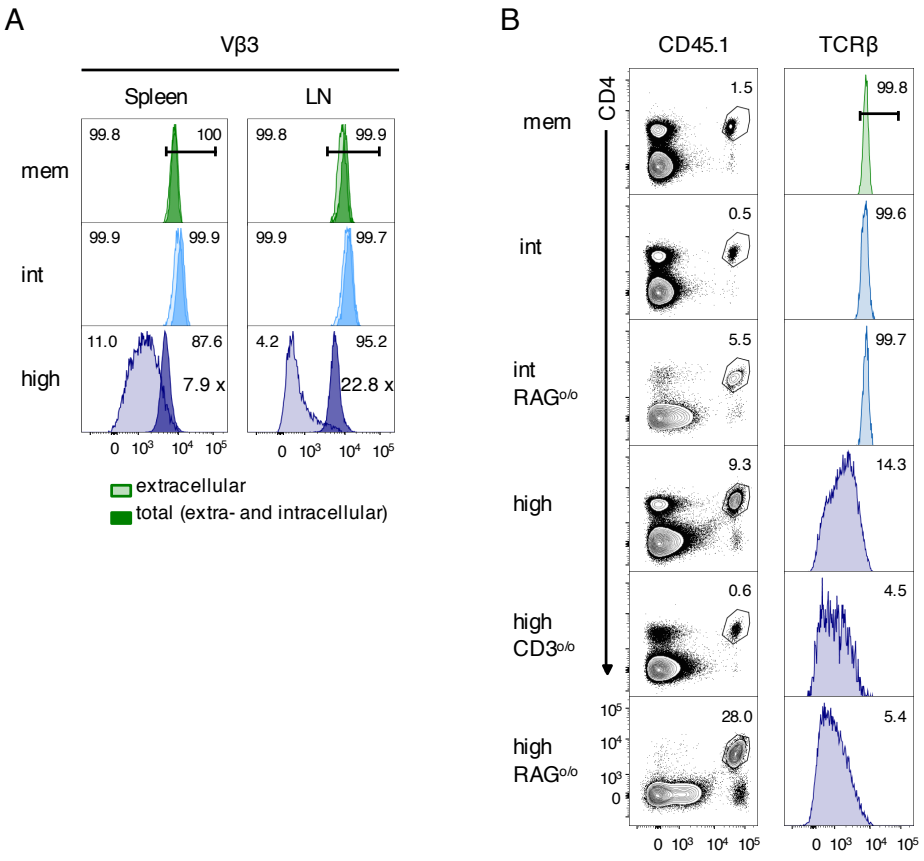

Figure 12: High quantity TCR stimulation drives TCR downregulation on antigen specific CD4⁺ T cells. (A, B) Quantification of 1 x 10^6 adaptively transferred AND T cells using flow cytometry. Organs were harvested 10 days post transfer, AND T cells shown were identified following the gating strategy described in Figure 8A. (A) Histograms showing extracellular and total (extra- plus intracellular) TCR (Vβ3) expression of AND T cells exposed to increasing amounts of antigen *in vivo*. Numbers indicate the percentage of AND T cells positive for TCR expression, top left: extracellular TCR, top right: total (intra- plus extracellular) TCR. (B) Flow cytometric quantification of TCR (Vβ3) surface expression of AND T cells isolated from the transgenic recipients, indicated data are from one experiment. Memory (mem), low, intermediate (int), and high represents the dose of antigen AND T cells have been exposed to after the priming phase as depicted in Figure 10A, RAG$^{o/o}$ and CD3$^{o/o}$ describe the recipients additional background genotype.

4.2.4 Persisting antigen anergizes CD4⁺ T cell effector functions

Exhaustion is a state of T cell dysfunctionality caused by persistent viral infections and cancer (Doering et al., 2012; Schietinger and Greenberg, 2014; Wherry, 2011). As a hallmark of exhaustion, CD8⁺ T cells show impaired effector functions in terms of cytokine production and cytotoxicity and increased expression of inhibitory receptors (Doering et al., 2012; Schietinger and Greenberg, 2014; Wherry, 2011). Less is known about CD4⁺ T cells under such chronic conditions. We investigated CD4⁺ T cell functionality 10 days after persistent presentation of different amounts of antigen. To do so, we generated naïve, memory, low, intermediate, and high AND T cells as described in Figure 10A and re-stimulated splenocytes from recipients with PMA/IM and Brefeldin A as depicted in Figure 13A. After *in vitro* re-stimulation intracellular

cytokines were measured by flow cytometry. In contrast to naïve T cells, memory T cells expressed significant amounts of effector cytokines, such as IL-2, TNF-α, and IFN-γ (Figure 13B, C). In response to persistent antigen-presentation AND T cells showed significantly impaired IL-2 production by all three different doses of antigen. TNF-α and IFN-γ production was significantly reduced by intermediate- and high-level antigen and showed a trend of reduction by low level TCR stimulation (Figure 13B, C). These results indicate that chronic antigen presentations impair effector functions in a dose-dependent fashion.

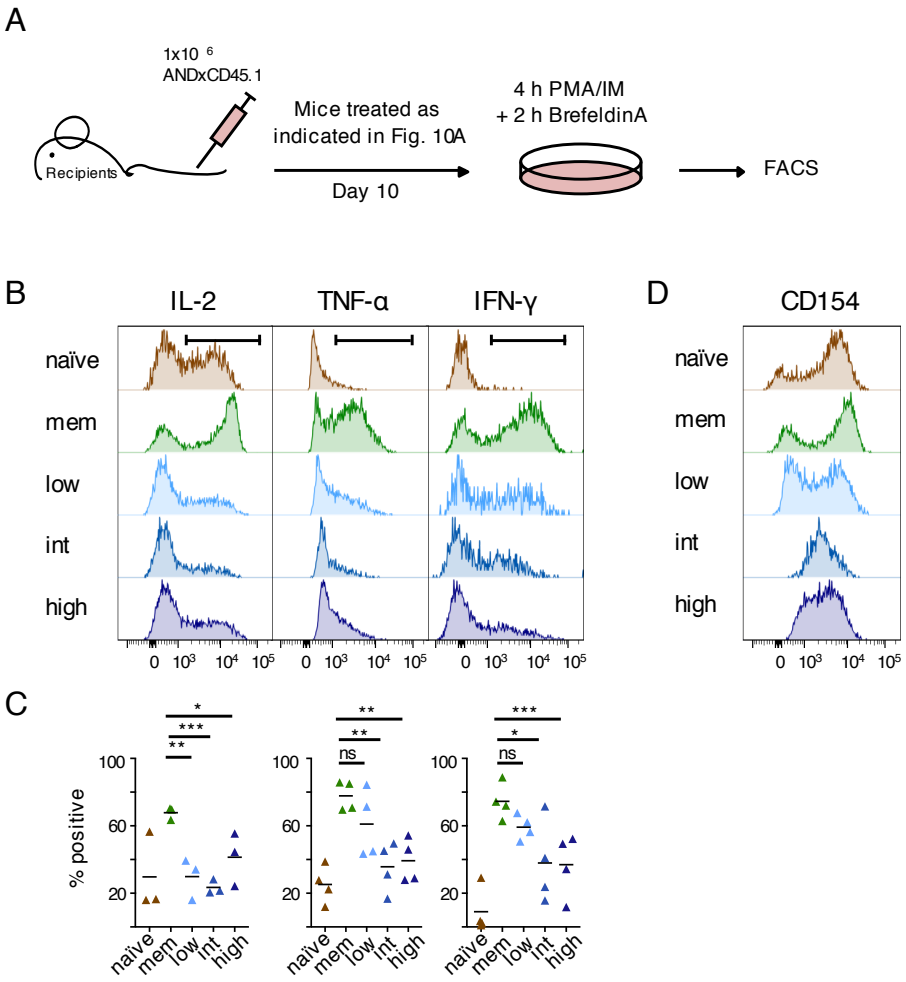

Figure 13: Effector function of antigen specific CD4+ T cell is hampered rapidly upon chronic TCR stimulation. (A) Schematic outline of the experimental set up. (B – D) Quantification of 1 x 10^6 adaptively transferred AND T cells using flow cytometry. Spleens were harvested 10 days post transfer, splenocytes were re-stimulated with PMA/IM for 4 h, Brefeldin A was added after 2 h of stimulation. AND T cells shown were identified using the gating strategy described in Figure 8B. (B) Representative histograms showing intracellular cytokine expression. (C) Statistical quantification of cytokine expression pattern. Delta geometrical means were calculated by $gMFI_{Sample}$ - $gMFI_{isotype\ control}$. Data were pooled from at least three independently performed experiments, each data point represents one mouse. *p < 0.05, **p < 0.001, ***p < 0.0001, ns = not significant, parametric unpaired two-tailed t-test. (D) Flow cytometric analysis for total CD154 (CD40L) expression. Data shown from one experiment. Memory (mem), low, intermediate (int), and high represents the dose of antigen AND T cells have seen beyond the priming phase as schemed in Figure 10A.

Professional APCs communicate with T cells via the CD40/CD40L route (Foy et al., 1996; Schrader et al., 1997). CD40L expression is induced upon T cells activation, transmits co-

stimulatory signals and thus contributes to proper T cell activation and induction of effector function (Grewal and Flavell, 1998; Kennedy et al., 1994; Ranheim and Kipps, 1993). Due to its rapid turnover induced by engagement with CD40 (Graf et al., 1995), we measured total (intra- and extracellular) CD40L (CD154) expression of AND T cells, persistently exposed to different amounts of antigen beyond the priming phase, using *in vitro* re-stimulation with PMA/IM and Brefeldin A (Kirchhoff et al., 2007). We found that the induction of CD40L expression was dose-dependently reduced in low, intermediate, and high $CD4^+$ T cells compared to naïve and memory $CD4^+$ T cells in respond to PMA/IM stimulation *in vitro* (Figure 13D). This suggests that chronic hyper-stimulations reduced the co-stimulatory signals transduced via CD40/CD40L pathway of cell communication. Yet, this is a preliminary finding that is currently reproduced in our laboratory.

As we have shown that in high AND T cells TCR surface expression rapidly recovers after overnight (o/n) rest in absence of antigen *in vitro* (described above) we asked if such rescued TCRs are responsive to TCR stimulation and are able to produce the effector cytokine IFN-γ triggered by TCR/pMHC interactions *in vitro*. To this end, Stefanie Pennavaria rested naïve, memory, and high AND T cells *in vitro* o/n and re-stimulated them with both, either PMA/IM bypassing the TCR as a control or B cells plus cognate antigen $MCC_{88\text{-}103}$ for four h in the presence of Brefeldin A during the last two h of stimulation. She showed that rested high AND T cells that had regained their TCR surface levels still fail to produce IFN-γ, despite the fact that their PMA/IM stimulated counterparts did do so (data not shown). Her data indicate that the TCR signal transduction pathway after o/n rest *in vitro* is still impaired proximal to the TCR.

4.3 TCR signal transduction following chronic TCR stimulation

4.3.1 Chronic high-dose TCR stimulation impairs TCR signal transduction

Upon TCR stimulation the protein tyrosine kinase ZAP-70 is activated and phosphorylates the transmembrane protein linker for activation of T cells (LAT) (Au-Yeung et al., 2018; Paz et al., 2001). LAT has a central role in TCR signal transduction as it recruits other adapter proteins and signaling molecules upon phosphorylation (Paz et al., 2001). Since we assume that chronically high dose antigen stimulations impaired TCR signaling proximal to the TCR we asked whether LAT expression was affected and compared intracellular LAT expression levels of memory, low, intermediate, and high AND T cells. We found LAT abundance being significantly reduced in high AND T cells only (Figure 13A). LAT reduction thus is correlated with TCR downregulation and might be involved in impaired TCR function. Data shown in Figure 24 will show that LAT is downregulated transcriptionally.

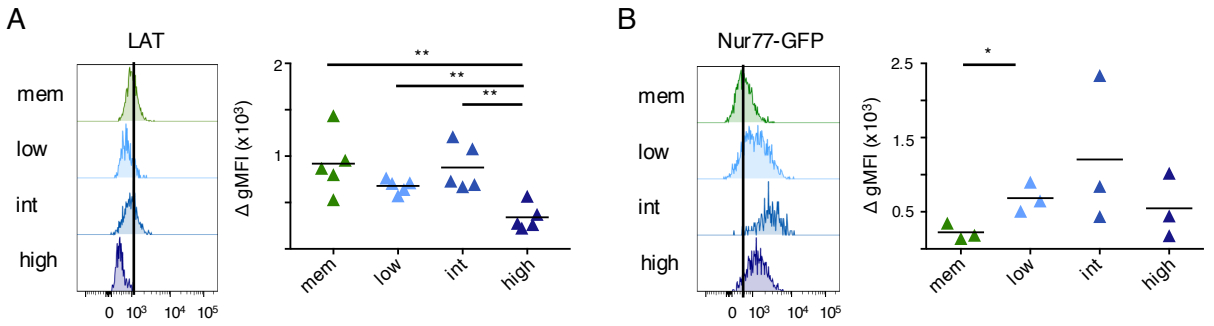

Figure 14: Chronic TCR stimulation of high quantity impairs TCR signal transduction. (A, B) Quantification of 1 x 10^6 adaptively transferred AND T cells using flow cytometry. Spleens were harvested 10 days post transfer. AND T cells shown were identified using the gating strategy described in Figure 8A. (A) Representative histograms showing intracellular LAT expression *ex vivo* on the left. Statistical quantification of LAT expression on the right. (B) Quantification of TCR signal transduction using Nur77-GFP reporter expression in ANDxNur77 T cells *ex vivo*. Representative histograms on the left and statistical analysis on the right. Delta geometrical means were calculated by (A) $gMFI_{sample}$ - $gMFI_{isotype\ control}$ and (B) $gMFI_{GFP\text{-}reporter}$ – $gMFI_{non\text{-}reporter\ AND}$. Data were pooled from (A) five and (B) three independent experiments, each data point represents one mouse. *$p < 0.05$, **$p < 0.001$, parametric unpaired two-tailed t-test. Memory (mem), low, intermediate (int), and high represents the dose of antigen AND T cells have seen beyond the priming phase as schemed in Figure 10A.

Next we asked whether all three conditions of chronic TCR stimulation are able to induce chronic TCR signals. Especially high dose TCR stimulation, which causes TCR downregulation and LAT reduction, is of interest, since it is unclear if internalized TCR complexes can still transmit TCR signals (Rothenberg, 1996; Saveanu et al., 2019). To measure TCR signal strength we used the Nur77-GFP reporter (Moran et al., 2011). Memory, low, intermediate, and high AND T cells were generated as described in Figure 10A, except that ANDxNur77 GFP-reporter T cells were co-transferred with non-reporter GFP-negative ANDx90.1 T cells. To exclude background signals measured GFP signals of reporter-negative AND T cells were subtracted from the values measured for GFP-reporter positive AND T cells. Spleens were harvested and analyzed by flow cytometry 10 dpt. GFP expression was increased in all three chronic conditions compared to memory ANDxNur77 T cells (Figure 13B). Interestingly, high AND T cells with internalized TCRs and reduced LAT expression levels, reported TCR signal transduction by induced Nur77-GFP expression. These findings suggest that TCR signal transduction is induced by persisting antigen-presentation of all three levels.

4.3.2 Calcium ion release and nuclear NFATc1 translocation by persisting antigen

Upon TCR stimulation T cells release Ca^{2+} ions from intracellular stores and the cellular environment to initiate activation programs (Baine et al., 2009; Hogan et al., 2010; Zhang et al., 2005). T cells chronically exposed to intermediate dose of antigen are able to flux Ca^{2+} (Han et

al., 2010), indicating that this pathway is not affected by intermediate levels of antigen. Whether high AND T cells are also able to induce Ca^{2+} flux is unclear. We thus asked whether Ca^{2+} flux-dependent pathways are also still intact. Ca^{2+} flux potential of rested high AND T cells was measured in our laboratory by Shu-Hung Wang. He showed that rested high AND T cells were not able to flux Ca^{2+} in response to TCR engagement (achieved by α-CD3/CD4 cross-linking with streptavidin). Ca^{2+} fluxes were not detectable after an o/n rest *in vitro,* nor after two days of rest *in vivo* accomplished by a secondary transfer into antigen-free hosts. These results indicate that Ca^{2+} flux is a rather robust pathway but rendered dysfunctional by the high dose of persisting antigen.

Upon Ca^{2+} influx, calcium ions bind to calmodulin and activate the protein phosphatase calcineurin (Klee et al., 1998). Activated calcineurin dephosphorylates the transcription factor NFATc1, a member of the NFAT family of Ca^{2+}-dependent transcription factors, and thus enables NFAT translocation from the cytoplasm to the nucleus (Martinez et al., 2015). In the nucleus NFAT cooperates with AP-1 (a heterodimer of Fos and Jun) to induce the transcription of effector genes. Recently it has been reported that NFAT, in cooperation with AP-1, favors T cell differentiation towards a memory phenotype and in absence of AP-1 towards an exhaustion-associated phenotype (Martinez et al., 2015). Hence, we investigated whether nuclear NFATc1 translocation was induced by chronic TCR stimulation. We first performed a pilot experiment to analyze NFATc1 translocation induced by PMA/IM stimulation *in vitro* using imaging flow cytometry (Figure 15A). AND T cells were transferred into wt mice to mimic later experimental conditions. Three days post transfer, splenocytes were either stimulated with PMA/IM *in vitro* or left untreated. NFATc1 was located in the cytoplasm of unstimulated $CD4^+$ T cells (Figure 15B, left part) and showed nuclear translocation upon PMA/IM stimulation (Figure 15B, right part), visualized by NFATc1 staining (green) surrounding the nucleus stained with Draq5 (red) in unstimulated cells. Following T cell stimulation, both markers overlapped in the nucleus (see merge) and demonstrated the nuclear translocation of NFATc1.

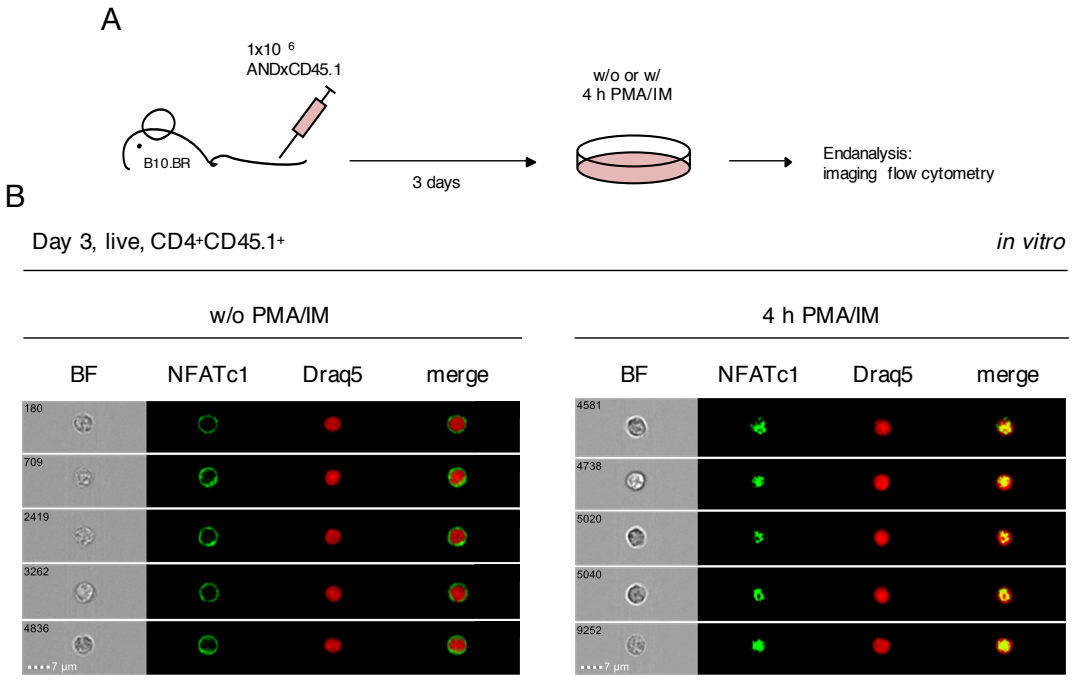

Figure 15: NFATc1 in PMA/IM stimulated CD4+ T cells localizes to the nucleus. (A) Schematic outline of the experimental set-up. As a pilot experiment to visualize nuclear NFATc1 translocation in response to PMA/IM stimulation *in vitro*, 1x 10^6 AND T cells were transferred into B10.BR wild type recipients to mimic the later experimental procedure. The spleen was harvested three days post transfer, splenocytes were isolated, and stimulated with (w/) PMA/IM for 4 h *in vitro* or left untreated (w/o). (B) Representative imaging-flow-cytometry images show examples of cytoplasmic NFATc1 (left) or nuclear NFATc1 (right). T cells shown were gated on singlets, live, CD4+CD45.1+, nuclear dye (Draq5) and NFATc1 double positive and autofluorescence negative cells. BF = bright field image, NFATc1 staining (green), nuclear dye Draq5 (red), merged overlap (yellow), scale bar: 7 μm.

We then compared memory, low, intermediate, and high CD4+ T cells with regard to nuclear NFATc1 translocation caused by chronic antigen stimulations *in vivo*. AND T cells were generated as described in Figure 10A, splenocytes were isolated on day 10 post transfer and fixed immediately *ex vivo* to prevent NFATc1 cytoplasmic relocation (Figure 16A). Comparisons of cellular NFATc1 expression levels indicated no difference in NFATc1 abundance under all four conditions (Figure 16B). NFATc1 expression is induced by T cell activation and apparently not affected by antigen persistence. However, looking at NFATc1 location within the cell compartments we found a significant increase of NFATc1 in the nucleus correlating with antigen dose. Interestingly, high ANDs showed the highest nuclear NFATc1 abundance (Figure 16C, D). These data imply that persisting TCR stimulation induces tonic TCR signal transduction that leads to nuclear NFATc1 translocation in a dose-dependent fashion. It is currently unclear whether TCR molecules send signals from the surface or endocytic compartments in the iMCC recipients (Saveanu et al., 2019).

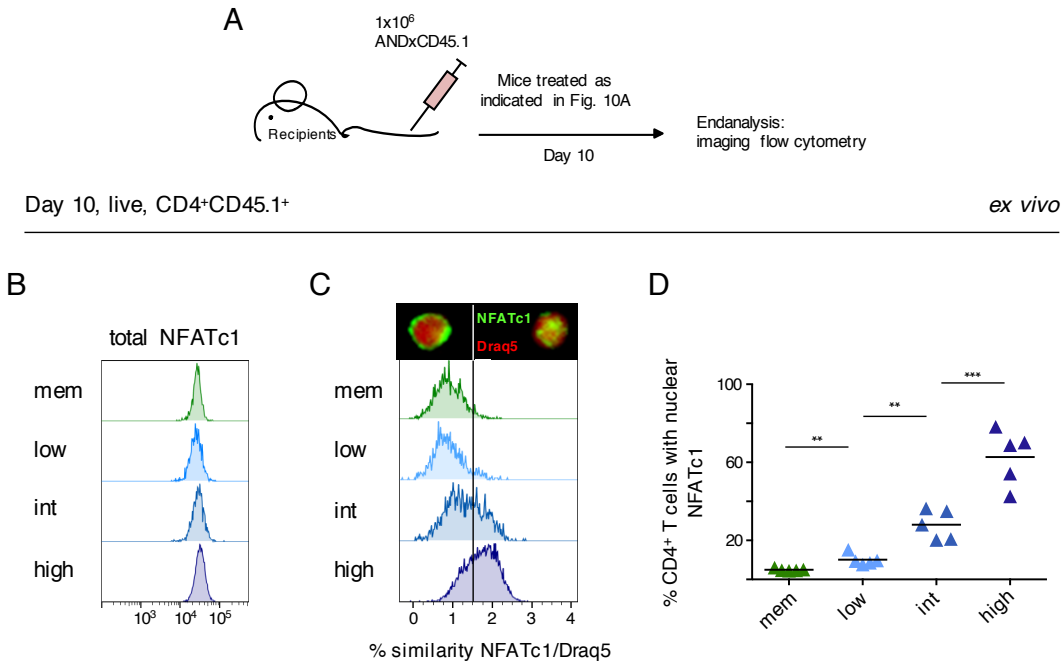

Figure 16: Chronic TCR stimulation causes dose-dependent nuclear NFATc1 translocation. (A) Schematic outline of the experimental set up. (B – D) Quantification of 1 x 10^6 adoptively transferred AND T cells using imaging flow cytometry. Memory, low, int, and high AND T cells were generated as described in Figure 10A. Spleens were harvested 10 days post transfer, splenocytes were fixed immediately *ex vivo*. T cells shown were gated on singlets, live, $CD4^+CD45.1^+$, nuclear dye (Draq5) and NFATc1 double positive and autofluorescence negative cells. (B) Representative histograms of total intracellular NFATc1 expression of the same experiments also analyzed in C and D. (C) Representative histograms on NFATc1 translocation. Co-localization of NFATc1 (green) and nuclear marker Draq5 (red) was calculated using the similarity feature implemented in the IDEAS analysis software to identify cells with NFATc1 located to the nucleus. A similarity score less than 1.5 represents cells with predominantly cytoplasmic NFATc1, while a score larger than 1.5 represents cells with predominantly nuclear NFATc1 location. On top of the histograms are two representative images of AND T cells with cytoplasmic NFATc1 (left) and nuclear NFATc1 location (right). Vertical line indicates the similarity score of 1.5. (D) Statistical quantification of AND T cells with nuclear NFATc1 location indicated by the percentages of cells with a similarity score larger than 1.5. Data were pooled from five independent experiments; each data point represents one mouse. **p < 0.001, ***p < 0.0001, parametric unpaired two-tailed t-test. Memory (mem), low, intermediate (int), and high represents the dose of antigen AND T cells have seen beyond the priming phase as schemed in Figure 10A.

Th1 effector cell differentiation is established during the initial T cell priming phase and is influenced by certain factors, such as antigen dose (signal 1), co-stimulatory signals transmitted by CD28 (signal 2), and cytokine environment (signal 3) (Constant and Bottomly, 1997). TCR stimulation activates the JNK/MAP kinase signaling pathway which controls the Th1 effector response (Ip and Davis, 1998; Whitmarsh and Davis, 1996; Yang et al., 1998) by inducing certain gene expression, such as the expression of *Il2*. Upon activation the JNK kinase phosphorylates its substrate c-Jun (Rincon and Flavell, 1994). Jun and Fos family members form heterodimers described as activator protein 1 (AP-1) and act as transcription factors (Foletta et al., 1998; Nakabeppu et al., 1988; Rincon and Flavell, 1994). Transcriptional activity of AP-1 depends on TCR stimulation and co-stimulation e.g. transmitted by CD28/B7.1 or B7.2 interaction (Rincon and Flavell, 1994) and on its DNA binding partners, such as NFAT proteins

(Jain et al., 1995; Jain et al., 1993; Rooney et al., 1995). Cooperative NFAT:AP-1 complexes are associated with $CD8^+$ T cell effector function and the induction of activation-induced genes (Martinez et al., 2015). In contrast, in absence of AP-1 NFAT homodimers drive exhaustion- and anergy-associated $CD8^+$ phenotypes by inducing exhaustion-related gene expression patterns (Martinez et al., 2015). Hence, we investigated Jun phosphorylation induced by chronic TCR stimulations of different antigen doses compared to naïve and memory AND T cells. These experiments were performed in our laboratory by Benedikt Lober. He found that upon additional TCR stimulation *in vivo* by injecting cognate antigen $pMCC_{88\text{-}103}$ for 1 h 10 dpt, high AND T cells were not able to phosphorylate and thus to activate c-Jun, whereas naïve, memory, and intermediate AND T cells did (data not shown). However, over time, chronic TCR stimulation of intermediate dose also impaired Jun phosphorylation, as 31 days post T cell transfer significantly reduced Jun phosphorylation in response to $pMCC_{88\text{-}103}$ injection for 1 h was reported (Han et al., 2010). Together, these findings suggest that high AND T cells with significantly reduced TCR surface expression could not activate the JNK/MAPK pathway and therefore lack the AP-1 transcription factor in the nucleus. As a result, partner-less NFATc1 may induce an altered gene-expression pattern.

4.4 Characterization of AND T cells exposed to antigen for 30 days

4.4.1 Experimental set-up and survival of AND T cells

To analyze the effects of antigen persistence on $CD4^+$ T cells over a truly chronic period of time we followed AND T cells for 30 days. We analyzed naïve, memory, low, intermediate, and high AND T cells on day 30 pt and included an additional condition where intermediate AND T cells were released from antigen on day 10 pt by switching off dox treatment and thus shutting down antigen presentation (int off) (Figure 17A).

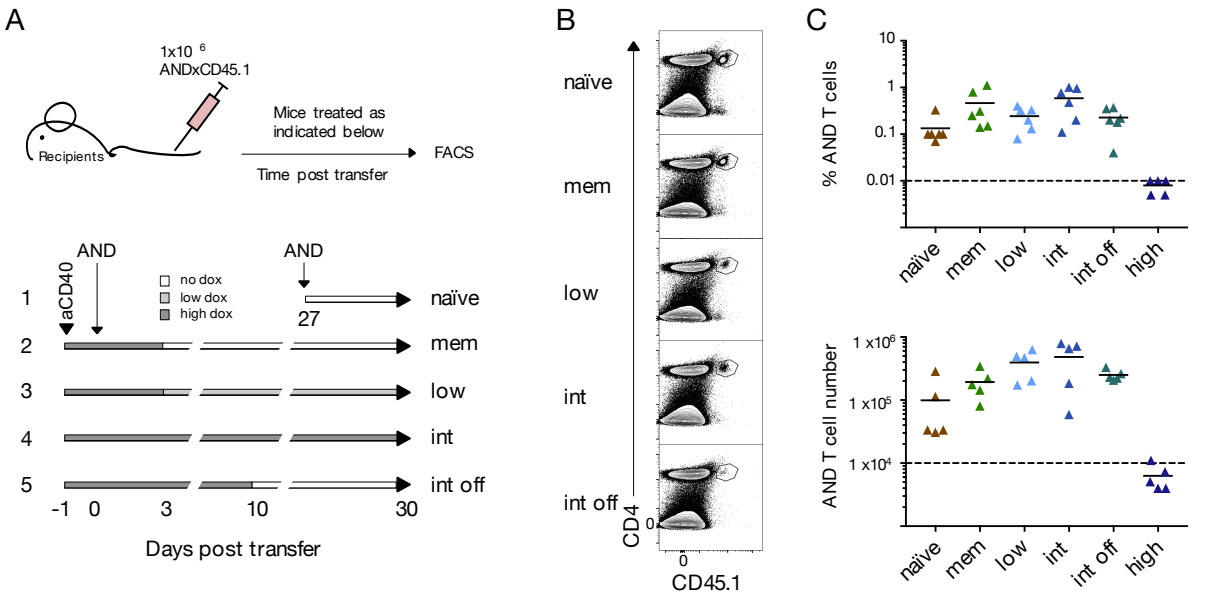

Figure 17: Long-term survival of AND T cells during chronic antigen stimulation and upon antigen removal in iMCC-transgenic recipients analyzed on day 30. (A) Schematic outline of the dox treatment to generate naïve, memory, low, intermediate (int), and intermediate off (int off) AND T cells analyzed 30 days post transfer (dpt). Recipient mice were treated with high-dose dox (100 μg/mL) in the drinking water and injected with 20 μg α-CD40 antibody one day before adoptive T cell transfer. Three dpt, dox treatment was either switched off to generate memory AND T cells, changed to low dose (10 μg/mL) to generate low AND T cells, or maintained on high dose (100 μg/mL) for int and int off ANDs. Int ANDs were continuously feed with high-dose dox. To generate int off AND T cells, mice were taken off dox treatment 10 dpt. Dox-water was changed regularly each three to five days. (B, C) Quantification of adoptively transferred AND T cells isolated from recipient spleens using flow cytometry. AND T cells shown were identified using the gating strategy described in Figure 8A. Recipient mice were treated as indicated in (A). Representative data of at least five independent experiments. (B) Identification of transferred AND T cells on day 30. (C) Graphs show percentage and absolute numbers of AND T cells 30 dpt.

All mice were injected with α-CD40 i.p. and fed with dox water (100 μg/mL) the day before adoptive T cell transfer (1 x 10^6 AND T cells). Dox treatments were continued as indicated in Figure 17A. Using the intermediate off condition we asked if the antigen-exhausted phenotype on day 10 can be reversed by antigen removal or whether it is rather irreversibly programmed. Analyses by cytometry on day 30 pt revealed that high AND T cells were hardly detectable as they appeared below the detection rate (less than 0.01%) (Figure 17C) leading to the suspicion that cell death is induced by high-level antigen stimulation. Hence, we excluded the high AND T cells from further day 30 experiments. Memory, low, intermediate, and intermediate off AND T cells were detectable 30 days post transfer (Figure 17B, C).

4.4.2 CD4$^+$ Tex cells recover upon antigen removal

When we analyzed the expression pattern of surface markers on day 30 by flow cytometry, we found CD44 expression still high upon antigen encounter, proving the recognition and activation

by cognate antigen. The homing receptor CD62L (Smalley and Ley, 2005) was expressed on naïve and memory CD4+ T cells but downregulated on antigen-exhausted T cells. Memory markers CD127 (IL-7 receptor alpha chain) (Huster et al., 2004; Wherry et al., 2003b) and Ly6C (Hale et al., 2013; Hanninen et al., 2011; Tokoyoda et al., 2009) were expressed on memory CD4+ T cells but were reduced by low and intermediate dosages of antigen persisting (Figure 18A). The expression of antigen sensitive markers, such as CD62L, CD127, and Ly6C tend to be reversible upon antigen-removal.

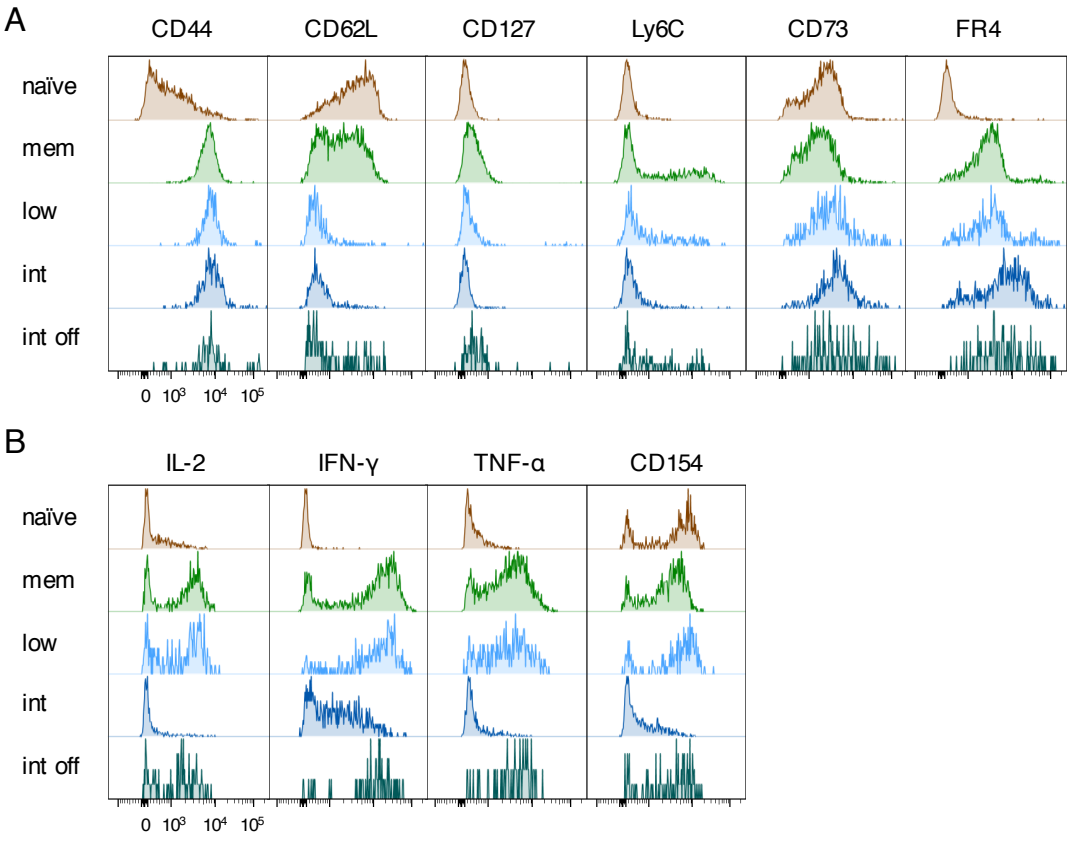

Figure 18: Characterization of chronically exhausted AND T cells upon persisting exposure to low and intermediate antigen doses in iMCC-transgenic recipients analyzed on day 30. (A, B) Quantification of 1 x 10^6 adoptively transferred AND T cells using flow cytometry. Spleens and LNs were harvested 30 days post transfer. Cells were generated as describes in Figure 16A. Naïve, memory (mem), low, intermediate (int), and intermediate off (int off) represents the time and dose of antigen AND T cells have seen beyond the priming phase. (A) Histograms showing surface marker expression of LN AND T cells. T cells shown were identified following the gating strategy described in Figure 8A. (B) Histograms showing intracellular cytokine expression of splenic AND T cells. Spleens were harvested 30 days post transfer, splenocytes were re-stimulated with PMA/IM for 4 h, Brefeldin A was added during the last 2 h of stimulation. T cells shown were identified using the gating strategy described in Figure 8B. Data are shown from one experiment.

To analyze the functionality of day 30 antigen-exhausted and rescued AND T cells we measured cytokine expression in response to *in vitro* re-stimulation with PMA/IM. Low dose of antigen

persistence resulted in a memory-like phenotype also shown by a cytokine-production profile similar to that of memory AND T cells. However, the intermediate dose of antigen impaired cytokine production (Figure 18B). Antigen removal on day 10 partially rescued this dysfunctional state, demonstrated by a cytokine-production profile comparable to the one of memory AND T cells (Figure 18B). These results suggest that the intermediate antigen-exhausted dysfunctional phenotype of CD4$^+$ T cells is reversible in terms of cytokine production. These data have recently been reproduced by Pallavi Kadam in our laboratory.

4.5 Transcriptome analysis of antigen-exhausted CD4$^+$ T cells

4.5.1 Sample preparation procedure to perform microarray analyses

In order to analyze dose-dependent gene-expression changes induced during early (day 10) and late (day 30) phase of antigen persistence we performed microarray analyses on the different conditions and time points. To this end, we generated five biological replicas of each condition (day 10 and day 30 samples), as described in Figure 10A and Figure 17A, respectively.

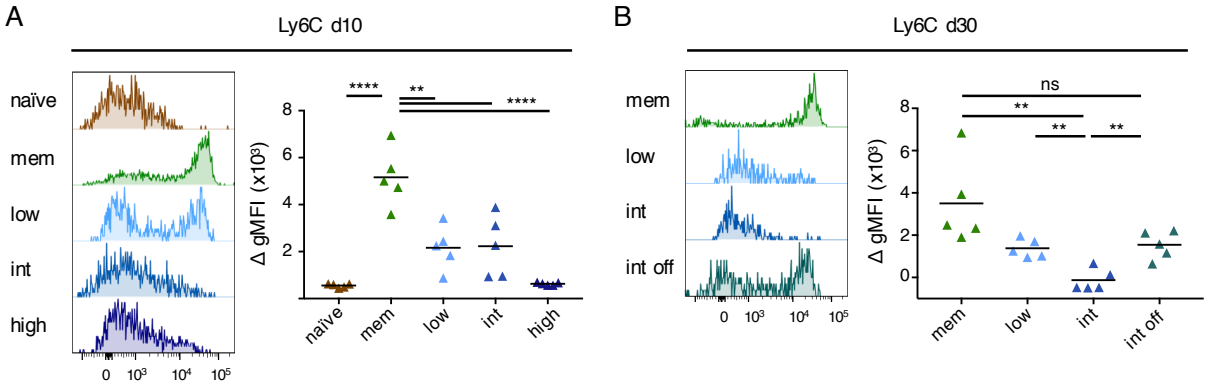

Figure 19: Characteristic Ly6C expression pattern validates the phenotypes of antigen-exhausted AND$^+$RAG$^{0/0}$ T cells at early (day 10) and late (days 30) time points for sorting. (A – D) Quantification of 1 x 10^6 adoptively transferred AND$^+$RAG$^{0/0}$ T cells using flow cytometry. Naïve, memory (mem), low, intermediate (int), intermediate off (int off), and high AND$^+$RAG$^{0/0}$ T cells were generated as described in Figure 10A and 17A respectively. Spleens and LNs were harvested, slenocytes and LN cells were pooled, Ly6C staining was performed for phenotype validation prior sorting these cells. AND$^+$RAG$^{0/0}$ T cells shown were identified following the gating strategy described in Figure 8A. (A) Representative histograms indicating Ly6C expression pattern of day 10 samples. (B) Statistical quantification of Ly6C expression on day 10 AND$^+$RAG$^{0/0}$ T cells. (C) Representative histograms indicating Ly6C expression pattern of day 30 samples. (D) Statistical quantification of Ly6C expression on day 30 AND$^+$RAG$^{0/0}$ T cells. Delta geometrical means were calculated by $gMFI_{sample}$ - $gMFI_{isotype\ control}$. Data were pooled from five independent experiments; each data point represents one mouse. ns = not significant, **$p < 0.001$, ***$p < 0.0001$, parametric unpaired two-tailed t-test.

Microarray analysis is a method to determine relative gene-expression changes. Using this technique, quantitative differences in RNA expression can be measured and compared between samples. Isolated RNA is converted to fluorescently labeled cDNA, which in turn is probed on the DNA-chip. The scanned fluorescence intensity of each gene is proportional to the gene-expression levels. Thus, the ratio between several fluorescent intensities can be used to measure relative gene-expression levels.

Phenotypes of $AND^{+}RAG^{0/0}$ T cells were confirmed by flow cytometry using Ly6C surface expression (Figure 19) before being used for microarray analyses. As expected, Ly6C was highly expressed by memory T cells on both, day 10 and day 30 samples and significantly reduced on the surface of chronically exposed T cells in a dose-dependent fashion. Rescued intermediate $AND^{+}RAG^{0/0}$ T cells (int off) showed significant increase in Ly6C surface expression compared to day 30 intermediate $AND^{+}RAG^{0/0}$ T cells. (Figure 19A – D). These results confirmed the expected phenotypes of the $AND^{+}RAG^{0/0}$ T cells to include these samples for microarray analyses accordingly.

$CD4^{+}$ T cells from all samples were negatively enriched and $AND^{+}RAG^{0/0}$ T cells were sorted twice to high purity and lysed in Trizol. Negative enrichment of $CD4^{+}$ T cells was performed by magnetic-activated cell sorting (MACS) as described in section 4.3.2.2. To do so, lymphocytes were pooled from spleen and LNs and were stained for “non-$CD4^{+}$-T-cell” markers using biotinylated mAbs. In a second step cells were bound via biotin to magnetic beads and small aliquots pre and post MACS were stained by streptavidin-PE (SA) to label cells to be depleted. Purity of MACS-enriched $CD4^{+}$ T cells was determined using the flow cytometric gating shown in Figure 20A. SA-labeled cells were successfully depleted as they were reduced from about 72% in pre-MACS samples to less than 2% in post MACS samples (Figure 20A).

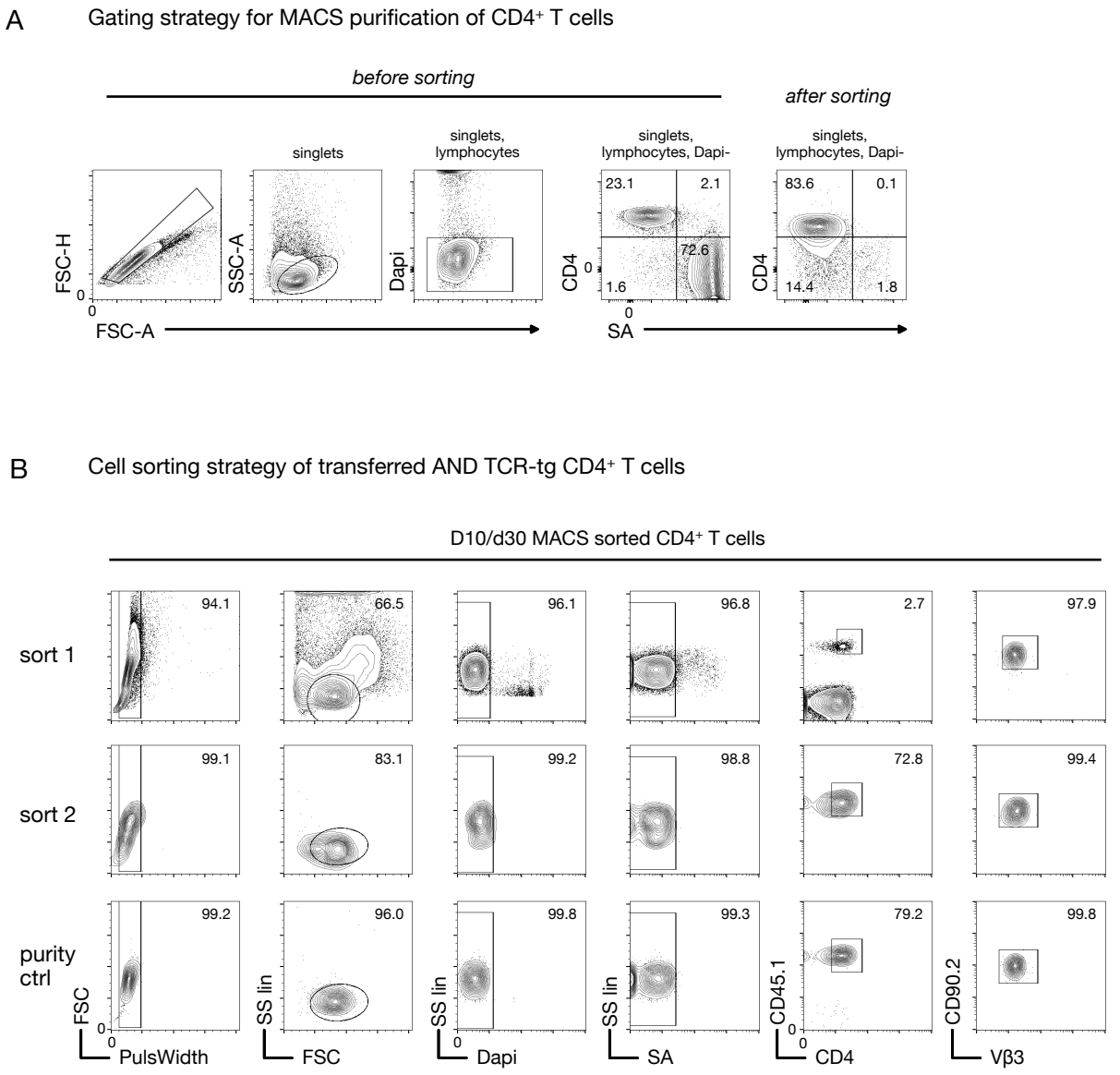

Figure 20: Representative sorting strategies and purity control of microarray samples. (A) Representative flow cytometric gating strategy of adoptively transferred AND^{+}RAG$^{0/0}$ T cells pre and post magnetic-activated cell sorting (MACS). Lymphocytes to be depleted were labeled by linage-specific biotinylated mAbs and identified by streptavidin-PE (SA). After cell sorting the SA positive cell population was depleted thus, CD4^{+} T cells were negatively enriched. (B) Representative gating strategy how AND^{+}RAG$^{0/0}$ T cells were flow cytometrically sorted from MACS purified CD4^{+} T cells and purity control of sorted AND^{+}RAG$^{0/0}$ T cells. Each sample was sorted twice (first and second row) to ensure the highest possible purity of sorted AND^{+}RAG$^{0/0}$ T cells. After the second sort cells were sorted into 500 μL Trizol for later analysis and a small aliquot of each sample was sorted into FACS buffer to check the purity of each sample (last row). AND^{+}RAG$^{0/0}$ T cells were identified and sorted as Dapi^{neg}SA^{neg}CD4^{+}CD45.1^{+}CD90.2^{+}Vβ3^{+}. All day 10 and day 30 samples for microarray analysis were sorted according to this strategy.

Subsequently, AND+RAG0/0 T cells were flow cytometrically sorted according to section 4.3.3.5 in cooperation with Mathias Schiemann and Lynette Henckel, TU München. For cell sorting AND+RAG0/0 T cells were labeled with CD45.1 and the TCR β-chain Vβ3, lineage markers CD4 and CD90.2, and SA to exclude other cells. Representative sorting data are shown in Figure 19B. Each sample was sorted twice to ensure maximal purity of sorted cells (Figure 19B, first and second row). Small aliquots of the second sort were taken for purity control performed by flow cytometry (Figure 20B, last row) before the rest of the samples were directly sorted into Trizol for RNA isolation. Cell numbers were collected during the sorting procedures of day 10 (Table 1) and day 30 (Table 2) samples. Between 1 x 10^4 and 6 x 10^5 AND+RAG0/0 T cells were sorted per sample with purities between 99 and 100% as revealed by purity control analysis (Table 1 and 2).

Day 10		MACS purification		FACS/Casy counter		Sort #1		Sort #2		
#	cell type	total cell # pre MACS (x107)	total cell # post MACS (x106)	AND %	total AND (x106)	total cell # pre Sort #1 (x106)	total cell # post Sort #1 (x104)	total cell # pre Sort #2 (x104)	total cell # post Sort #2 (x104)	RIN
1	naive	32,4	12,4	0,5	1,5	9,9	9,2	7,5	6,0	9,3
2	naive	31,5	25,2	0,6	1,9	18,0	25,0	20,0	17,0	9,3
3	naive	27,9	17,6	0,5	1,5	12,0	8,8	6,2	5,0	9
4	naive	34,2	19,2	0,6	1,9	11,0	6,8	4,7	3,7	8,9
5	naive	26,3	10,8	0,5	1,2	9,3	7,7	5,8	4,9	8,8
6	memory	16,8	12,5	1,8	3,1	8,6	35,0	25,0	19,0	9,5
7	memory	13,4	24,4	0,1	0,2	39,0	13,0	12,0	8,1	9,5
8	memory	54,0	112,0	0,7	4,0	13,0	73,0	63,0	52,0	9,3
9	memory	21,4	29,2	3,7	7,9	15,0	63,0	56,0	44,0	9,4
10	memory	19,8	30,4	3,3	6,5	15,0	51,0	44,0	37,0	9,5
11	low	16,8	9,6	1,9	3,1	4,5	17,0	14,0	13,0	9,6
12	low	66,0	6,0	2,8	1,8	3,3	21,0	18,0	17,0	9,7
13	low	11,1	12,4	2,3	2,5	5,6	27,0	22,0	21,0	9,7
14	low	82,8	12,8	1,5	1,2	5,8	19,0	16,0	14,0	9,7
15	low	63,6	8,8	1,7	1,5	4,7	18,0	14,0	13,0	9,4
16	int	5,4	3,0	0,8	0,4	1,6	2,8	2,0	1,7	9,5
17	int	8,8	6,7	1,0	0,9	4,1	7,8	6,0	4,9	9,4
18	int	8,6	3,7	0,6	0,5	1,9	3,2	2,1	1,7	9,5
19	int	14,9	9,2	0,6	0,9	3,2	6,4	4,7	4,1	9,2
20	int	14,1	8,3	0,8	1,1	3,8	9,2	6,9	6,1	Nd
21	high	24,0	15,2	3,3	7,8	10,0	100,0	85,0	59,0	9,4
22	high	9,2	10,4	3,3	3,0	7,6	700,0	140,0	93,0	9,7
23	high	9,3	12,0	4,5	4,2	5,6	49,0	41,0	25,0	9,8
24	high	6,9	12,3	3,5	2,4	5,9	45,0	39,0	25,0	9,8
25	high	14,4	22,8	4,0	5,7	9,3	31,0	25,0	18,0	9,5

Table 5: Cell numbers of day 10 sorted naïve, memory, low, int, and high AND+RAG0/0 T cells.

Day 30		MACS purification		FACS/Casy counter		Sort #1		Sort #2		
#	cell type	total cell # pre MACS (x107)	total cell # post MACS (x106)	AND %	total AND # (x105)	total cell # pre Sort #1 (x106)	total cell # post Sort #1 (x104)	total cell # pre Sort #2 (x104)	total cell # post Sort #2 (x104)	RIN
1	memory	5,6	8,2	0,3	1,8	3,2	3,6	2,6	2,4	9,5
2	memory	4,3	7,7	0,8	3,4	4,4	1,1	5,5	4,9	9,2
3	memory	5,4	7,8	0,2	0,8	4,2	2,3	1,4	1,2	9
4	memory	8,8	9,6	0,3	2,2	5,7	4,8	2,5	2,3	9,7
5	memory	1,0	12,8	0,1	1,4	6,1	2,4	1,8	1,7	8,3
6	low	15,5	9,3	0,3	4,9	6,4	4,3	3,8	3,4	8,2
7	low	15,8	9,4	0,4	6,3	5,9	5,1	4,0	3,7	9,6
8	low	10,2	6,5	0,2	2,0	4,1	2,0	1,6	1,5	9
9	low	21,6	6,8	0,1	1,7	4,2	3,3	2,7	2,4	9
10	low	14,2	16,5	0,3	4,7	6,3	4,5	3,3	2,7	8,8
11	int	4,9	7,4	0,3	1,5	4,7	4,1	2,4	1,6	9,2
12	int	10,3	6,1	0,8	7,9	4,3	3,2	2,6	2,4	9,5
13	int	4,2	4,2	0,3	1,4	2,5	4,0	2,8	2,6	8,8
14	int	7,1	4,5	1,0	7,2	3,1	2,8	2,0	1,8	8,5
15	int	6,9	8,4	1,0	6,6	5,5	4,2	3,1	2,9	9,4
16	int off	11,5	23,6	0,2	2,0	12,0	5,7	3,2	2,7	9,2
17	int off	9,5	12,3	0,4	3,3	7,4	6,2	3,3	2,8	9,6
18	int off	11,2	13,2	0,2	2,2	8,5	4,5	2,3	2,1	9
19	int off	6,2	12,6	0,4	2,3	6,3	4,9	2,6	2,4	8,8
20	int off	12,0	19,2	0,2	2,6	9,3	3,7	2,1	1,9	9,2

Table 6: Cell numbers of day 30 sorted naïve, memory, low, int, and high $AND^{+}RAG^{0/0}$ T cells.

Total RNA was isolated as described in section 3.3.4. RNA quality indicated by the RNA integrity number (RIN, 0 – 10, with 10 representing the highest purity) and total RNA concentrations (Table 5 and 6) were measured as described in section 3.3.1.5 using a Bioanalyzer. Samples with high RIN values (> 8) were converted to cDNA and used for gene expression analysis (see 3.3.6). Microarray technique was performed by Martin Irmler, Helmholtz Zentrum München. All RIN values are listed in Table 5 and Table 6.

4.5.2 Chronic TCR stimulation causes unique gene expression pattern

Principle component analysis (PCA) is a popular statistical method to visualize genetic distance and relation between distinct cell populations. In cooperation with Tobias Straub at the Bioinformatics Core Facility at the BMC, München we performed PCA on gene-expression patterns measured at early (Figure 21A) and late (Figure 21B) time points to determine and quantify the distance between both, the samples within a unique group and between the different groups. Unique samples that failed the quality control by PCA were excluded from further analyses. PCA analysis was done separately for day 10 and day 30 samples to avoid batch effects.

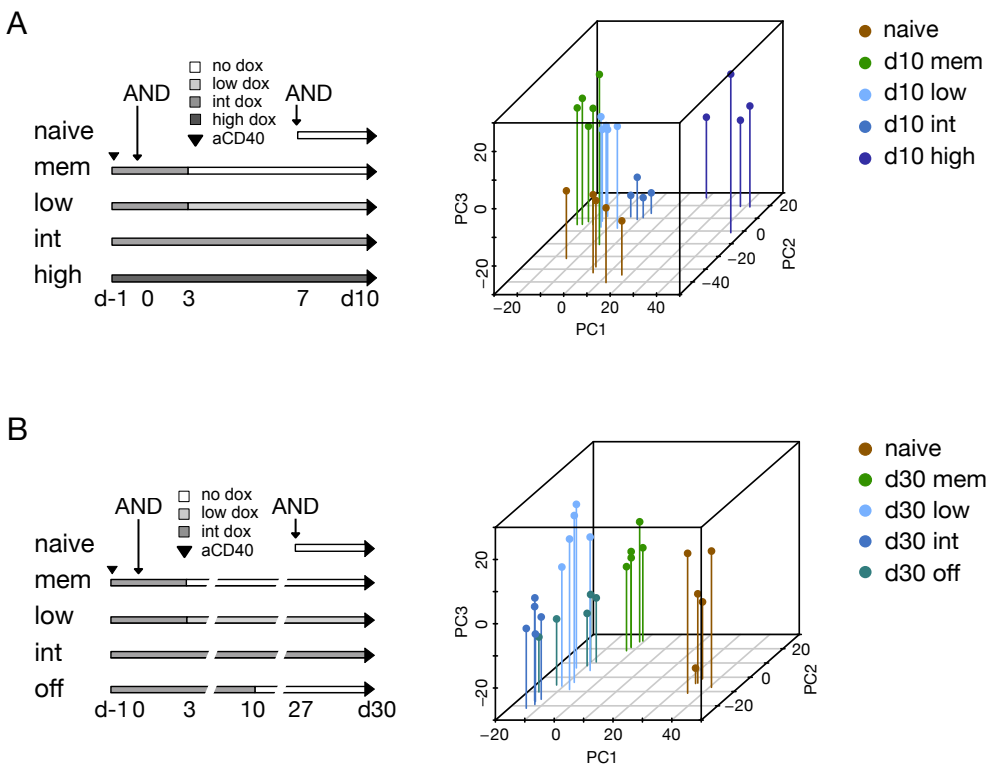

Figure 21: Gene expression pattern of antigen-exhausted CD4⁺ T cells clearly distinguish from memory CD4⁺ T cells. Principle component analysis (PCA) of day 10 and day 30 generated AND⁺RAG$^{0/0}$ T cells exposed to varying antigen levels. (A) PCA of naïve, memory, low, int, and high AND⁺RAG$^{0/0}$ T cells. Cells were generated as indicated and analyzed on day 10. Samples were phenotype-checked according to Figure 18 and sorted as described in Figure 19. (B) PCA of naïve, memory, low, int, and int off AND⁺RAG$^{0/0}$ T cells. Cells were generated as indicated and analyzed on day 30. Naïve AND⁺RAG$^{0/0}$ T cells were generated once, together with day 10 samples and were re-used for day 30 analysis. Samples were phenotype-checked according to Figure 18 and sorted as described in Figure 19. Statistical analyses were performed by Dr. Tobias Straub, LMU. Naïve, memory (mem), low, intermediate (int), intermediate off (int off), and high represents the time and dose of antigen AND⁺RAG$^{0/0}$ T cells have seen beyond the priming phase.

PCA illustrated that the samples clustered according to their conditions of treatment. The more antigen persisted beyond the priming phase, the further separated from each other clustered the unique groups. The same pattern holds true over time. Low ANDs clustered very close to memory ANDs on day 10 and separated further away on day 30, indicating a closer relatedness in gene expression during the early phase than compared to the later time point (Figure 21A, B, light blue and green). Thus, low level of TCR stimulation induces a memory-like gene-expression pattern that change slowly over time. Looking at the day 30 induced gene-expression pattern of intermediate off ANDs with terminated antigen presentation on day 10 we found that this population spread among intermediate and low AND groups towards the memory population (Figure 21B, turquoise), indicating that some gene-expression changes are reversible. Together, these data indicate that the longer and the more antigen CD4⁺ T cells see beyond the priming phase, the more gene-expression changes and divergence occur, which are, at least partially, reversible by antigen removal.

To gain a deeper insight into gene-expression patterns and changes induced by chronic antigen presentations of different doses we analyzed, in cooperation with Tobias Straub at the BMC, the induced gene-expression profiles of all 15 possible gene-expression patterns as 15 clusters. To do so, we set the criteria to FC ≥ 1.5 and FDR ≤ 0.05 and defined the 15 clusters of upregulated gene-expression patterns containing genes that were either uniquely expressed or shared between the different conditions for both, day 10 (Figure 22A) and day 30 (Figure 22B). We identified memory-associated clusters, such as cluster 1 and cluster 5, containing genes significantly induced in memory or in both, memory and low AND T cells, respectively. In these clusters, we found memory-associated genes, such as *Jun*, *Fos*, and *Il7r* on day 10 and on day 30.

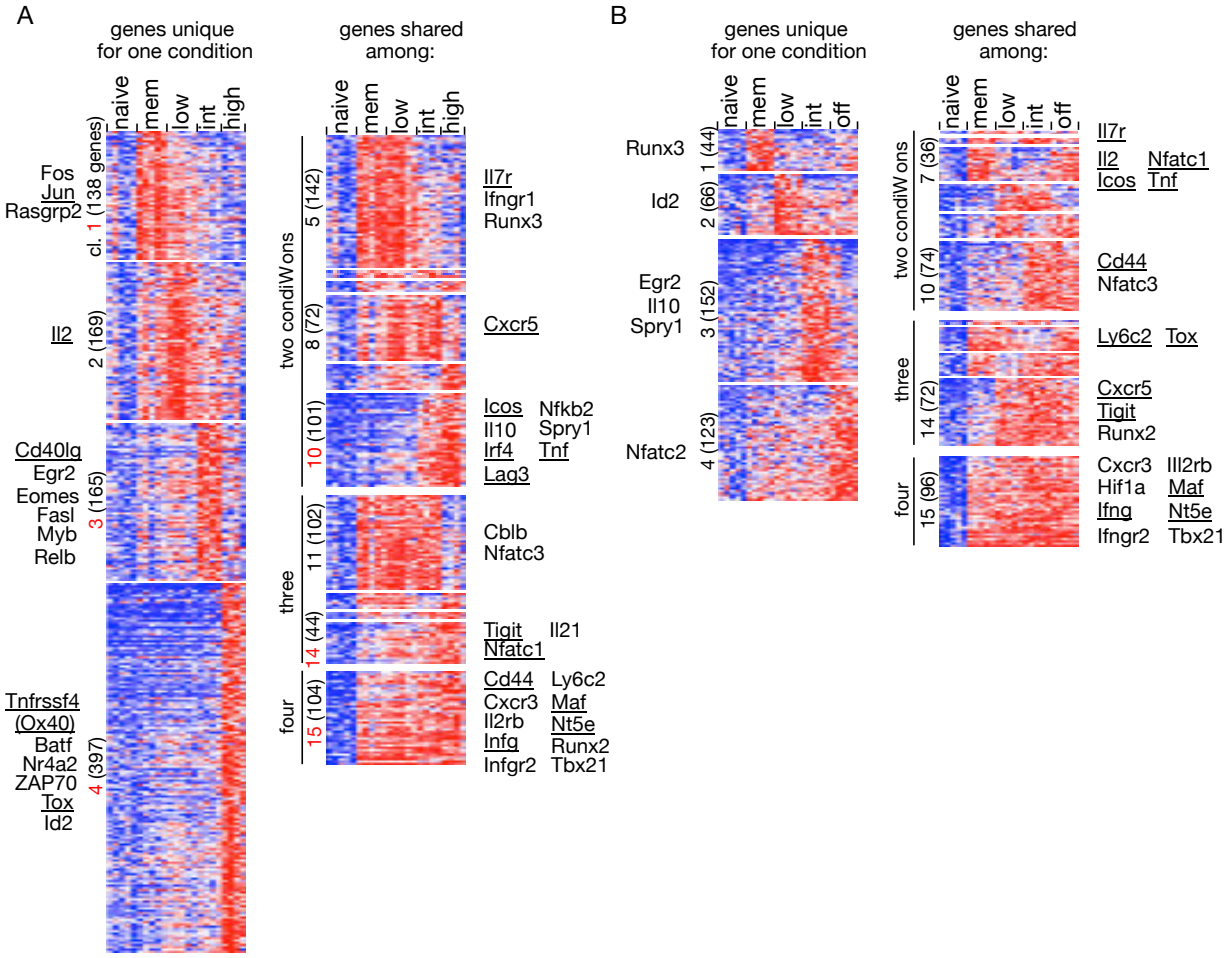

Figure 22: Persisting antigen upregulates dose-dependently unique gene expression patter in specific CD4+ T cells. Cluster analyses of microarray data comparing gene expression pattern of naïve, memory, low, int, int off, and high, AND+RAG0/0 T cells early on day 10 or late on day 30. Samples were generated as describes in Figure 22. cDNA was probed with Mogene 2.0 microarrays. 15 clusters were identified for each analysis. All genes depicted fulfill the criteria FC≥1.5 and FRD≤0.05. (A) Gene-expression upregulated (red) early on day 10 compared to naïve T cells. (B) Gene-expression upregulated (red) late on day 30 compared to naïve T cells. Genes uniquely expressed in one condition are depicted in the left column and genes expressed in two or more conditions in the right column. Naïve, memory (mem), low, intermediate (int), intermediate off (int off), and high represents the time and dose of antigen AND+RAG0/0 T cells have seen beyond the priming phase. Red numbers on the left side of the columns indicate the cluster number followed by the number of regulated genes within the according cluster (black number). Representative genes of the corresponding cluster are listed next to its cluster, underlined genes were further analyzed in this thesis. FC: fold change, FDR: false discovery rate.

Genes that were re-induced by antigen termination on day 10, such as *Il2*, *Tnf*, *Icos*, and *Nfatc3*, were found in cluster 7, and genes that were antigen-dependently induced were found in cluster 8 (Figure 22B). Within the chronic-associated clusters (4, 10, 14, and 15) we found genes encoding exhaustion-associates markers, such as PD-1, Lag-3, TIGIT, CD200/Ox2, Ox40, TOX, Maf, NFAT, Batf, as well as genes, encoding the Tfh-associated markers ICOS, CXCR5, IL-21, and the anergy-associated marker CD73 (*Nt5e*, cluster 15) (Figure 22A). These analyses suggest that chronic antigen presentation beyond the priming phase induces CD4+ T cell plasticity in a dose- and time-dependent manner.

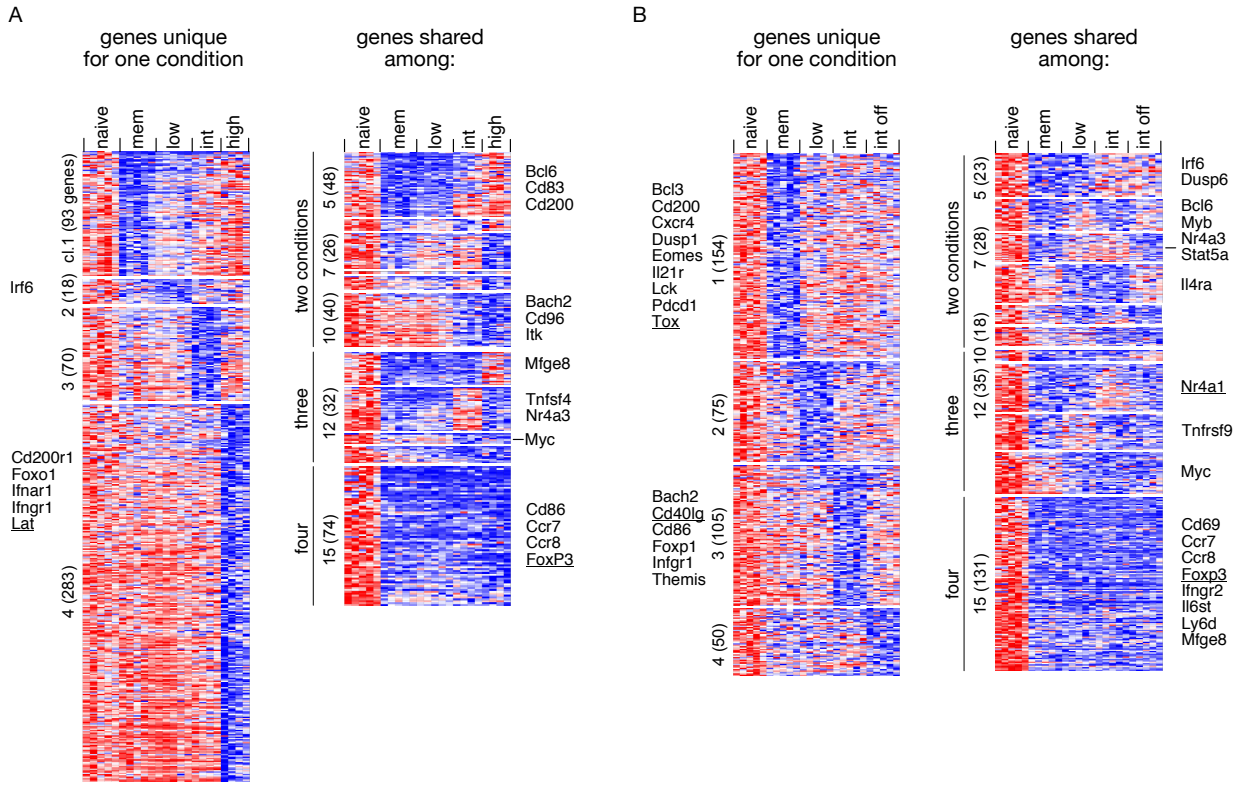

Figure 23: Persisting antigen dose-dependently downregulates certain gene expression in specific CD4+ T cells. Cluster analyses of microarray data comparing gene expression pattern of naïve, memory, low, int, int off, and high, AND+RAG0/0 T cells early on day 10 or late on day 30. Samples were generated as describes in Figure 22. cDNA was probed with Mogene 2.0 microarrays. 15 clusters were identified for each analysis. All genes depicted fulfill the criteria FC≥1.5 and FRD≤0.05. (A) Gene-expression downregulated (blue) early on day 10 compared to naïve T cells. (B) Gene-expression downregulated (blue) late on day 30 compared to naïve T cells. Genes uniquely expressed in one condition are depicted in the left column and genes expressed in two or more conditions in the right column. Naïve, memory (mem), low, intermediate (int), intermediate off (int off), and high represents the time and dose of antigen AND+RAG0/0 T cells have seen beyond the priming phase. Red numbers on the left side of the columns indicate the cluster number followed by the number of regulated genes within the according cluster (black number). Representative genes of the corresponding cluster are listed next to its cluster, underlined genes were further analyzed in this thesis. FC: fold change, FDR: false discovery rate.

We also defined the 15 possible patterns of gene-expression as 15 clusters with downregulated genes compared to naïve T cells among the different groups on day 10 (Figure 23A) and on day 30 (Figure 23B). Interestingly, we found *Lat* in cluster 4, a cluster representing genes that

were exclusively downregulated by chronic high TCR stimulation. This finding is in agreement with our finding that LAT protein is significantly decreased in high AND T cells (Figure 14A).

Gene Ontology (GO) enrichment analysis is used to perform statistically analyses on gene sets to identify significant similarities or differences between genomic samples and to gain insights into the functions and dynamics of gene sets. To identify molecular mechanisms induced or repressed by dose-dependent chronic antigen presentation we performed GO enrichment analysis of day 10 clusters upregulated in chronic condition (3, 4, 10, 11, 12, 14, and 15). We identified several statistically significant GO terms, including the ones listed in Figure 24. The diameter of the circles indicates the number of regulated genes associated with the corresponding terms and the color indicates the p-Values as indicated.

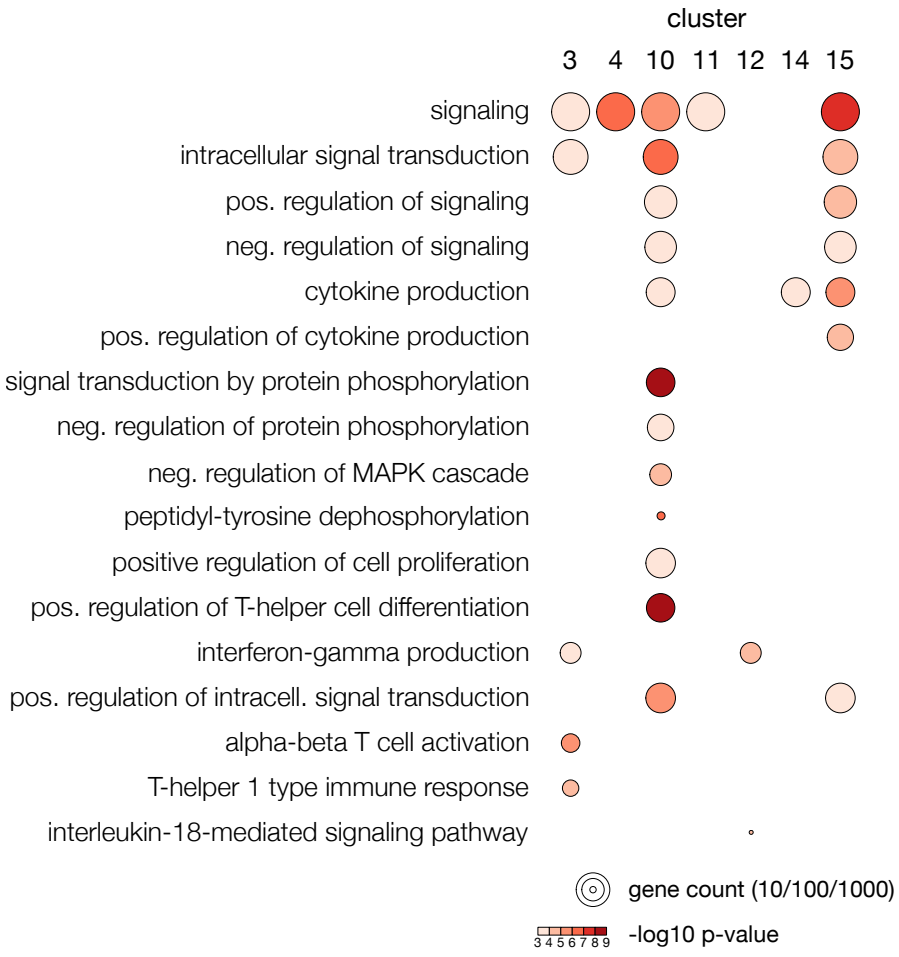

Figure 24: Gene Ontology (GO) enrichment analysis of upregulated gene-expression clusters on day 10 revealed gene-expression pattern associated with negative regulation of the MAPK cascade. GO terms enriched in gene sets upregulated within gene-expression clusters identified on day 10 (cluster 3, 4, 10, 11, 12, 14, and 15) described in Figure 22A. Each column represents a cluster; each row represents a GO pathway or process. The significances (p-values of student's t-test) are color coded and the number of genes per GO term is indicated by the diameters of the circles. Analyses were performed by Tobias Straub, BMC, LMU.

We found the highest number of significantly regulated GO terms associated to clusters with induced gene expression, either by intermediate antigen-dose only (cluster 3), shared by intermediate and high dose (cluster 10), or shared by all activating conditions (cluster 15). The gene-expression profile of cluster 10 indicates that signaling is affected and that gene-expression modulates MAPK signaling, which is in agreement with our finding that c-Jun and S6 phosphorylation was significantly reduced under chronic conditions (describes above, data not shown) (Han et al., 2010). Cytokine production was positively regulated by all stimulating conditions (cluster 15) suggesting a post-transcriptional regulation, as cytokine production was antigen-dose-dependently impaired (Figure 13).

In contrast, analyzing GO terms of downregulated genes, we found not many genes downregulated by chronic intermediate or high TCR stimulation (cluster 10). NF-κB signaling is significantly downregulated by high TCR stimulation (cluster 4) (Figure 25).

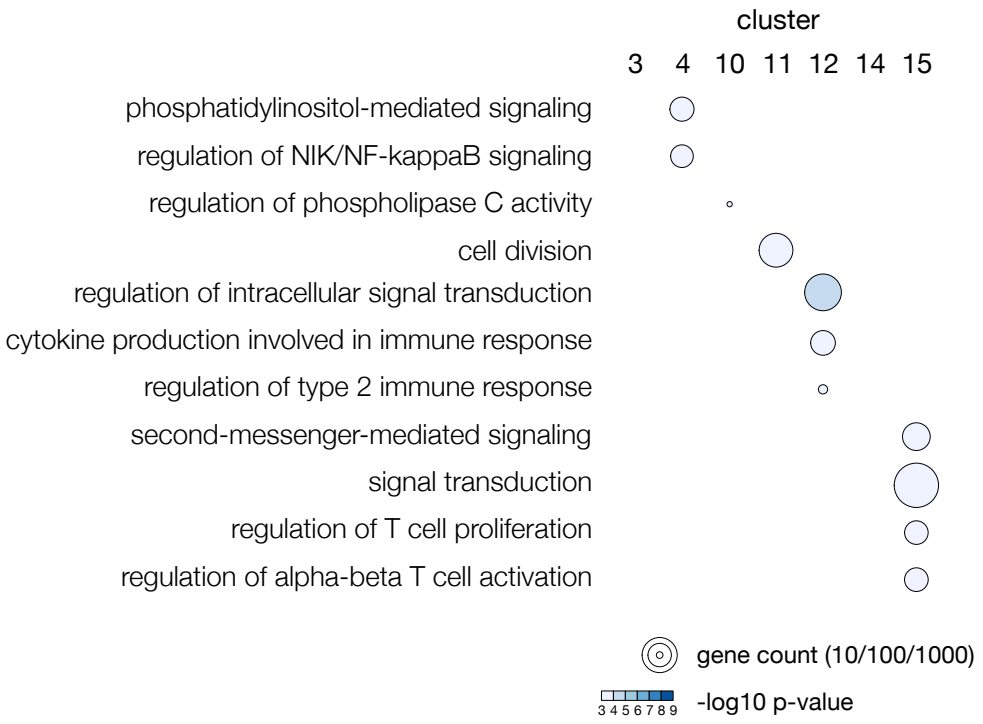

Figure 25: Gene Ontology (GO) enrichment analysis of gene-expression clusters of downregulated genes on day 10. GO terms significantly associated with gene sets downregulated within gene-expression clusters identified on day 10 (cluster 3, 4, 10, 11, 12, 14, and 15) described in Figure 22A. Each column represents a cluster; each row represents a GO pathway or process. The significances (p-values of student's t-test) are color coded and the number of genes per GO term is indicated by the diameters of the circles. Analyses were performed by Tobias Straub, BMC.

4.5.3 Gene-expression differences on day 10 are predictive for later gene expression patterns

To examine if induced gene-expression patterns on day 10 correlate with the gene-expression profile of day 30 we compared upregulated day 10 gene-expression clusters shown in Figure 22A (Figure 26A, red dots) with day 30 identified gene-expression profile of intermediate vs. memory AND T cells (Figure 26A, black dots). Genes identified in the day 10 memory-associated cluster 1 were equally distributed among day 30 memory and intermediate AND T cells (Figure 26A). Gene Set Enrichment Analysis (GSEA) also revealed no significant correlation, indicated by the high false discovery rate (FDR) of 0.14 (Figure 26B). In contrast, gene clusters associated with chronic stimulation (cluster 3, 4, 10, 14, and 15) are significantly (indicated by very low FDR, Figure 26B) enriched in the int/mem comparison on day 30 (Figure 26). This comparison indicates that gene-expression changes induced by persisting antigen by day 10 are predictive for later gene expression on day 30.

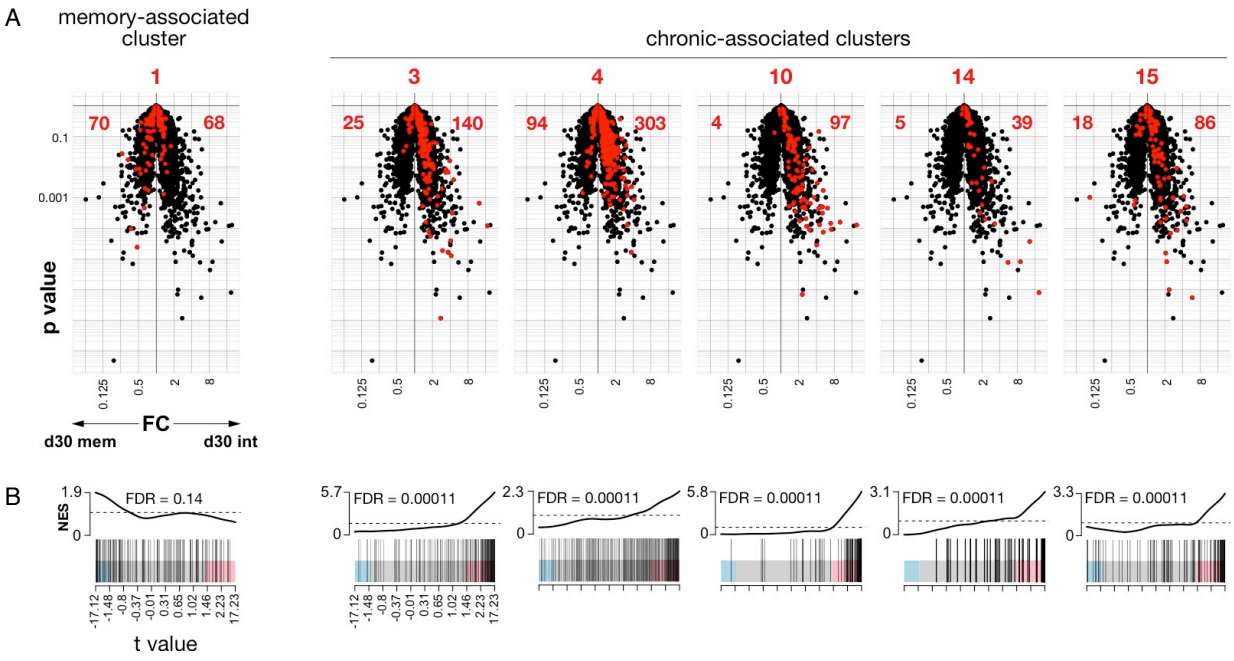

Figure 26: Early induced gene expression pattern (on day 10) are predictive for later gene-expression pattern (on day 30). (A) Gene expression pattern of day 30 memory (mem) and intermediate (int) AND^{+}RAG$^{0/0}$ T cells identified in Figure 22B are visualized in volcano plots (black dots). Genes expressed in AND^{+}RAG$^{0/0}$ T cells on day 10 according to the conditions defined for unique clusters 3 and 4, or shared clusters 10, 14, and 15 were projected in red onto day 30 induced gene-expression pattern of int vs. mem AND^{+}RAG$^{0/0}$ T cells. Numbers on top of the volcano plots indicate the cluster number, the two red numbers within the panels indicate the cluster genes with an FDR < 1 and >1, respectively. (B) Gene set enrichment analysis (GSEA) showing the FDR of the corresponding comparisons. FDR: false discovery rate, FC: fold change, NES: Normalized enrichment score, t: t-value of Student´s test.

4.5.4 Exhaustion-associated surface markers and transcription factors are induced by persisting antigen in a dose-dependent fashion

Chronic infections and cancer cause a dysfunctional state of T cells termed exhaustion and is associated with the loss of effector function, impaired proliferative capacity, upregulation of multiple inhibitory receptors, and altered expression of key transcription factors (Crawford et al., 2014; McLane et al., 2019; Schietinger et al., 2016; Wherry and Kurachi, 2015; Yi et al., 2010). What role chronic antigen presentation itself plays in such a scenario and what influence the dose of presented antigen has on CD4$^+$ T cells is not clear. We found increased RNA expression levels of several exhaustion-associated inhibitory receptors (Figure 22). To validate surface expression of the respective proteins, flow cytometric analyses were performed (Figure 27A, B). We found LAG-3, TIGIT, and Ox2 (CD200) being highly sensitive to persisting antigen levels as they showed a dose-dependent surface expression. Other markers responded exclusively to high dose antigen. Among them we found the expression of PD-1, Ox40, and IL18R significantly induced and the expression of CD137L significantly repressed on high AND T cells. These data show that the amount of antigen presentation beyond the priming phase matters for the upregulation of inhibitory receptors.

Flow cytometric analysis of the induced transcription factors TCF-1, cMaf, and TOX (Figure 22) demonstrated different responses to chronic antigen presentations (Figure 27). TCF-1, which is associated with CD8$^+$ T memory generation (Lin et al., 2016; Utzschneider et al., 2016b; Zhou et al., 2010) is not induced on protein-level but significantly reduced in high ANDs. The transcription factor cMaf was shown to be involved in Tr1 differentiation and in CD8$^+$ T cell exhaustion (Chien et al., 2017; Gagliani et al., 2013; Giordano et al., 2015; Pot et al., 2009; Roncarolo et al., 2018). We found that cMaf expression was induced by high-dose antigen and the transcription factor TOX, which is associated with CD8$^+$ T cell exhaustion (Alfei et al., 2019; Khan et al., 2019; Scott et al., 2019) to be dose-dependently induced, suggesting a more sensitive regulator (Figure 27). These data indicate that AND CD4$^+$ T cells sense and respond to different antigen doses after the initial priming phase with the induction of transcription factors involved in CD8$^+$ Tmem and Tex cell differentiation in viral and cancer models.

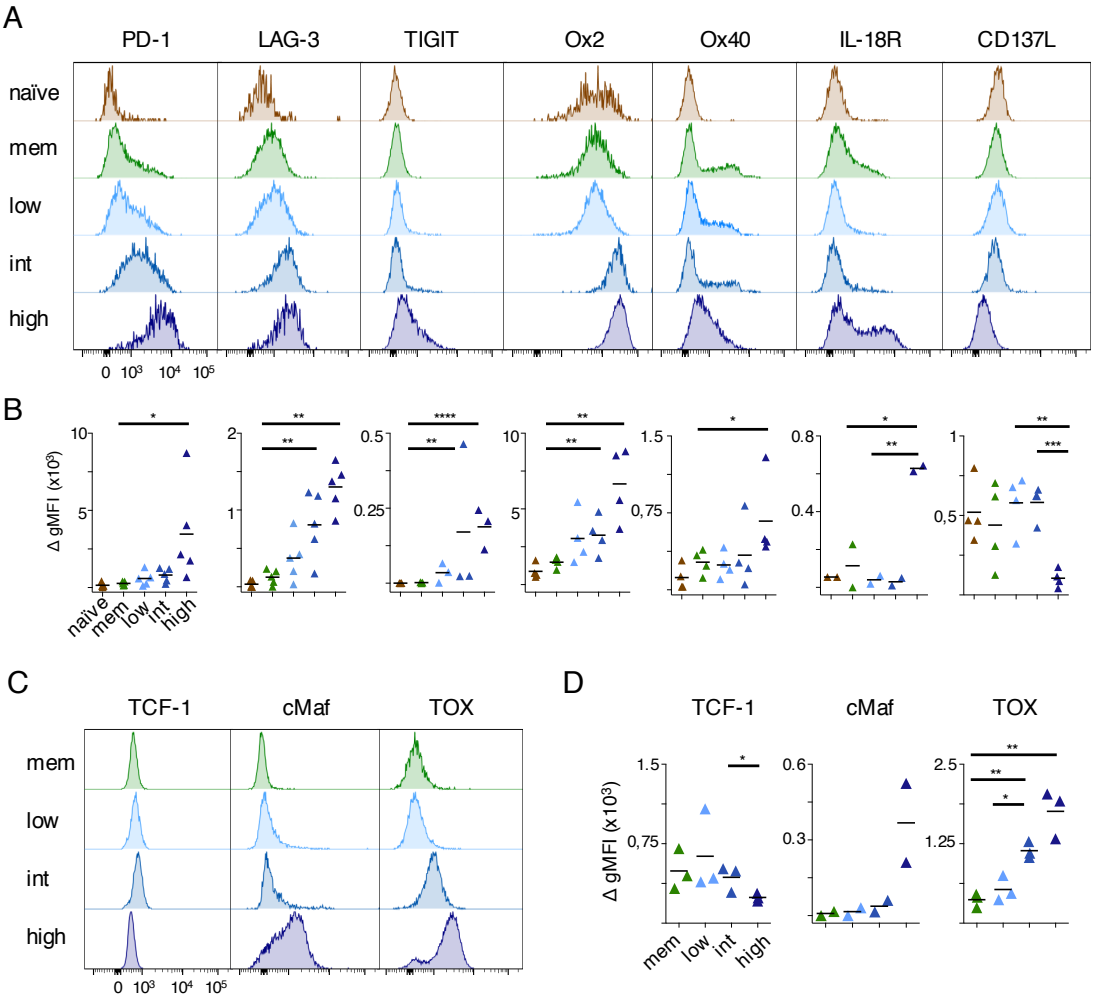

Figure 27: Exhaustion-associated markers and transcription factors respond dose-dependently to persisting antigen. Quantification of 1 x 10^6 adoptively transferred AND T cells using flow cytometry. Naïve, memory (mem), low, intermediate (int), and high AND $CD4^+$ T cells were generated as described in Figure 10A. Spleens were harvested 10 days post transfer. AND T cells shown were identified using the gating strategy described in Figure 8A. (A) Representative histograms showing surface expression of inhibitory receptors identified by microarray analyses. (B) Statistical quantification. (C) Representative histograms of intracellular transcription factor expression identified by microarray analysis. (D) Statistical quantification. Delta geometrical means were calculated by $gMFI_{Sample}$ - $gMFI_{isotype\ control}$. Data were pooled from at least two independently performed experiments, each data point represents one mouse. *$p < 0.05$, **$p < 0.001$, ***$p < 0.0001$, parametric unpaired two-tailed t-test.

Analyzing the transcription factor expression pattern on day 30 we found IRF4 and cMaf responding to chronic intermediate amount of antigen presentations (Figure 28). TOX expression was repressed on day 30, indicating a rather early role in T cell dysfunctionality of the transcription factor, in contrast to IRF4 and cMaf, which are expressed in intermediate AND T cells also at later stages of stimulation.

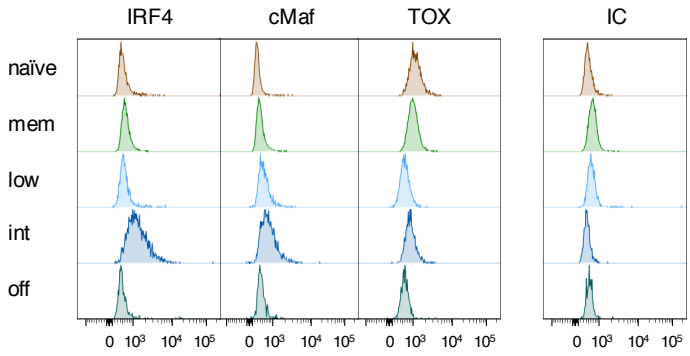

Figure 28: Characterization of transcription factors in AND T cells chronically exposed to low and intermediate Ag doses in iMCC-transgenic recipients analyzed on day 30. Quantification of 1 x 10^6 adoptively transferred AND T cells using flow cytometry. Cells were generated as describes in Figure 10A. Spleens were harvested 30 dpt, T cells shown were identified by CD4 and CD45.1 expression using the gating strategy described in Figure 8B. Histograms showing intracellular transcription factor expression of splenic AND T cells. Data shown from one experiment. Memory (mem), low, intermediate (int), and high represents the dose of antigen AND T cells have seen beyond the priming phase as schemed in Figure 10A. IC = isotype control.

4.5.5 Antigen-exhausted CD4⁺ T cells share gene-expression pattern with LCMV cl13-exhausted CD4⁺ T cells

Chronic Lymphocytic Choriomeningitis Virus (LCMV) infection is one of the best-studied systems of chronic infections in mice. During chronic LCMV cl13 infections T cells become exhausted. Thus, we compared mRNAs induced in antigen-exhausted CD4⁺ T cells with the ones induced in LCMV cl13-exhausted CD4⁺ T cells, published by Crawford et al., 2014. We identified shared induced genes (Figure 29, red dots) with LCMV cl13-exhausted CD4⁺ T cells analyzed 15 days (Figure 29A black dots, B) and 30 days post infection (Figure 29C black dots, D). Genes grouped in memory-associated cluster 5 (day 10) correlate with LCMV Armstrong (Arm) challenged CD4⁺ T cells (day 15), when memory CD4⁺ T cells are generated. This indicates that gene-expression pattern induced by transient antigen-presentation is similar to the one induced by LCMV Arm-specific memory CD4⁺ T cells. Exhaustion-associated clusters (cluster 10, and 14) correlate with LCMV cl13-exhausted phenotype analyzed on da 15 (Figure 29A, B) as well as on day 30 (Figure 29C, D) indicating shared exhaustion-induced gene-expression patterns. The observed differences in gene-expression patterns between LCMV- and antigen-exhausted T cells might be induced in an inflammation-driven manner.

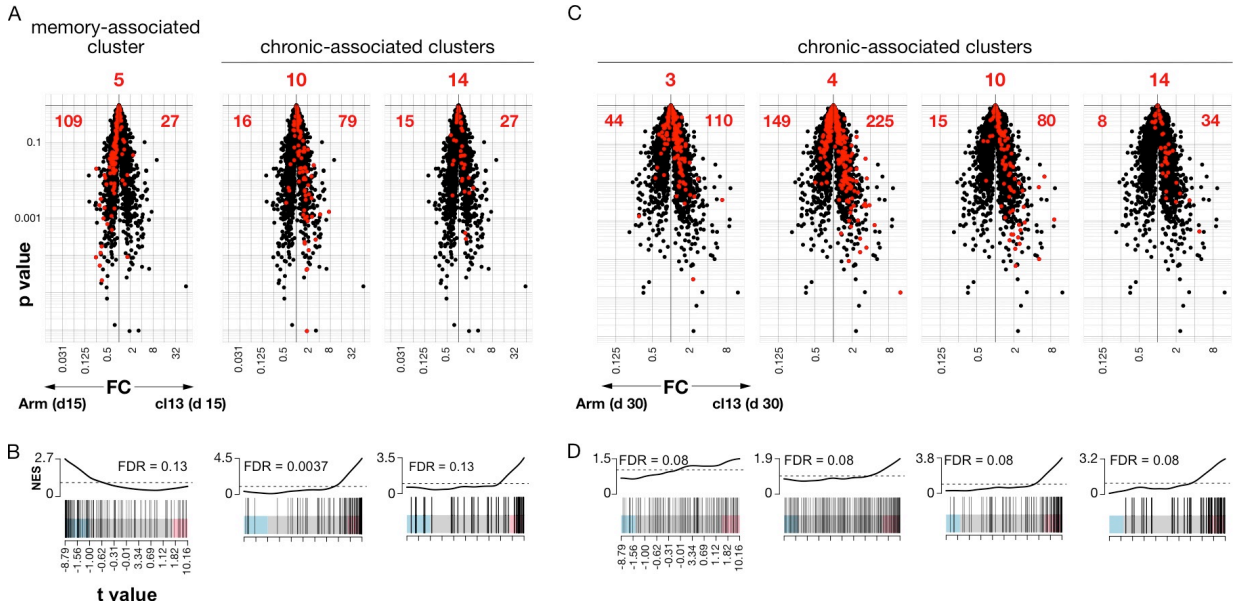

Figure 29: Antigen-exhausted AND T cells share gene-expression pattern with LCMV cl13-exhausted CD4⁺ T cells. Gene expression pattern of antigen specific CD4⁺ T cells isolated upon 15 or 30 days of LCMV Armstrong (Arm) or clone13 (cl13) infections respectively, are visualized in volcano plots (black dots). Gene expression upregulated in acute LCMV arm infection fall to the left and genes upregulated in chronic cl13 infection fall to the right. Genes expressed in AND⁺RAG$^{0/0}$ T cells on day 10 according to the conditions defined for the memory-associated cluster 5 and exhaustion-associated clusters 4, 10 and 14 were projected in red onto (A) day 15 analyzed LCMV induced gene-expression pattern of Arm vs. cl13 CD4⁺ T cells and (C) day 30 LCMV induced gene-expression pattern of Arm vs. cl13 CD4⁺ T cells. Numbers on top of the volcano plots indicate the cluster number, the two red numbers within the panels indicate the cluster genes with an FDR < 1 and >1, respectively. (B and D) Gene set enrichment analysis (GSEA) showing the FDR of the corresponding comparisons. FDR: false discovery rate, FC: fold change, NES: Normalized enrichment score, t: t-value of Student´s test.

4.5.6 Anergy-associated surface marker-expression is antigen dose-dependent and reversible

The markers FR4 and CD73 are associated with T cell anergy (Kalekar et al., 2016; Martinez et al., 2012). We found *Nt5e*, the gene encoding for CD73, highly induced on gene-expression level in all antigen-experienced AND T cells (Figure 22, cluster 15). Thus, we assessed surface expression of CD73 with the surface expression of FR4 (which is not probed by the microarray used) on day 10 by flow cytometry. Naïve and memory AND CD4⁺ T cells barely expressed these markers, only approximately two and three percent, respectively. FR4 and CD73 surface expression was induced by antigen persistence beyond the priming phase in correlation with antigen-dose. The more antigen AND T cells have seen, the stronger FR4 and CD73 surface expression was upregulated (Figure 30A, B).

Looking at the abundance of endogenous anergic CD4⁺ T cells of the recipient mice there was no significant difference detectable in percentage and absolute numbers, indicating there is no competition (Figure 30A, B). These data indicated that persisting antigen-stimulation induce the expression of anergy-associated markers in a dose-dependent fashion.

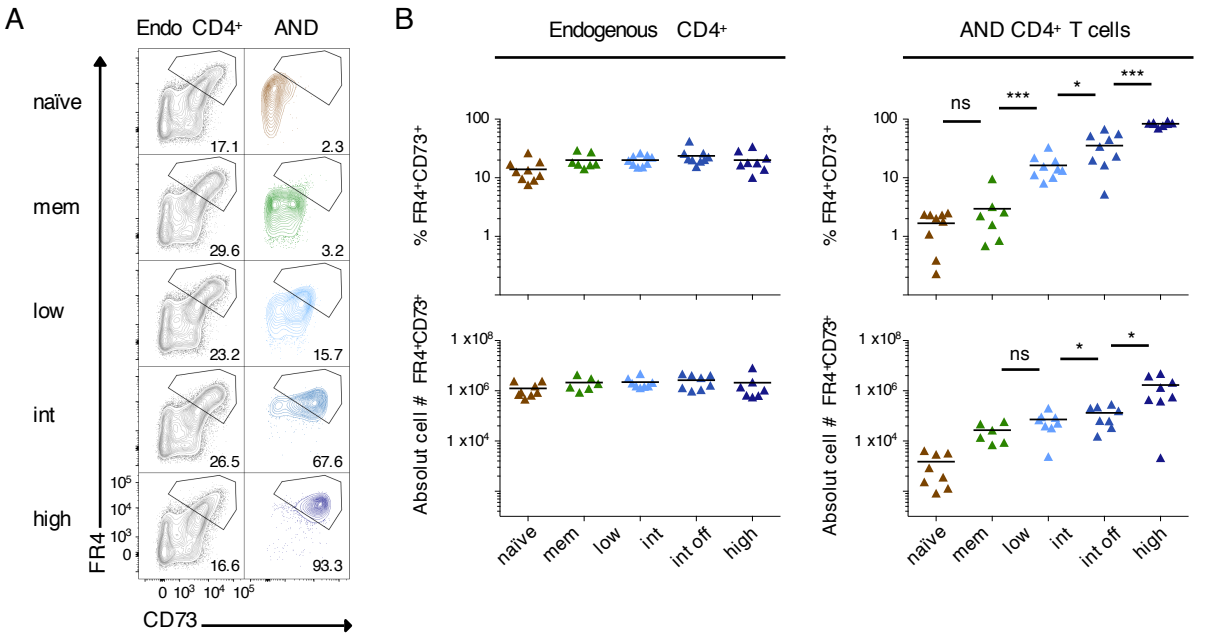

Figure 30: Anergy-associated markers respond to antigen dose (day 10). Quantification of 1 x 10^6 adoptively transferred AND T cells using flow cytometry. Naïve, memory (mem), low, intermediate (int), and high AND CD4+ T cells were generated as described in Figure 10A. Spleens were harvested 10 days post transfer. AND T cells shown were identified following the gating strategy described in Figure 8A. (A) Representative results showing increasing surface expression of the anergy-associated markers FR4 and CD73 on the surface of ANDs (color coded, right column) chronically exposed to increasing antigen dose and on endogenous anergic CD4+ T cells (in grey, left column). (B) Graphs show percentage and absolute numbers of AND T cells and endogenous anergic CD4+ T cells expressing the anergy-associated markers FR4 and CD73. Data are shown of eight independent experiments; each data point represents one mouse. *$p < 0.05$, **$p < 0.001$, ***$p < 0.0001$, parametric unpaired two-tailed t-test. Naïve, memory (mem), low, intermediate (int), and high represents the dose of antigen AND T cells have seen beyond the priming phase as schemed in Figure 10A.

Next, we asked if the expression of the anergy-associated markers FR4 and CD73 depends on persisting antigen or is rather fixed. To this end we *rescued* intermediate and high AND T cells on day 10 by terminating dox treatment of intermediate mice (int off) and performed secondary transfer from high ANDs into antigen-free wt mice (high off). As controls we included memory and intermediate (int on) AND T cells as well as high ANDs secondarily transferred back into cMCC recipients presenting MCC at a high dose (high on) (Figure 31A). Splenocytes were analyzed on day 21 post primary transfer. The expression patterns of FR4 and CD73 on day 21 pt represent the expression patterns shown on day 10 post transfer (Figure 30). Upon antigen withdrawal by either terminating dox treatment or secondary transfer surface expression of FR4 and CD73 was significantly reduced (Figure 31B, C) indicating that the expression of these anergy markers depend on persisting antigen presentation. Thus, the anergic phenotype might be reversible upon antigen removal. This conclusion is in agreement with Kalekar et al., 2016 showing that most anergic T cells downregulated their surface expression of FR4 and CD73 when transferred into lymphopenic recipients.

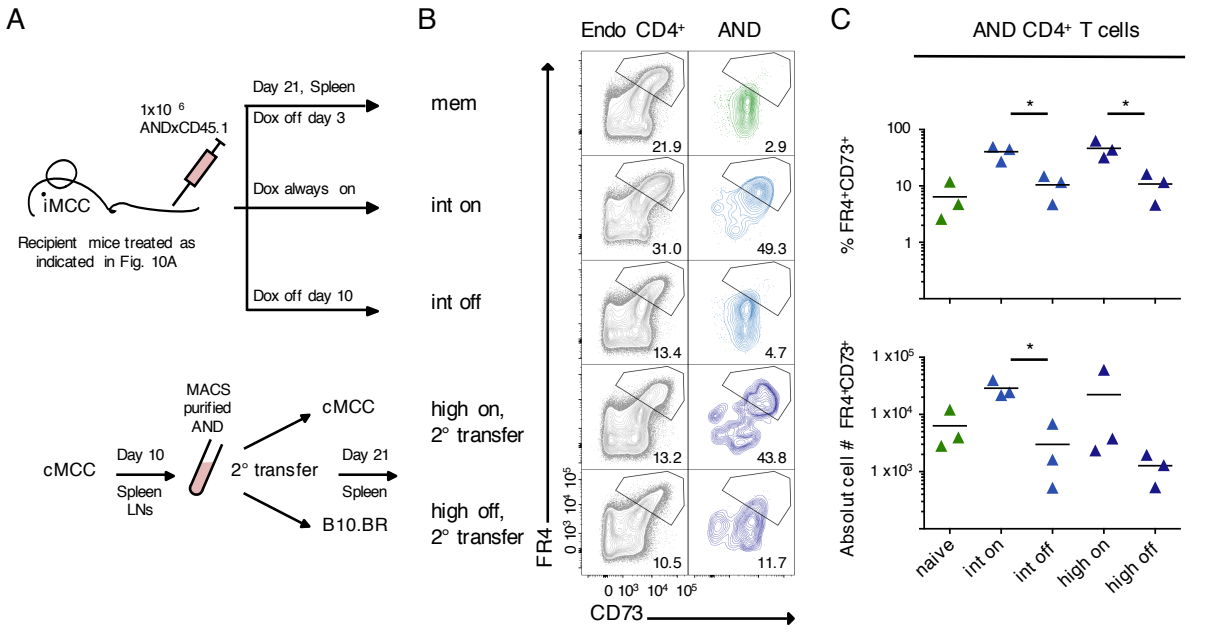

Figure 31: The expression of the CD73 and FR4 markers associated with anergy is reversible upon discontinuation of antigen stimulation. Quantification of 1 x 10^6 adoptively transferred AND T cells using flow cytometry. (A) Schematic outline describing the treatment strategy to generate memory (mem), intermediate (int), intermediate off (int off), high and high off AND CD4+ T cells. Mem, int, and int off cells were generated as described in (Figure 10A) and analyzed 21 days post transfer (dpt). "High on" and "high off" AND T cells were generated by secondary transfer 10 days post primary transfer. High CD4+ T cells were MACS purified and 3x10^6 CD4+ T cells secondarily transferred into either high-dose antigen presenting cMCC or antigen-free wildtype mice. Spleens were analyzed on 21 dpt. T cells shown were identified according to the gating strategy described in Figure 8A. (B) Representative results showing reversible surface expression of the anergy-associated markers FR4 and CD73 on AND T cells rescued *in vivo* by terminating antigen presentation (color coded, right column) and on endogenous anergic CD4+ T cells (in grey, left column). (C) Graphs show percentage and absolute numbers of AND T cells expressing the anergy-associated markers FR4 and CD73 analyzed on day 21 post transfer. Data are shown of three independent experiments; each data point represents one mouse. *$p < 0.05$ parametric unpaired two-tailed t-test.

4.5.7 Gene expression profile of antigen-exhausted CD4+ T cells strongly correlate with the one of anergic CD4+ T cells

The finding that the expression of anergy markers FR4 and CD73 was induced dose-dependently (Figure 30) suggested comparisons of the gene-expression profiles described with those of endogenous anergic CD4+ T cells. To this end, we sorted endogenous anergic CD4+ T cells based on CD4+CD44+FR4+CD73+ and non-anergic control CD4+ T cells based on CD4+CD44+FR4−CD73− surface expression (according to Figure 32 and Table 7). Total RNA was isolated and microarray analysis was performed as described in section 3.3.1.6).

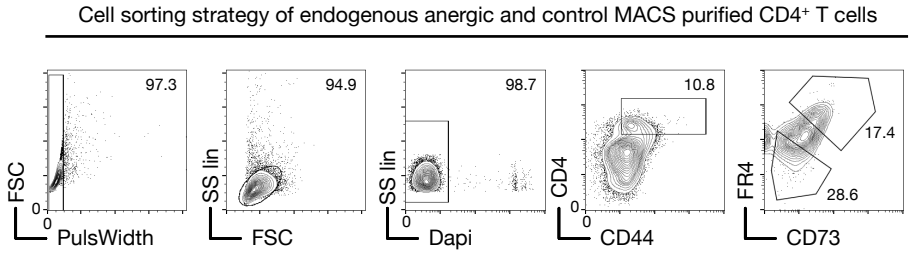

Figure 32: Sorting strategies for endogenous anergic and control CD4⁺ T cells used for microarray analysis. Representative gating strategy for sorting endogenous anergic and naïve non-anergic cells. Samples were sorted directly into Trizol for later analysis. Anergic cells were sorted based on Dapi^{neg}CD4⁺CD44⁺FR4⁺CD73⁺ and non-anergic control cells based on Dapi^{neg}CD4⁺CD44⁺FR4⁻CD73⁻.

Anergy		MACS purification		Sort #1	
#	cell type	total cell # pre MACS (x107)	total cell # post MACS (x106)	total cell # post Sort #1 (x105)	RIN
1	FR4+CD73+	2,0	16,4	2,0	9,9
2	FR4+CD73+	10,4	9,7	2,0	9,8
3	FR4+CD73+	8,8	7,9	2,0	9,8
4	FR4+CD73+	9,2	10,6	2,0	9,4
5	FR4+CD73+	7,9	8,6	2,0	9,7
6	FR4-CD73-	2,0	16,4	2,9	9,4
7	FR4-CD73-	10,4	9,7	4,9	9,2
8	FR4-CD73-	8,8	7,9	3,4	9,2
9	FR4-CD73-	9,2	10,6	4,2	7,7
10	FR4-CD73-	7,9	8,6	3,8	9,3

Table 7: Cell numbers of sorted endogenous anergic (FR4⁺CD73⁺) and non-anergic control (FR4⁻CD73⁻) cells.

The gene-expression pattern of endogenous anergic cells were plotted against expression pattern of non-anergic control cells (Figure 33A, black dots). We highlighted the genes of the memory-associated day 10 cluster 1 and the exhaustion-associated clusters (3, 4, 10, 14, and 15) on to anergic vs. control gene-expression volcano plots (Figure 33A, red dots). Genes of the memory-associated cluster 1 were preferentially expressed in non-anergic cells, though the false discovery rate FDR = 0,15 indicated no statistical significance (Figure 33B). Comparing exhaustion-associated clusters of interest with anergy-induced gene-expression pattern, genes strongly correlate with the anergic phenotype (Figure 33A, right) with low FDRs (FDR = 0.000125) calculated by GSEA. Thus, these results show a significant correlation of genes preferentially expressed by anergic and antigen-exhausted cells.

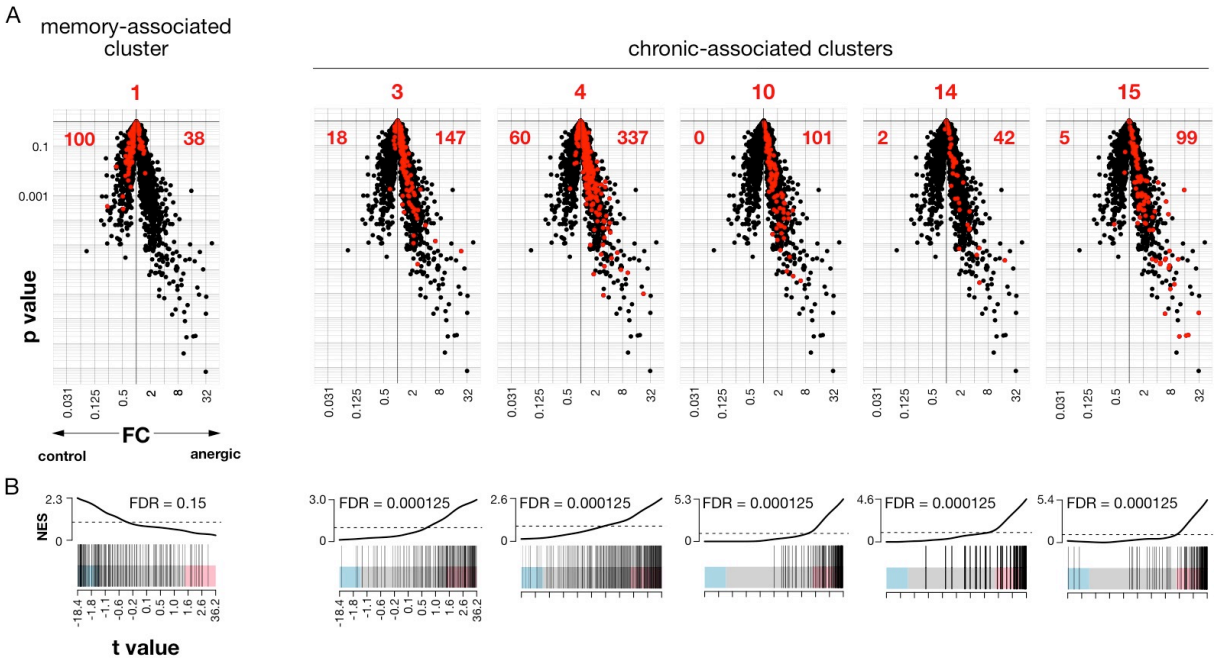

Figure 33: Early antigen-exhausted AND^{+}RAG$^{0/0}$ T cells share gene-expression patterns with endogenous anergic CD4^{+} T cells. Gene expression pattern of polyclonal anergic CD4^{+} T cells and polyclonal naïve, non-anergic CD4^{+} T cells, both from untreated wildtype B10.BR mice were analyzed with microarrays and visualized in volcano plots (black dots). Gene expression specific to non-anergic control cells fall to the left and genes identified for polyclonal anergic cells fall to the right. Genes expressed in AND^{+}RAG$^{0/0}$ T cells on day 10 according to the conditions defined for the memory-associated cluster 1 and exhaustion-associated clusters 3, 4, 10, 14, and 15 were projected in red onto anergic vs. non-anergic gene-expression pattern. (B) Gene set enrichment analysis (GSEA) showing the FDR of the corresponding comparisons. FDR: false discovery rate, FC: fold change, NES: Normalized enrichment score, t: t-value of Student´s test.

4.5.8 Chronic TCR stimulation is not sufficient to induce precursor cells of regulatory FoxP3^{+}CD4^{+} T cells

Anergic CD4^{+} T cells have been suggested to include precursor cells of regulatory FoxP3^{+}CD4^{+} T cells (Treg) (Kalekar et al., 2016). It also has been shown that low level antigen can induce peripheral Treg cell differentiation *in vivo* (Kretschmer et al., 2005; Verginis et al., 2008). Therefore, we measured intracellular FoxP3 expression by flow cytometry to ask if Treg cells were generated in our experimental system. Naïve, memory, low, intermediate, and high AND T cells were generated (Figure 10A) and splenocytes were analyzed 10 dpt. FoxP3 expression was induced in none of our conditions (Figure 34), indicating that persistent antigen presentation itself is not sufficient to induce Treg precuror cells in this model. Our finding is in agreement with Szymczak-Workman et al., showing that TCR stimulation is not absolutely required for Treg activation (Szymczak-Workman et al., 2009).

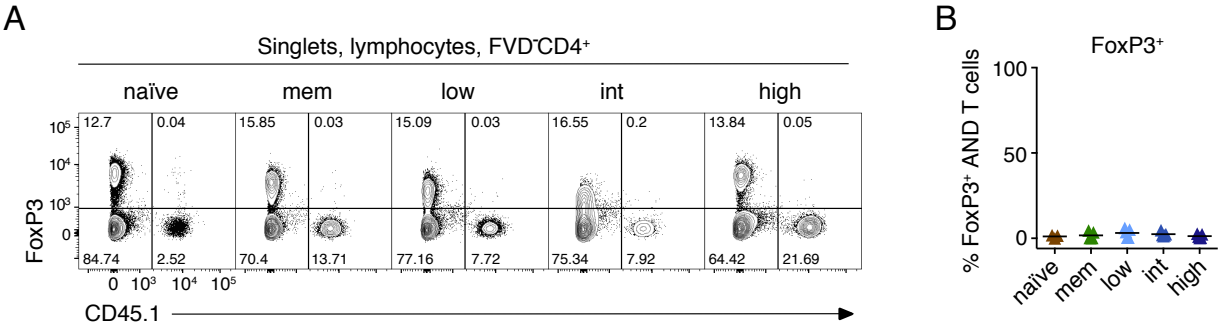

Fig 34: Treg differentiation is not induced by persisting antigen presentation in the periphery. Quantification of 1 x 10^6 adoptively transferred AND T cells using flow cytometry. Naïve, memory (mem), low, intermediate (int), and high AND $CD4^+$ T cells were generated as described in Figure 10A. Spleens were harvested 10 days post transfer. AND T cells shown were identified using the gating strategy described in Figure 8B. (A) Representative histograms showing intracellular expression levels of the Treg-specific transcription factor FoxP3 in endogenous ($CD4^+CD45.1^-$) and transferred AND T cells ($CD4^+CD45.1^+$). (B) Statistical quantification. Data were pooled from three independently performed experiments, each triangle represents one mouse.

4.5.9 $CD4^+$ T cells chronically exposed to antigen fail to transmit B cell help

During acute infections, Tfh cells promote B-cell-mediated immunity (Crotty, 2015; Hale et al., 2013). Whether $CD4^+$ T cells differentiate towards Tfh(-like) cells during chronic conditions (Brooks et al., 2006a; Elsaesser et al., 2009; Fahey et al., 2011) or become exhausted (Vella et al., 2017) is unclear. To address this question, we analyzed Tfh-associated markers and B cell proliferation transmitted by antigen-exhausted AND T cells. Gene-expression analyses showed significantly increased RNA levels encoding Tfh-associated markers such as PD-1, CXCR5, and ICOS, the key transcription factor Bcl-6, and interleukin IL-21. Dose-dependent induction of PD-1 expression was validated in Figure 27A. Here, we tested for surface expression of CXCR5 and ICOS on naïve, memory, low, intermediate, and high AND T cells using flow cytometry. Cells were generated according to Figure 10A, splenocytes were isolated and analyzed. In all three antigen-persisting conditions CXCR5 and ICOS expression was significantly induced. Intermediate AND T cells showed the highest expression of CXCR5. ICOS expression was induced with increasing antigen dose (Figure 35A, B).

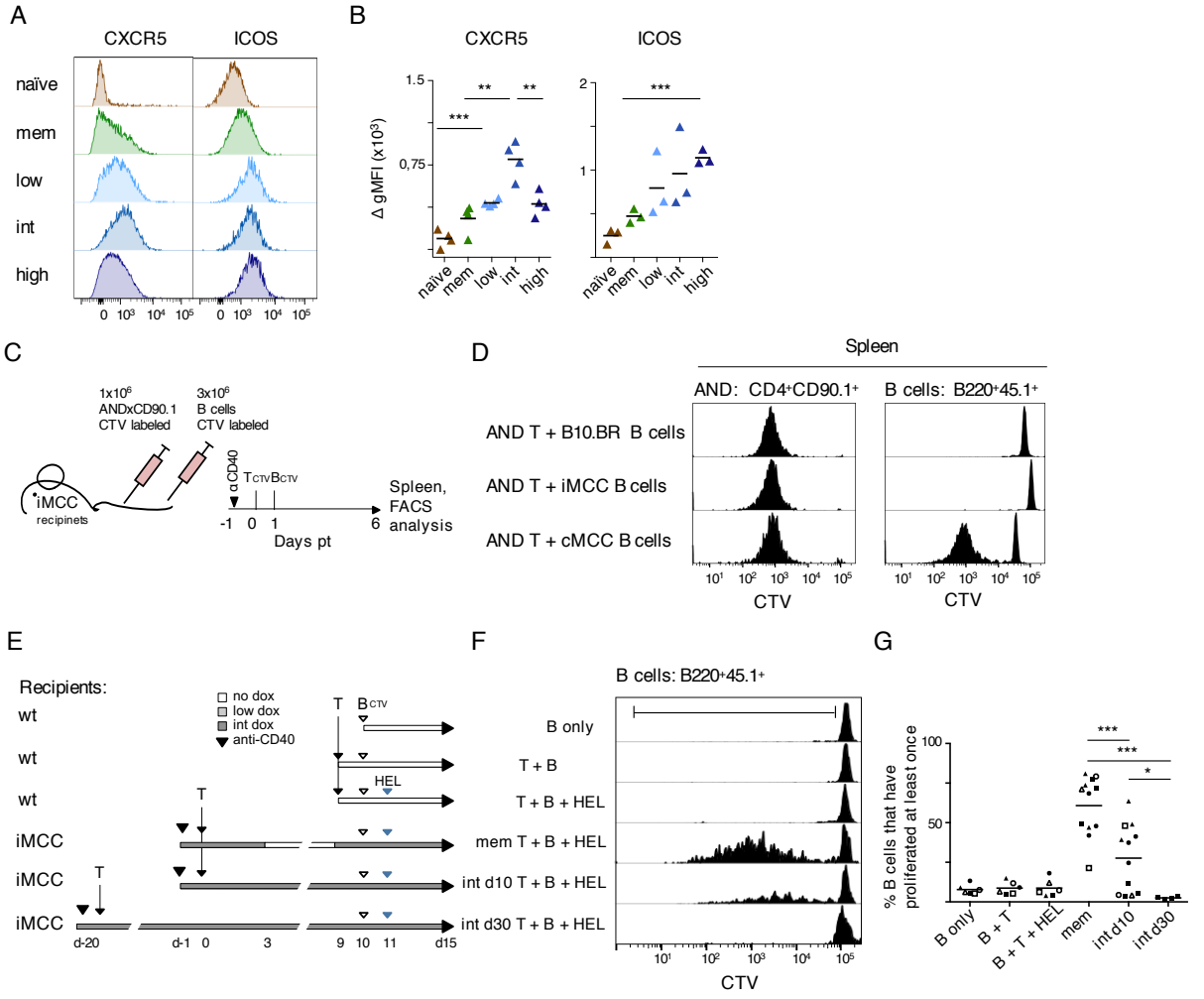

Figure 35: CD4⁺ T cells chronically exposed to antigen failed to transmit help to B cells. (A and B) Quantification of 1 x 10^6 adoptively transferred AND T cells using flow cytometry. Naïve, memory, low, int, and high AND CD4⁺ T cells were generated as described in Figure 10A. Spleens were harvested 10 days post transfer (dpt). AND T cells shown were identified using the gating strategy described in Figure 8A. Memory (mem), low, intermediate (int), and high represents the dose of antigen AND T cells have seen beyond the priming phase as schemed in Figure 10A. (A) Representative histograms showing surface expression of Tfh-associated markers CXCR3 and ICOS analyzed on day 10 pt. (B) Statistical quantification of the markers described in (A). Delta geometrical means were calculated by $gMFI_{Sample}$ - $gMFI_{isotype\ control}$. (C, D) Pilot experiment to analyze B and T cell proliferation in response to antigen presentation. (C) Schematic outline of the experimental set up. (D) CTV dilution of AND T cells and different B cells; B10.BR (wt) B cells as non-antigen presenting B cells, iMCC B cells without dox treatment also serve as non-antigen presenting B cells, and cMCC B cells presenting cognate antigen to AND T cells constitutively. (E – G) B cell help transmitted by antigen-exhausted AND T cells. (E) Experimental set up and treatment strategy to analyze T and B cell interaction upon chronically T cells stimulation. Memory, int (day 10), and int (day 30) were generated as indicated. Dox treatment of memory mice was switched on again on day 9 pt. Control mice were all set the same day as indicated, AND T cells were transferred into wt hosts. 10 dpt 5x10^6 CTV labeled cMCC B cells were transferred into the mice hosting AND T cells. One day after B cell transfer 1 ng hen egg lysozyme (HEL) was injected ip. Five days post B cell transfer Spleens were harvested and analyzed using flow cytometry. (F) Representative results showing CTV dilution of B cells. (G) Graph shows the percentage of B cells that have proliferated at least once. Data were pooled from at least three (B), one (D), and 15 (G) independently performed experiments, each data point represents one mouse. *$p < 0.05$, **$p < 0.001$, ***$p < 0.0001$, parametric unpaired two-tailed t-test.

These data suggest that chronic antigen stimulation induces a Tfh-like phenotype. Therefore, we examined if antigen-exhausted AND T cells were able to transmit help to B cells. As a readout we used B cell proliferation induced by intermediate day 10 and day 30 AND T cells. To establish T and B cell interaction we ran a pilot experiment which showed that B cell proliferation was induced only in antigen-expressing B cells. CTV-labeled AND T cells were transferred into iMCC recipient mice and CTV-labeled, congenically marked B cells were transferred one day later (Figure 35C). Recipient #1 received B10.BR wt B cells, #2 iMCC B cells, both are not antigen-specific and do not express MCC on E^k, and #3 received cMCC B cells expression MCC on E^k. Splenocytes were analysed five days post B cell transfer. AND T cells proliferated in all recipients in response to MCC expressed by host DCs (Figure 35D, left) but only antigen-presenting B cells (#3) proliferated (Figure 35D, right). These results demonstrate that AND T cells mediate proliferation of antigen-presenting B cells. Thus, indicating that effector AND T cells are able to transmit help to B cells inducing proliferation.

We then asked if antigen-exhausted AND T cells are also able to provide help to B cells. We analyzed B cell proliferation induced by day 10 and day 30 antigen-exhausted AND T cells, compared to day 10 memory AND T cells. T cell phenotypes were established before B cells were transferred (Figure 35E) to read out the effect of antigen-persistence at an intermediate dose on T cell functionality. A set of negative controls were included to establish that B cell proliferation was induced by functional T cell help only. $3x10^6$ CTV-labeled cMCCxSW B cells, expressing MCC on E^k (MHC II) and a hen egg lysozyme (HEL)-specific transgenic BCR (Brink et al., 2015), were used. Very low dose of HEL (1 ng) was injected as indicated. HEL was not sufficient to induce B cell proliferation itself, as there was no B cell proliferation detectable in control #3 (Figure 35F). All spleens were harvested and analyzed on the same day, 5 days post B cell transfer. Memory AND T cells were able to induce B cell proliferation (Figure 35F, G). However, the B cell proliferation rate was significantly reduced by antigen-persistence in a time-dependent manner. B cells interacting with day 10 antigen-exhausted AND T cells showed significantly reduced proliferation, which was completely lost when AND T cells were exposed to antigen for 30 days (Figure 35F, G). These results indicate that even though AND T cells up-regulate Tfh-associated surface markers, such as CXCR5, ICOS, and PD-1, they fail to transmit help to B cells.

5. Discussion

Protective immunity against chronic infections or tumor cells significantly relies on intact CD4+ T cell functionality. An important question concerning protective immunity is whether and how CD4+ T cells become exhausted by chronic antigen presentation. In contrast to CD8+ T cell exhaustion, the cause of CD4+ T cell dysfunctionality and its plasticity are rarely investigated. Both, CD4+ T cell exhaustion as well as Tfh cell differentiation caused by chronic TCR stimulation have been reported. Here, we have analyzed the effects of mere antigen persistence beyond the priming phase, with the focus on antigen dose and timing, on phenotype, functionality, signaling, and transcription of antigen-specific CD4+ T cells. We have shown that chronically stimulated CD4+ T cells have impaired cytokine production and exhibit a dose-dependent upregulation of exhaustion-, anergy-, and Tfh-associated genes. Our data further demonstrated that chronic CD4+ T cells are able to continuously sense persistent antigen, even at the highest dose where TCR/CD3 complexes and downstream signaling molecules and pathways were chronically downregulated. Furthermore, qualitative and quantitative changes in the cells' transcriptional profiles highlighted a common signature describing antigen-induced T cell anergy and exhaustion. We have also shown that antigen-exhausted CD4+ T cells lose their ability to provide help to B cells over time. Together, our results underline the importance of antigen disappearance after priming to generate functional Tmem cells. Persistent antigen, dependent on dose and timing, contribute to the plasticity of CD4+ T cells and determine their range of dysfunctionality or anergy.

5.1 CD4+ T cells are sensitive to initial antigen quality

Different amounts of cognate antigen during the priming phase of CD4+ T cells induced dose-dependent T cell activation and proliferation. Intermediate- and high-doses of antigen activated antigen specific CD4+ T cells already 16 hours post transfer *in vivo* and induced rapid phenotypic changes. In contrast, low-level antigen failed to do so, evidenced by baseline expression of the early activation marker CD69 and Nur77-GFP, a reporter for TCR signal strength (Moran et al., 2011). Thus, this indicates that CD4+ T cells require a certain degree of stimulation to become activated. If the stimulating dose of antigen was low, T cell activation was delayed, and phenotypic changes established only slowly. Further, the proliferative capacity of specific CD4+ T cells reflected a dose-dependent response. The more antigen T cells encountered, the more homogenous were the proliferation profiles. This indicates that CD4+ T cells accumulate weak TCR stimulations over time to overcome a certain threshold of activation. Thus, we conclude

that CD4+ T cells are able to sense and discriminate antigen quality and respond antigen-dose-dependently. This conclusion is in agreement with the finding that CTLs, stimulated by increasing amount of cognate antigen presented by APCs in a coculture system *in vitro*, revealed a dose-dependent cytotoxic activity, which exhibited hyporesponiveness in response to high-dose pMHC (Wolchinsky et al., 2014).

5.2 Persisting antigen impairs CD4+ T cell memory differentiation

In the mouse model used here, antigen removal by day five allows for the differentiation of a T cell memory phenotype, as shown by efficient production of IL-2, TNF-α, and IFN-γ (Han et al., 2010; Obst et al., 2007). In contrast, persistent antigen presentation beyond the priming phase impaired memory cell formation. The dose of persistent antigen determined the level of reduced IL-2, TNF-α, and IFN-γ production in response to PMA/IM re-stimulation on day 10. Loss of effector function appeared in a dose-dependent and progressive fashion with IL-2 being most sensitive to antigen dose, while TNF-α and IFN-γ production was reduced more gradually in correlation with antigen quality. Our data confirm the findings of Brooks et al., 2006a and Crawford et al., 2014, showing that IL-2, TNF-α, and IFN-γ production are impaired in LCMV cl13-exhausted CD4+ T cells. Several studies on CD8+ T cell exhaustion caused by chronic LCMV cl13 infections reported that cytokine production is being lost progressively. IL-2 production is lost first, followed by TNF-α and subsequently, by IFN-γ (Agnellini et al., 2007; Fuller et al., 2004; Mackerness et al., 2010; Shin et al., 2009; Wherry et al., 2003a) thus, supporting our findings. Additionally, surface-expression levels of the memory-associated markers CD127 (Boettler et al., 2006; Huster et al., 2004; Kaech et al., 2003), CD62L (Smalley and Ley, 2005), and Ly6C (Hale et al., 2013; Hanninen et al., 2011; Tokoyoda et al., 2009) were reduced, suggesting phenotypic changes induced by persistent antigen. Taken together, our data demonstrate that CD4+ T cell memory differentiation is affected early if chronic TCR stimulation exceeds a certain threshold. Mere chronic antigen presentation caused the loss of the regular Th1-associated effector functions and impaired memory generation. Thus, we postulate that CD4+ T cells are sensitive to persistent TCR stimulation and adjust their functional unresponsiveness to the dose of persisting antigen.

5.3 Features of antigen-exhausted/anergic CD4+ T cells

After CD4+ T cell depletion, LCMV-cl13-infected mice establish a lifelong unresolving viremia (Matloubian et al., 1994). There is evidence suggesting that CD4+ T cells are not entirely dysfunctional during chronic viral infections but rather differentiate away from a regular Th1-associated phenotype towards a Tfh-associated one (Elsaesser et al., 2009; Fröhlich et al.,

2009). As we and others showed that chronic CD4+ T cells lose their regular effector mechanisms (Crawford et al., 2014; Han et al., 2010) and enter a hyporesponsive state, considered to be an important tolerance mechanism (Schwartz, 2003; Wells, 2009; Wolchinsky et al., 2014), it is important to investigate the changes antigen-specific CD4+ T cells undergo during chronic conditions.

5.3.1 Persisting antigen alters effector function and phenotype

In addition to the progressive loss of the regular Th1 memory-associated cytokine profile, several research groups published that CD4+ Tex cells skew their cytokine production towards Tfh-associated cytokines, such as IL-21 (Brooks et al., 2006b; Crawford et al., 2014; Elsaesser et al., 2009; Fahey et al., 2011; Fröhlich et al., 2009). Our transcriptome analyses support these findings. *Il-21* mRNA expression was significantly increased in CD4+ T cells chronically stimulated by persistent antigen (day 10, up cluster 10 and cluster 14 respectively). In agreement with the hypothesis of Tfh-like differentiation induced by chronic TCR stimulation (Fahey et al., 2011), the Tfh-associated markers ICOS, CXCR5, and PD-1 were significantly upregulated on mRNA and protein levels. ICOS and PD-1 expression positively correlated with antigen dose, while CXCR5 expression was highest at intermediate strength. Our findings agree with data on LCMV cl13-exhausted CD4+ T cells demonstrating high-level surface expression of CXCR5, ICOS and PD-1 (Crawford et al., 2014). Further, expression of the key Tfh-specific master transcription factor B cell lymphoma 6 (BCL-6) is induced in LCMV cl13-exhausted CD4+ T cells (Crawford et al., 2014). In our experiments, *bcl-6* mRNA expression was also elevated by persistent TCR stimulations of intermediate and high amount compared to the conditions leading to memory differentiation (day 10, down cluster 5). A key feature of Tfh cells is to ensure B cell-mediated immunity by driving GC development, promoting antibody affinity maturation, and supporting long-lived plasma cell differentiation (Crotty, 2015). We have shown that chronically stimulated CD4+ T cells downregulate CD154 (CD40L) expression in an antigen dose-dependent fashion. CD40L is a specific ligand for CD40 expressed on professional APCs, such as B cells. CD40L/CD40 ligation triggers bi-directional signals between antigen-specific T and antigen-specific B cells and is necessary for proliferation of both (Evans et al., 2000), provides costimulatory signals by inducing or sustaining co-stimulatory receptor (CR) expression such as CD80 (B7-1) and CD86 (B7-2) (Grewal and Flavell, 1998; Kennedy et al., 1994; Ranheim and Kipps, 1993) and mediates contact-dependent T cell help for B cell differentiation and proliferation (Evans et al., 2000). Humans and mice deficient in either CD40 or CD40L expression lack T cell-mediated antibody responses and GCs (Foy et al., 1996; Kawabe et al., 1994). Our experiments found a reduced CD40L expression and the limited

capacity of chronically stimulated CD4+ T cells to induce B cell proliferation. Nevertheless, there is evidence that chronic TCR stimulation induces Tfh differentiation (Elsaesser et al., 2009; Fahey et al., 2011; Fröhlich et al., 2009). Tfh-associated markers are induced and significant amounts of virus-specific T-cell-dependent antibodies are generated during chronic LCMV cl13 infections in mice and during HCV infections in man (Bartosch et al., 2003; Buchmeier et al., 1980; Vella et al., 2017). Additionally, broadly neutralizing antibodies are generated in HIV patients several years after infection, even if they appear only very rarely (Caskey et al., 2019; West et al., 2013). Tfh-like T cells have also been described in cancer patients (Crotty, 2019) and autoimmune disease (Crotty, 2019) such as rheumatic disease (Deng et al., 2019). Thus, it is tempting to speculate that at least some features of T cell help to B cells remain intact.

5.3.2 Persisting antigen causes surface expression of multiple IRs

Another key feature of CD8+ Tex cells is an increased and sustained surface expression of multiple IRs (Bengsch et al., 2010; Blackburn et al., 2009; Day et al., 2006; Kaufmann et al., 2007; Petrovas et al., 2006; Radziewicz et al., 2007; Trautmann et al., 2006; Urbani et al., 2006; Wherry et al., 2007). IRs negatively influence T cell activation and function. Transient expression is important to restrain immune responses and attenuating T cell activation when the infection is cleared to prevent dangerous auto-pathology. Prolonged IRs surface expression, however, was described to induce dysfunctional states of CD8+ Tex cells (Bengsch et al., 2010; Blackburn et al., 2009; Day et al., 2006; Kaufmann et al., 2007; Petrovas et al., 2006; Radziewicz et al., 2007; Trautmann et al., 2006; Urbani et al., 2006; Wherry et al., 2007). Previously, IR surface expression was also reported on LCMV cl13-exhausted CD4+ T cells (Crawford et al., 2014). In line with this, we show in this study a dose-dependent increase in expression levels of PD-1, LAG-3, TIGIT, and CD200/Ox2 on chronically stimulated CD4+ T cells. Since antigen dose and surface-expression levels of IRs positively correlated we suggest that the dose of persistent antigen beyond the priming phase determines the degree of CD4+ T cell dysfunctionality and can be used to characterize the different states of unresponsiveness/ anergy.

5.3.3 Chronic high-dose TCR stimulation results in loss of CD4+ T cells

Recently, several authors described the heterogeneity of the CD8+ Tex pool, consisting of stem-like progenitor Tex cells with the potential of self-renewal and more terminally differentiated exhausted T cells (Paley et al., 2012). Bengsch et al. identified nine different subsets of CD8+ Tex cells based on their specific surface marker expression characteristics (Bengsch et al., 2018). The majority of Tex cells represent terminal CD8+ Tex cells, which have lost the ability

to proliferate and finally enter activation-induced cell death when high-dose antigen stimulation continues to persist (Paley et al., 2012).

Accordingly, even though chronic antigen stimulations allowed CD4+ T cell accumulation on day 10 post transfer to a similar extent when compared to memory CD4+ T cells, we failed to detect chronically high-dose stimulated CD4+ T cells 30 days post transfer. In contrast, low- and intermediate-dose TCR stimulation induced a long-lived phenotype (> 30 days). Since exclusively T cells stimulated with a high-dose failed to survive, we hypothesize that high-dose antigen stimulation possibly drives activation-induced cell death as a physiological negative feedback mechanism, preventing overstimulation/overactivation-mediated auto-pathology within a chronic stimulatory microenvironment.

5.4 Development of antigen-exhausted CD4+ T cells

CD8+ Tex cells isolated within the first two weeks from chronically LCMV cl13 infected animals and transferred back into acutely infected wild type mice are able to reverse their exhausted phenotype and recover towards functional memory T cells (Angelosanto et al., 2012; Brooks et al., 2006a). In contrast, extended priming by persistent antigen stimulation induces irreversible CD8+ T cell dysfunction and an exhausted immunophenotype (Angelosanto et al., 2012; Brooks et al., 2006a; Utzschneider et al., 2016b). This is evidence to conclude that CD8+ T cell exhaustion develops in a progressive way and that its severity depends on the duration of antigen persistence. For CD4+ T cells such experiments have not been done. Here, we addressed the role of chronic TCR stimulation during CD4+ Tex differentiation.

5.4.1 Role of chronic TCR signaling during CD4+ Tex cell differentiation

The severity of CD8+ T cell exhaustion correlates with the dose of antigen and its exposure time, as shown during LCMV cl13 infections in mice and during HBV, HCV, and HIV infections in man (Boni et al., 2007; Goepfert et al., 2000; Reignat et al., 2002; Shankar et al., 2000; Wherry and Kurachi, 2015; Wherry et al., 2003b; Zajac et al., 1998). One observation of this study was that TCR/CD3-complex surface expression is exclusively downregulated by high-dose TCR stimulation. This phenomenon is associated with T cell activation (Cai et al., 1997; Valitutti et al., 1995b; Viola and Lanzavecchia, 1996), and is induced especially by high affinity TCR/pMHC engagement (Cai et al., 1997; Rothenberg, 1996; Valitutti et al., 1995a; Valitutti et al., 1996; Zanders et al., 1983). It has been suggested that TCR/CD3 downmodulation is a mechanism to protect against autoimmunity caused by extensive TCR signaling (Alcover et al., 2018; Rothenberg, 1996). In the experimental system used here, TCR downregulation was induced early, already by day three, and persisted. TCR/CD3-complex degradation has been described

as a modulatory mechanism to reduce TCR surface expression and facilitating or promoting intracellular signal transduction (Alcover et al., 2018; Rothenberg, 1996). We found that TCR/CD3 complexes are intracellularly maintained upon downmodulation and rapidly recycle back to the cell surface in absence of antigenic stimulations. These re-expressed surface TCR/CD3 complexes are not able to transmit TCR signals when stimulated directly via TCR, even though the cells still remained their capacity to produce IFN-γ when stimulated indirect via PMA/IM bypassing TCR/CD3 complexes. This suggests a problem in signal transduction proximal to the TCR/CD3 complex.

With the help of network analysis, we identified *lat* mRNA expression, encoding for the linker of activated T cells (LAT), being significantly reduced exclusively upon high-dose TCR stimulations. We validated this finding also on the protein level. Usually, after productive TCR stimulation LAT is phosphorylated by zeta-chain-associated protein kinase 70 (ZAP-70) (Au-Yeung et al., 2018; Paz et al., 2001). Once phosphorylated, LAT serves as a central adaptor protein recruiting several signaling molecules and thus mediates TCR-mediated signals leading to T cell activation, proliferation, differentiation, and cytokine production. Besides reduced *lat* mRNA expression in high $CD4^+$ T cells LAT protein is also degraded, while TCR/CD3 complexes were maintained intracellular. There is evidence that internalized TCR complexes are still able to transmit TCR signals (Rothenberg, 1996; Saveanu et al., 2019). With the help of the Nur77-GFP reporter for TCR signaling (Moran et al., 2011) we were able to measure TCR signal transduction induced by all three persistently stimulating conditions, even at the highest dose, at which TCR/CD3 complexes were internalized. Thus, it is tempting to speculate that LAT downregulation serves as a negative regulatory mechanism to prevent stimulation-induced T cell overactivation. Reduced LAT protein level might explain why rescued TCR/CD3 complexes fail to transmit productive T cell activating signals and thus, failed to induce Ca^{2+} flux and cytokine production. Thus, LAT downregulation/degradation might play an important role during the progression of T cell exhaustion/dysfunctionality. Hence, it is of interest to investigate the dynamics of this adaptor molecule especially in regard to therapeutic approaches trying to reinvigorate/improve effector functions. In a next step, it would be interesting to analyze if *lat* mRNA expression will also recover after *TCR* re-appearance at the cell surface in absence of antigen and to see whether its protein expression will be re-induced.

5.4.2 Transcriptional profile of antigen-induced $CD4^+$ Tex cells

Previous studies have demonstrated that $CD8^+$ Tex cells represent a unique cell lineage, which is clearly distinct from Teff and Tmem cells regarding their phenotype and functionality (McLane et al., 2019). Network analyses revealed that gene expression profiles of $CD8^+$ and $CD4^+$ LCMV

cl13-exhausted T cells exhibit unique gene-expression patterns and simultaneously share a common gene-expression signature of exhaustion (Crawford et al., 2014). To gain further insights into the mechanisms and pathways involved in CD4+ T cell exhaustion we performed genome-wide transcriptional profiling of naïve, memory, antigen-exhausted, and endogenous anergic T cells. We aimed to identify impaired signal-transduction pathways and genes potentially involved in CD4+ T cell exhaustion. We have shown that antigen-exhausted CD4+ T cells have adjust their gene expression to persisting antigen quantity and quality. We could not identify an obvious skewing towards one specific T helper cell subset. Comparing exhaustion-associated gene-expression clusters with the gene-expression profile of endogenous anergic CD4+ T cells revealed a strong correlation between the gene-expression of both differentiation states. Thus, there is evidence suggesting that persistent antigen presentation induces multiple states of anergy. Interestingly, comparing exhaustion-associated gene-expression clusters identified at an early exhaustion phase (10 days post T cell transfer) with a later chronic phase (30 days post transfer) we found a substantial overlap of induced genes (FDR = 0.00011), indicating that gene-expression patters induced on day 10 are predictive for later induced gene-expression profiles. Hence, genetic changes driving CD4+ T cell dysfunction/anergy induction are probably induced early and are maintained over time.

5.4.3 Transcriptional driver of T cell exhaustion/anergy

Transcriptome analyses revealed an antigen-dependent increase in RNA expression of several transcription factors. As expected, *Fos* and *Jun* expression levels were significantly induced in early memory T cells (Foletta et al., 1998). Cluster analyses identified *Fos* and *Jun* message within the day 10 memory-associated cluster 1. Monomers of Fos and Jun form heterodimers called AP-1, a transcription factor family associated with T cell memory generation (Nakabeppu et al., 1988). *NFATc1* expression was found (together with *Tigit* and *Il-21)* in cluster 14*,* a cluster representing genes that were antigen-dose-dependently expressed. Interestingly, NFATc1 was equally expressed on protein levels in mem, low, intermediate, and high CD4+ T cells. The transcription factors *Tbx21, Runx2, and Maf* were found in cluster 15 (together with *CD44* and *CXCR3*), a cluster representing genes that were induced upon antigen encounter, irrespective of the TCR stimulation intensity beyond the priming phase.

We found cMaf protein expression exclusively upregulated by high-dose TCR stimulation. Thus, post-transcriptional regulation of the transcription factors NFATc1 and cMaf is likely. In cluster 4, which contains genes significantly induced exclusively upon high TCR stimulation, we identified the transcription factors *Tox* and *Id2*. Surprisingly, we found TOX protein expression dose-dependently and uniquely induced by persistent TCR stimulations. The more antigen T

cells encountered beyond the priming phase, the more TOX was expressed. Therefore, we conclude that *Tox* induction is dependent on the stimulants´ nature, e.g. antigen quantity and quality. So far, TOX has been described to be important during thymic CD4+ T cell development (Wilkinson et al., 2002) and there was no correlation to chronic infections or cancer. However, very recently TOX was identified as a key transcription factor driving CD8+ T cell exhaustion (Alfei et al., 2019; Khan et al., 2019; Scott et al., 2019). Kahn, Scott, and Alfei described simultaneously the central role of this transcription factor for CD8+ Tex differentiation. The authors showed that *Tox* expression is induced in CD8+ T cells by chronic high-dose antigen stimulations (Alfei et al., 2019; Khan et al., 2019; Scott et al., 2019). Elevated *Tox* expression-levels were found upon chronic LCMV cl13 infections in mice and HCV infections in human, as well in human CD8+ TILs and peripheral blood mononuclear cells (PBMCs) isolated from melanoma, breast, lung, and ovarian cancers. Further, robust *Tox* expression correlates with increased surface expression of multiple IRs, such as PD-1, Lag-3, 2B4, and Tim-3 (Alfei et al., 2019; Khan et al., 2019; Scott et al., 2019) and translates chronic TCR stimulations into a certain CD8+ Tex gene-expression profile fostering CD8+ Tex commitment (Khan et al., 2019). *Tox*-depleted CD8+ T cells normally differentiate into Teff and Tmen cells upon acute LCMV Armstrong infections demonstrating a redundant role of TOX for Teff and Tmem differentiation (Scott et al., 2019). *Tox*-depleted tumor-specific T cells fail to survive within the chronic tumor microenvironment. Together, there is evidence to suggest that the TOX-driven Tex program is induced by persistent TCR stimulations during chronic viral infections and within the TME and prevents overstimulation/activation-induced cell death (Scott et al., 2019). This finding coincides with the strong contraction observed for CD8+ Tex cells expressing a TOX variant, with a mutated DNA-binding domain that can no longer function as a transcription factor (Alfei et al., 2019). This mutant, however, shows reduced PD-1 expression and increased cytokine-production leading to a polyfunctional phenotype (Alfei et al., 2019). These findings agree with Scott et al., showing that *Tox* depleted CD8+ T cells failed to induce an exhaustion-associated program, as mRNAs encoding for IRs (*Pdcd1, Entpd1, Havcr2, Cd244, Tigit*) were not induced by persisting antigen even though their chromatin accessibility was still intact (Scott et al., 2019). The non-exhausted immunophenotype of Tox-depleted or -mutated “Tex cells” and the fact that ectopic TOX expression induces a Tex-associated gene-expression profile (Scott et al., 2019) provides evidence for TOX being a key transcription factor driving CD8+ T cell exhaustion and dysfunction (Alfei et al., 2019; Khan et al., 2019; Scott et al., 2019). Taking these data on CD8+ Tex cells and our own data demonstrating an antigen-dose-dependent expression of TOX into consideration, it is likely that TOX plays also a central role in controlling CD4+ T cell hypo-responsiveness. To address this hypothesis directly, a $Tox^{fl/fl}$ locus has to be deleted in the exhaustion phase and the effects monitored.

Scott et al. compared Chip-seq data previously published by Martinez et al. (Martinez et al., 2015) with their own ATAC-seq data (Philip et al., 2017; Scott et al., 2019) and found that NFAT binds to regions within the *Tox* locus of $CD8^+$ TILs exhibiting increased chromatin accessibility (Khan et al., 2019; Scott et al., 2019). This suggests a hierarchical role of NFAT in regulating TOX expression. NFAT is a Ca^{2+}-dependent transcription factor that has to be dephosphorylated by activated calcineurin in order to translocate from the cytoplasm into the nucleus to function as a transcriptional regulator (Jain et al., 1993). Inhibition of calcineurin-mediated dephosphorylation of NFAT (using the inhibitor FK506 (Flanagan et al., 1991; Jain et al., 1993; Philip et al., 2017)) prevents nuclear NFAT translocation and causes reduced TOX and PD-1 expression-levels (Scott et al., 2019). These findings are consistent with results reporting that TOX expression requires Ca^{2+} signaling and NFATc1 transcriptional activity (Khan et al., 2019). Here, we demonstrate that nuclear NFATc1 correlates with the dose of persistent antigen. The higher the antigen stimulus of $CD4^+$ T cells was beyond the priming phase, the more NFATc1 translocated into the nucleus. Interestingly, $CD4^+$ T cells stimulated with the strongest stimulus exhibited the highest amount of nuclear NFATc1, even though these cells downregulated TCR/CD3 surface complexes, had reduced LAT protein levels, and did not show detectable Ca^{2+} release. Yet, it is unclear if high-dose TCR stimulations caused undetectable tonic Ca^{2+} release close to base-line levels and thus provoked NFATc1 translocation or whether NFATc1 relocation mechanisms were inhibited by high-dose antigen causing NFATc1 to be trapped inside the nucleus upon its translocation in response to very early, strong TCR stimulation. Nevertheless, once in the nucleus NFAT regulates gene-expression pattern depending on its binding partner. For instance, cooperative NFAT:AP-1 complexes act to favor T cell differentiation towards a memory phenotype, are associated with $CD8^+$ T cell effector functions and trigger activation-induced genes (Martinez et al., 2015). In contrast, NFAT homodimers, so-called partnerless NFAT that are generated in the absence of AP-1, drive an exhaustion-associated immunophenotype (Martinez et al., 2015). AP-1 itself is a heterodimer of Jun and Fos family members (Foletta et al., 1998; Nakabeppu et al., 1988; Rincon and Flavell, 1994), which drives Th1 effector responses (Ip and Davis, 1998; Whitmarsh and Davis, 1996; Yang et al., 1998). AP-1 generation depends on TCR-mediated activation of the JNK/MAP kinase signaling pathways (Ip and Davis, 1998; Whitmarsh and Davis, 1996; Yang et al., 1998). Activated JNK kinase phosphorylates its substrate c-Jun (Rincon and Flavell, 1994), which is subsequently able to generate heterodimers with Fos. We found that $CD4^+$ T cells stimulated with intermediate- or high-doses of antigen were impaired or not able to phosphorylate c-Jun, hence no heterodimers with Fos were formed and no AP-1 transcription factors generated. Consequently, high-quality TCR stimulations that downregulated TCR/CD3 surface complexes and intracellular LAT abundance, failed to activate the JNK/MAPK pathway and therefore lack

AP-1 transcription factors in the nucleus generating partnerless NFATc1 to induce an altered, exhaustion-associated transcriptional profile. Taken together, partnerless NFATc1 and IR expression, such as PD-1, Lag-3, and Ox2, correlate with the strength of TCR stimulation. These findings, together with the observations described for chronic $CD8^+$ T cells, strengthen the hypothesis that “asymmetrical” signaling via partnerless NFATc1 drives *Tox* expression within chronically stimulated $CD4^+$ T cells in an antigen-dose-dependent manner. This may mean that TOX is a key transcription factor driving $CD4^+$ T cell exhaustion/dysfunction/anergy and requires experimental investigations.

5.5 Dysfunctional $CD4^+$ T cells maintain plasticity

Anergy has been described as an acquired state of immune cells hallmarked by unresponsiveness and describes an antigen-specific state of dysfunctionality. It is been seen as a mechanism to protect from autoimmune disorders (Chappert and Schwartz, 2010; Kalekar et al., 2016; Schwartz, 1990; Wells, 2009) and immunopathology (Knoechel et al., 2005; Martinez et al., 2012). Mueller and colleagues, have described two surface markers that characterize anergic T cells: CD73 (*Nt5e*) and FR4 (*Izumolr*) (Kalekar et al., 2016; Martinez et al., 2012). Interestingly, both markers positively correlate with the amount of antigen presented beyond the priming phase to $CD4^+$ T cells. So far, anergic T cells have been described in cancer patients where positive signal 2/co-stimulation is missing or is being overwritten by a negative signal 2 mediated by IRs (Blank et al., 2004; Curiel et al., 2003; Zou and Chen, 2008). Since anergic T cells are additionally characterized by reduced IL-2 production, increased IR surface expression (PD-1, CTLA-4, and Lag-3), and impaired mTOR and MAPK signaling (Zheng et al., 2012), we performed transcriptome analyses of endogenous anergic $CD4^+$ T cells to compare their specific gene signature with the signature of antigen-exhausted $CD4^+$ T cells. We found that the transcriptional profiles of antigen-exhausted and endogenous anergic $CD4^+$ T cells strongly overlapped. A central role in anergy induction was ascribed to the homodimers of the transcription factors early growth response gene 2 (Egr2) and NFAT (Anandasabapathy et al., 2003; Soto-Nieves et al., 2009; Zheng et al., 2012). The mRNA levels of both transcription factors were significantly induced by persisting TCR stimulation. *Nfatc1* was induced upon TCR stimulation independent of antigen dose, while *Egr2,* according to transcriptome analysis, was uniquely induced by an intermediate dose of persistent TCR stimulation. As discussed above, while nuclear NFATc1 correlated with the strength of stimulation, MAPK pathway activity showed an inverse correlation. As a consequence of an interrupted MAPK pathway by high-dose TCR stimulations, Jun phosphorylation was inhibited, AP-1 generation disrupted and thus,

NFAT homodimer generation induced. NFAT homodimers were linked previously to the generation of CD8+ T cell exhaustion (Martinez et al., 2015).

Further, anergic T cells have been proposed to be precursor cells for peripheral FoxP3-expressing Treg cells (Kalekar et al., 2016). We analyzed FoxP3 expression levels of antigen-exhausted AND T cells and found no FoxP3 induction detectable, neither on mRNA nor on protein levels. Therefore, we conclude that mere antigen persistence is not sufficient to induce Treg differentiation of AND T cells, a clone generally unlikely to commit to the Treg fate (Szymczak-Workman et al., 2009).

We found that surface expression of anergy-associated markers FR4 and CD73 remained reversible upon antigen removal on day 10. Thus, our data confirm the observation that T cell anergy is reversible when anergic CD4+CD44+FR4+CD73+ T cells were transferred into lymphopenic mice (Kalekar et al., 2016). Under a lymphopenic condition, anergic T cells downregulated their FR4 and CD73 surface expression and regained their proliferative capacity (Kalekar et al., 2016). We further found that the expression of the memory-associated markers CD127 and Ly6C, for CD154/CD40L also remained reversible. The same was true for surface expression of IRs such as PD-1 and even for the production of regular Th1-associated effector cytokines, such as IL-2, TNF-α, and IFN-γ. Our results are in agreement with the finding that progenitor CD8+ Tex cells are able to re-establish effector functions when isolated early, within the first two weeks of chronic LCMV cl13 infections, while terminal Tex cells fail to do so (McLane et al., 2019). Thus, there is evidence to suggest that CD4+ T cell dysfunction remain reversible upon antigen removal. All together, we conclude that mere antigen presentation beyond the priming phase drives CD4+ T cell differentiation towards multiple states of anergy depending on antigen-dose and -timing, thus on quality and quantity of chronic antigen presentation and that the dysfunctional state of CD4+ T cells can be reversed.

CD4+ T cells chronically exposed to different levels of antigen beyond the priming phase deviate towards multiple states of anergy. Our data demonstrate that functional unresponsiveness/anergy is caused in the periphery by mere chronic antigen presentation as a gradual and reversible process. Anergy induction is important to protect from dangerous autoimmune disorders and immunopathology, but it comes with the cost of an impaired/lost defense against chronic viral infections and cancer.

5.6 Therapeutic implications

Our findings may be exploited for the generation of novel immunotherapeutic strategies. Only about 20 – 30% of cancer patients treated with immune checkpoint blocking antibodies benefit from therapy (Fesnak et al., 2016). In these patients Tex cells, the key cells responding to

checkpoint blockades (Huang et al., 2017; Kamphorst et al., 2017; Twyman-Saint Victor et al., 2015) fail to proliferate, lack cytotoxic activity, and reveal reduced effector cytokine production *ex vivo*. This indicates that T cell exhaustion can hamper immunotherapies. Thus, our results provide important clues on how to optimize dose and timing of therapeutic antibodies or adapter molecules (specific antibody conjugates) that recruit endogenous and/or CAR T cells to the tumor, in order to minimize the induction of T cell exhaustion or anergy. As T cell dysfunctionality is caused by persisting TCR stimulation and is still reversible during early stages, therapeutic antibody derivates should be administered discontinuously. This way T cells will not be persistently stimulated and consequently, hopefully do not enter anergic states. It is tempting to speculate that a defined pause of treatment could prevent T cell exhaustion. This, however, has to be further investigated. Moreover, since we show that the dose of TCR stimulus plays a decisive role in the loss of effector function, the amount of administered therapeutic antibodies could be given a careful consideration.

5.7 Graphical summary

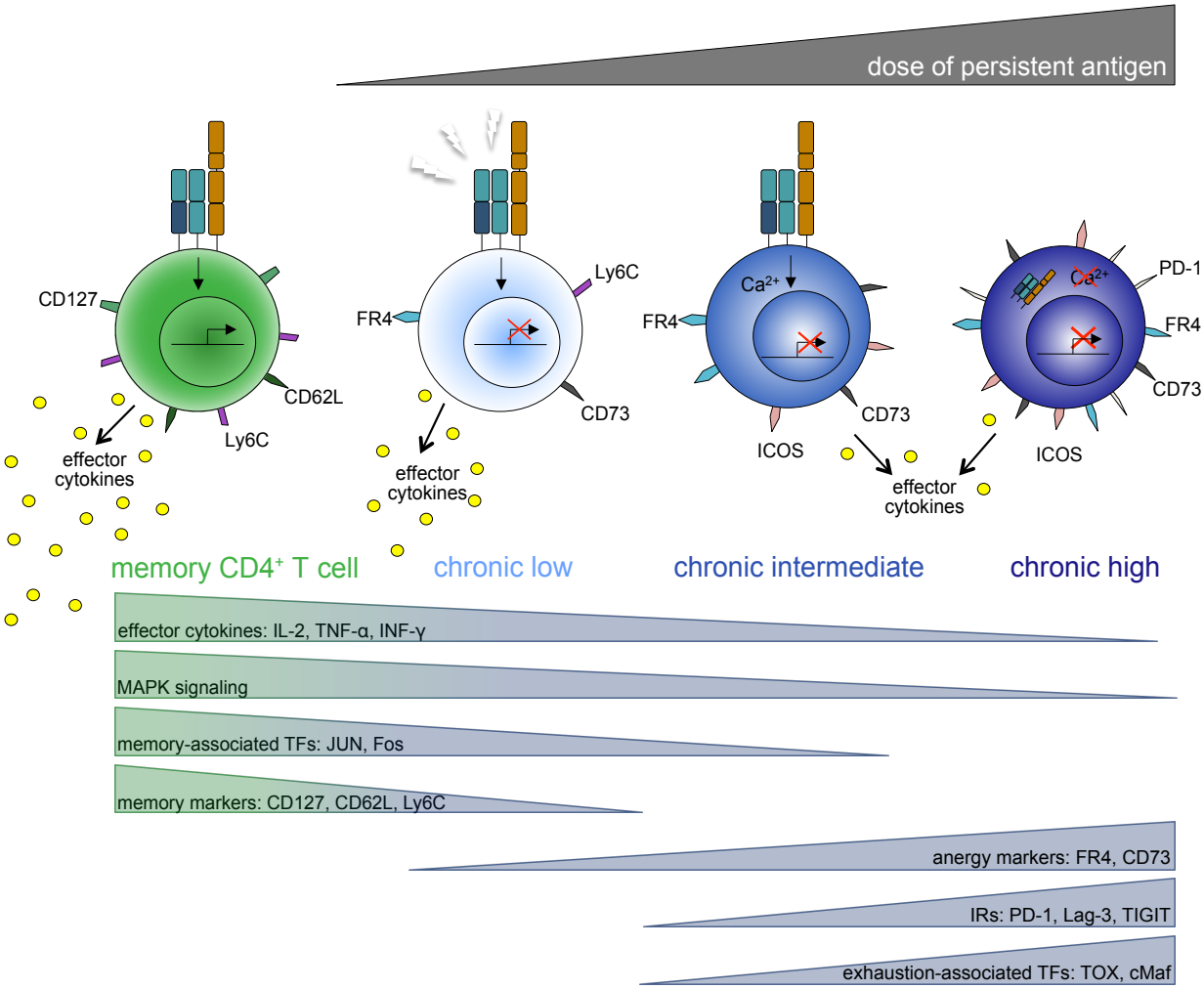

Figure 36: Gradually induced functional unresponsiveness of antigen-exhausted CD4⁺ T cells. Transient antigen presentation drives functional CD4⁺ Tmem generation (green cell). Low level of persistent cognate antigen generated an anergic state, which progressed slowly over time and was characterized by a memory-like phenotype and transcriptional profile but also by impaired IL-2 production, reduced memory marker expression (CD127 and CD62L), and low but significant upregulation of anergy-associated markers (FR4 and CD73) (light-blue cell). Intermediate antigen-level generated an anergic state, characterized by unique gene expression patterns, impaired effector functions (IL-2, TNF-α, and IFN-γ production), reduced memory- (CD127, Ly6C, and CD62L), and increased anergy-marker expression (FR4 and CD73). An exhaustion-associated transcription factor profile (partnerless nuclear NFATc1 and intermediate dose of TOX) and impaired transmission of B cell help were further characteristics (middle-blue cell). And high-level of chronic antigen presentation caused an anergic state, characterized by unique gene expression patterns, impaired effector functions (IL-2, TNF-α, and IFN-γ production), reduced memory- (CD127, Ly6C, and CD62L), and increased anergy-associated marker expression (FR4 and CD73), as well as upregulated multiple IRs (PD-1, LAG-3, TIGIT, Ox2/CD200). An exhaustion-associated transcription factor profile (partnerless nuclear NFATc1, high dose of TOX and cMaf), and modified TCR signal pathway (MAPK) including significantly reduced surface TCR complexes and LAT expression levels and finally activation induced cell death defined this anergic state (dark-blue cell). However, anergic CD4⁺ T cells revealed their plasticity upon the termination of chronic TCR stimulation (FR4 and CD73, as well as IRs expression, and cytokine production was reversible upon antigen termination). Nevertheless, they might not be able to skew (back) towards a common memory path of differentiation (Crawford et al., 2014) but rather represent a unique redirected program (Hale et al., 2013). Hence, implying that the dose and time of antigen presented beyond the priming phase has the power to fundamentally change the transcriptional and translational regulation and thus, the phenotype and functionality of CD4⁺ T cells.

6. References

Abel, M., Sene, D., Pol, S., Bourliere, M., Poynard, T., Charlotte, F., Cacoub, P., and Caillat-Zucman, S. (2006). Intrahepatic virus-specific IL-10-producing CD8 T cells prevent liver damage during chronic hepatitis C virus infection. Hepatology 44, 1607-1616.

Agnellini, P., Wolint, P., Rehr, M., Cahenzli, J., Karrer, U., and Oxenius, A. (2007). Impaired NFAT nuclear translocation results in split exhaustion of virus-specific CD8+ T cell functions during chronic viral infection. Proc Natl Acad Sci USA 104, 4565-4570.

Ahmadzadeh, M., Johnson, L.A., Heemskerk, B., Wunderlich, J.R., Dudley, M.E., White, D.E., and Rosenberg, S.A. (2009). Tumor antigen-specific CD8 T cells infiltrating the tumor express high levels of PD-1 and are functionally impaired. Blood 114, 1537-1544.

Ahmed, R., Byrne, J.A., and Oldstone, M.B. (1984). Virus specificity of cytotoxic T lymphocytes generated during acute lymphocytic choriomeningitis virus infection: role of the H-2 region in determining cross-reactivity for different lymphocytic choriomeningitis virus strains. J Virol 51, 34-41.

Aivazian, D., and Stern, L.J. (2000). Phosphorylation of T cell receptor zeta is regulated by a lipid dependent folding transition. Nat Struct Biol 7, 1023-1026.

Alcover, A., Alarcon, B., and Di Bartolo, V. (2018). Cell Biology of T Cell Receptor Expression and Regulation. Annu Rev Immunol 36, 103-125.

Alfei, F., Kanev, K., Hofmann, M., Wu, M., Ghoneim, H.E., Roelli, P., Utzschneider, D.T., von Hoesslin, M., Cullen, J.G., Fan, Y., et al. (2019). TOX reinforces the phenotype and longevity of exhausted T cells in chronic viral infection. Nature 571, 265-269.

Alfei, F., and Zehn, D. (2017). T cell exhaustion: an epigenetically imprinted phenotypic and functional makeover. Trends Mol Med 23, 769-771.

Althage, A., Odermatt, B., Moskophidis, D., Kundig, T., Hoffman-Rohrer, U., Hengartner, H., and Zinkernagel, R.M. (1992). Immunosuppression by lymphocytic choriomeningitis virus infection: competent effector T and B cells but impaired antigen presentation. Eur J Immunol 22, 1803-1812.

Anandasabapathy, N., Ford, G.S., Bloom, D., Holness, C., Paragas, V., Seroogy, C., Skrenta, H., Hollenhorst, M., Fathman, C.G., and Soares, L. (2003). GRAIL: an E3 ubiquitin ligase that inhibits cytokine gene transcription is expressed in anergic CD4+ T cells. Immunity 18, 535-547.

Anderson, A.C., Joller, N., and Kuchroo, V.K. (2016). Lag-3, Tim-3, and TIGIT: Co-inhibitory Receptors with Specialized Functions in Immune Regulation. Immunity 44, 989-1004.

Angelosanto, J.M., Blackburn, S.D., Crawford, A., and Wherry, E.J. (2012). Progressive loss of memory T cell potential and commitment to exhaustion during chronic viral infection. J Virol 86, 8161-8170.

Araki, K., Youngblood, B., and Ahmed, R. (2013). Programmed cell death 1-directed immunotherapy for enhancing T-cell function. Cold Spring Harb Symp Quant Biol 78, 239-247.

Au-Yeung, B.B., Shah, N.H., Shen, L., and Weiss, A. (2018). ZAP-70 in signaling, biology, and disease. Annu Rev Immunol 36, 127-156.

Aubert, R.D., Kamphorst, A.O., Sarkar, S., Vezys, V., Ha, S.J., Barber, D.L., Ye, L., Sharpe, A.H., Freeman, G.J., and Ahmed, R. (2011). Antigen-specific CD4 T-cell help rescues exhausted CD8 T cells during chronic viral infection. Proc Natl Acad Sci U S A 108, 21182-21187.

Baine, I., Abe, B.T., and Macian, F. (2009). Regulation of T-cell tolerance by calcium/NFAT signaling. Immunol Rev 231, 225-240.

Baitsch, L., Baumgaertner, P., Devevre, E., Raghav, S.K., Legat, A., Barba, L., Wieckowski, S., Bouzourene, H., Deplancke, B., Romero, P., et al. (2011). Exhaustion of tumor-specific CD8+ T cells in metastases from melanoma patients. J Clin Invest 121, 2350-2360.

Baixeras, E., Huard, B., Miossec, C., Jitsukawa, S., Martin, M., Hercend, T., Auffray, C., Triebel, F., and Piatier-Tonneau, D. (1992). Characterization of the lymphocyte activation gene 3-encoded protein. A new ligand for human leukocyte antigen class II antigens. J Exp Med 176, 327-337.

Balachandran, V.P., Luksza, M., Zhao, J.N., Makarov, V., Moral, J.A., Remark, R., Herbst, B., Askan, G., Bhanot, U., Senbabaoglu, Y., et al. (2017). Identification of unique neoantigen qualities in long-term survivors of pancreatic cancer. Nature 551, 512-516.

Barber, D.L., Wherry, E.J., Masopust, D., Zhu, B., Allison, J.P., Sharpe, A.H., Freeman, G.J., and Ahmed, R. (2006). Restoring function in exhausted CD8 T cells during chronic viral infection. Nature 439, 682-687.

Barber, E.K., Dasgupta, J.D., Schlossman, S.F., Trevillyan, J.M., and Rudd, C.E. (1989). The CD4 and CD8 antigens are coupled to a protein-tyrosine kinase (p56lck) that phosphorylates the CD3 complex. Proc Natl Acad Sci U S A 86, 3277-3281.

Barnstorf, I., Borsa, M., Baumann, N., Pallmer, K., Yermanos, A., Joller, N., Spörri, R., Welten, S.P.M., Kräutler, N.J., and Oxenius, A. (2019). Chronic virus infection compromises memory bystander T cell function in an IL-6/STAT1-dependent manner. J Exp Med 216, 571-586.

Bartosch, B., Bukh, J., Meunier, J.C., Granier, C., Engle, R.E., Blackwelder, W.C., Emerson, S.U., Cosset, F.L., and Purcell, R.H. (2003). In vitro assay for neutralizing antibody to hepatitis C virus: evidence for broadly conserved neutralization epitopes. Proc Natl Acad Sci U S A 100, 14199-14204.

Bengsch, B., Martin, B., and Thimme, R. (2014). Restoration of HBV-specific CD8+ T cell function by PD-1 blockade in inactive carrier patients is linked to T cell differentiation. J Hepatol 61, 1212-1219.

Bengsch, B., Ohtani, T., Herati, R.S., Bovenschen, N., Chang, K.M., and Wherry, E.J. (2018). Deep immune profiling by mass cytometry links human T and NK cell differentiation and cytotoxic molecule expression patterns. J Immunol Methods 453, 3-10.

Bengsch, B., Seigel, B., Ruhl, M., Timm, J., Kuntz, M., Blum, H.E., Pircher, H., and Thimme, R. (2010). Coexpression of PD-1, 2B4, CD160 and KLRG1 on exhausted HCV-specific CD8+ T cells is linked to antigen recognition and T cell differentiation. PLoS Pathog 6, e1000947.

Bi, J., and Tian, Z. (2017). NK cell exhaustion. Front Immunol 8, 760.

Blackburn, S.D., Shin, H., Haining, W.N., Zou, T., Workman, C.J., Polley, A., Betts, M.R., Freeman, G.J., Vignali, D.A., and Wherry, E.J. (2009). Coregulation of CD8+ T cell exhaustion by multiple inhibitory receptors during chronic viral infection. Nat Immunol 10, 29-37.

Blank, C., Brown, I., Peterson, A.C., Spiotto, M., Iwai, Y., Honjo, T., and Gajewski, T.F. (2004). PD-L1/B7H-1 inhibits the effector phase of tumor rejection by T cell receptor (TCR) transgenic CD8+ T cells. Cancer Res 64, 1140-1145.

Bluestone, J.A., Mackay, C.R., O'Shea, J.J., and Stockinger, B. (2009). The functional plasticity of T cell subsets. Nat Rev Immunol 9, 811-816.

Boettler, T., Panther, E., Bengsch, B., Nazarova, N., Spangenberg, H.C., Blum, H.E., and Thimme, R. (2006). Expression of the interleukin-7 receptor alpha chain (CD127) on virus-specific CD8+ T cells identifies functionally and phenotypically defined memory T cells during acute resolving hepatitis B virus infection. J Virol 80, 3532-3540.

Boni, C., Fisicaro, P., Valdatta, C., Amadei, B., Di Vincenzo, P., Giuberti, T., Laccabue, D., Zerbini, A., Cavalli, A., Missale, G., et al. (2007). Characterization of hepatitis B virus (HBV)-specific T-cell dysfunction in chronic HBV infection. J Virol 81, 4215-4225.

Bonifaz, L.C., Bonnyay, D.P., Charalambous, A., Darguste, D.I., Fujii, S., Soares, H., Brimnes, M.K., Moltedo, B., Moran, T.M., and Steinman, R.M. (2004). In vivo targeting of antigens to maturing dendritic cells via the DEC-205 receptor improves T cell vaccination. J Exp Med 199, 815-824.

Borrow, P., Evans, C.F., and Oldstone, M.B. (1995). Virus-induced immunosuppression: immune system-mediated destruction of virus-infected dendritic cells results in generalized immune suppression. J Virol 69, 1059-1070.

Brink, R., Paus, D., Bourne, K., Hermes, J.R., Gardam, S., Phan, T.G., and Chan, T.D. (2015). The SW(HEL) system for high-resolution analysis of in vivo antigen-specific T-dependent B cell responses. Methods Mol Biol 1291, 103-123.

Brooks, D.G., Ha, S.J., Elsaesser, H., Sharpe, A.H., Freeman, G.J., and Oldstone, M.B. (2008). IL-10 and PD-L1 operate through distinct pathways to suppress T-cell activity during persistent viral infection. Proc Natl Acad Sci U S A 105, 20428-20433.

Brooks, D.G., McGavern, D.B., and Oldstone, M.B. (2006a). Reprogramming of antiviral T cells prevents inactivation and restores T cell activity during persistent viral infection. J Clin Invest 116, 1675-1685.

Brooks, D.G., Trifilo, M.J., Edelmann, K.H., Teyton, L., McGavern, D.B., and Oldstone, M.B. (2006b). Interleukin-10 determines viral clearance or persistence in vivo. Nat Med 12, 1301-1309.

Buchmeier, M.J., Welsh, R.M., Dutko, F.J., and Oldstone, M.B. (1980). The virology and immunobiology of lymphocytic choriomeningitis virus infection. Adv Immunol 30, 275-331.

Bucks, C.M., Norton, J.A., Boesteanu, A.C., Mueller, Y.M., and Katsikis, P.D. (2009). Chronic antigen stimulation alone is sufficient to drive $CD8^+$ T cell exhaustion. J Immunol 182, 6697-6708.

Cai, Z., Kishimoto, H., Brunmark, A., Jackson, M.R., Peterson, P.A., and Sprent, J. (1997). Requirements for peptide-induced T cell receptor downregulation on naive $CD8^+$ T cells. J Exp Med 185, 641-651.

Caskey, M., Klein, F., and Nussenzweig, M.C. (2019). Broadly neutralizing anti-HIV-1 monoclonal antibodies in the clinic. Nat Med 25, 547-553.

Caza, T., and Landas, S. (2015). Functional and phenotypic plasticity of $CD4^+$ T cell subsets. Biomed Res Int 2015, 521957.

Chappert, P., and Schwartz, R.H. (2010). Induction of T cell anergy: integration of environmental cues and infectious tolerance. Curr Opin Immunol 22, 552-559.

Chauvin, J.M., Pagliano, O., Fourcade, J., Sun, Z., Wang, H., Sander, C., Kirkwood, J.M., Chen, T.H., Maurer, M., Korman, A.J., et al. (2015). TIGIT and PD-1 impair tumor antigen-specific $CD8^+$ T cells in melanoma patients. J Clin Invest 125, 2046-2058.

Chemnitz, J.M., Parry, R.V., Nichols, K.E., June, C.H., and Riley, J.L. (2004). SHP-1 and SHP-2 associate with immunoreceptor tyrosine-based switch motif of programmed death 1 upon primary human T cell stimulation, but only receptor ligation prevents T cell activation. J Immunol 173, 945-954.

Chew, G.M., Fujita, T., Webb, G.M., Burwitz, B.J., Wu, H.L., Reed, J.S., Hammond, K.B., Clayton, K.L., Ishii, N., Abdel-Mohsen, M., et al. (2016). TIGIT marks exhausted T cells, correlates with disease progression, and serves as a target for immune restoration in HIV and SIV infection. PLoS Pathog 12, e1005349.

Chien, C.H., Yu, H.C., Chen, S.Y., and Chiang, B.L. (2017). Characterization of c-Maf^+Foxp3^- regulatory T cells induced by repeated stimulation of antigen-presenting B cells. Sci Rep 7, 46348.

Chiodetti, L., Choi, S., Barber, D.L., and Schwartz, R.H. (2006). Adaptive tolerance and clonal anergy are distinct biochemical states. J Immunol 176, 2279-2291.

Constant, S.L., and Bottomly, K. (1997). Induction of Th1 and Th2 $CD4^+$ T cell responses: the alternative approaches. Annu Rev Immunol 15, 297-322.

Crabtree, G.R., and Olson, E.N. (2002). NFAT signaling: choreographing the social lives of cells. Cell 109 Suppl, S67-79.

Crawford, A., Angelosanto, J.M., Kao, C., Doering, T.A., Odorizzi, P.M., Barnett, B.E., and Wherry, E.J. (2014). Molecular and transcriptional basis of $CD4^+$ T cell dysfunction during chronic infection. Immunity 40, 289-302.

Crotty, S. (2015). A brief history of T cell help to B cells. Nat Rev Immunol 15, 185-189.

Crotty, S. (2019). T follicular helper cell biology: A decade of discovery and diseases. Immunity 50, 1132-1148.

Cui, W., and Kaech, S.M. (2010). Generation of effector CD8+ T cells and their conversion to memory T cells. Immunol Rev 236, 151-166.

Curiel, T.J., Wei, S., Dong, H., Alvarez, X., Cheng, P., Mottram, P., Krzysiek, R., Knutson, K.L., Daniel, B., Zimmermann, M.C., et al. (2003). Blockade of B7-H1 improves myeloid dendritic cell-mediated antitumor immunity. Nat Med 9, 562-567.

Curtsinger, J.M., Schmidt, C.S., Mondino, A., Lins, D.C., Kedl, R.M., Jenkins, M.K., and Mescher, M.F. (1999). Inflammatory cytokines provide a third signal for activation of naive CD4+ and CD8+ T cells. J Immunol 162, 3256-3262.

Day, C.L., Kaufmann, D.E., Kiepiela, P., Brown, J.A., Moodley, E.S., Reddy, S., Mackey, E.W., Miller, J.D., Leslie, A.J., DePierres, C., et al. (2006). PD-1 expression on HIV-specific T cells is associated with T-cell exhaustion and disease progression. Nature 443, 350-354.

Deng, J., Wei, Y., Fonseca, V.R., Graca, L., and Yu, D. (2019). T follicular helper cells and T follicular regulatory cells in rheumatic diseases. Nat Rev Rheumatol.

Derynck, R., and Zhang, Y.E. (2003). Smad-dependent and Smad-independent pathways in TGF-beta family signalling. Nature 425, 577-584.

Doering, T.A., Crawford, A., Angelosanto, J.M., Paley, M.A., Ziegler, C.G., and Wherry, E.J. (2012). Network analysis reveals centrally connected genes and pathways involved in CD8+ T cell exhaustion versus memory. Immunity 37, 1130-1144.

Dorsey, M.J., Tae, H.J., Sollenberger, K.G., Mascarenhas, N.T., Johansen, L.M., and Taparowsky, E.J. (1995). B-ATF: a novel human bZIP protein that associates with members of the AP-1 transcription factor family. Oncogene 11, 2255-2265.

Ejrnaes, M., Filippi, C.M., Martinic, M.M., Ling, E.M., Togher, L.M., Crotty, S., and von Herrath, M.G. (2006). Resolution of a chronic viral infection after interleukin-10 receptor blockade. J Exp Med 203, 2461-2472.

El-Far, M., Halwani, R., Said, E., Trautmann, L., Doroudchi, M., Janbazian, L., Fonseca, S., van Grevenynghe, J., Yassine-Diab, B., Sekaly, R.P., et al. (2008). T-cell exhaustion in HIV infection. Curr HIV/AIDS Rep 5, 13-19.

Elsaesser, H., Sauer, K., and Brooks, D.G. (2009). IL-21 is required to control chronic viral infection. Science 324, 1569-1572.

Evans, D.E., Munks, M.W., Purkerson, J.M., and Parker, D.C. (2000). Resting B lymphocytes as APC for naive T lymphocytes: dependence on CD40 ligand/CD40. J Immunol 164, 688-697.

Fahey, L.M., Wilson, E.B., Elsaesser, H., Fistonich, C.D., McGavern, D.B., and Brooks, D.G. (2011). Viral persistence redirects CD4 T cell differentiation toward T follicular helper cells. J Exp Med 208, 987-999.

Faroudi, M., Utzny, C., Salio, M., Cerundolo, V., Guiraud, M., Muller, S., and Valitutti, S. (2003). Lytic versus stimulatory synapse in cytotoxic T lymphocyte/target cell interaction: manifestation of a dual activation threshold. Proc Natl Acad Sci U S A 100, 14145-14150.

Fazilleau, N., Mark, L., McHeyzer-Williams, L.J., and McHeyzer-Williams, M.G. (2009). Follicular helper T cells: lineage and location. Immunity 30, 324-335.

Feldmann, M., and Steinman, L. (2005). Design of effective immunotherapy for human autoimmunity. Nature 435, 612-619.

Ferber, I., Schonrich, G., Schenkel, J., Mellor, A.L., Hammerling, G.J., and Arnold, B. (1994). Levels of peripheral T cell tolerance induced by different doses of tolerogen. Science 263, 674-676.

Fesnak, A.D., June, C.H., and Levine, B.L. (2016). Engineered T cells: the promise and challenges of cancer immunotherapy. Nat Rev Cancer 16, 566-581.

Flanagan, W.M., Corthesy, B., Bram, R.J., and Crabtree, G.R. (1991). Nuclear association of a T-cell transcription factor blocked by FK-506 and cyclosporin A. Nature 352, 803-807.

Foletta, V.C., Segal, D.H., and Cohen, D.R. (1998). Transcriptional regulation in the immune system: all roads lead to AP-1. J Leukoc Biol 63, 139-152.

Fourcade, J., Sun, Z., Benallaoua, M., Guillaume, P., Luescher, I.F., Sander, C., Kirkwood, J.M., Kuchroo, V., and Zarour, H.M. (2010). Upregulation of Tim-3 and PD-1 expression is associated with tumor antigen-specific CD8+ T cell dysfunction in melanoma patients. J Exp Med 207, 2175-2186.

Foy, T.M., Aruffo, A., Bajorath, J., Buhlmann, J.E., and Noelle, R.J. (1996). Immune regulation by CD40 and its ligand GP39. Annu Rev Immunol 14, 591-617.

Fraietta, J.A., Lacey, S.F., Orlando, E.J., Pruteanu-Malinici, I., Gohil, M., Lundh, S., Boesteanu, A.C., Wang, Y., O'Connor, R.S., Hwang, W.T., et al. (2018). Determinants of response and resistance to CD19 chimeric antigen receptor (CAR) T cell therapy of chronic lymphocytic leukemia. Nat Med 24, 563-571.

Frebel, H., Richter, K., and Oxenius, A. (2010). How chronic viral infections impact on antigen-specific T-cell responses. Eur J Immunol 40, 654-663.

Fröhlich, A., Kisielow, J., Schmitz, I., Freigang, S., Shamshiev, A.T., Weber, J., Marsland, B.J., Oxenius, A., and Kopf, M. (2009). IL-21R on T cells is critical for sustained functionality and control of chronic viral infection. Science 324, 1576-1580.

Fuller, M.J., Khanolkar, A., Tebo, A.E., and Zajac, A.J. (2004). Maintenance, loss, and resurgence of T cell responses during acute, protracted, and chronic viral infections. J Immunol 172, 4204-4214.

Fuller, M.J., and Zajac, A.J. (2003). Ablation of CD8 and CD4 T cell responses by high viral loads. J Immunol 170, 477-486.

Gagliani, N., Magnani, C.F., Huber, S., Gianolini, M.E., Pala, M., Licona-Limon, P., Guo, B., Herbert, D.R., Bulfone, A., Trentini, F., et al. (2013). Coexpression of CD49b and LAG-3 identifies human and mouse T regulatory type 1 cells. Nat Med 19, 739-746.

Gallimore, A., Glithero, A., Godkin, A., Tissot, A.C., Pluckthun, A., Elliott, T., Hengartner, H., and Zinkernagel, R. (1998). Induction and exhaustion of lymphocytic choriomeningitis virus-specific cytotoxic T lymphocytes visualized using soluble tetrameric major histocompatibility complex class I-peptide complexes. J Exp Med 187, 1383-1393.

Gandhi, M.K., Lambley, E., Duraiswamy, J., Dua, U., Smith, C., Elliott, S., Gill, D., Marlton, P., Seymour, J., and Khanna, R. (2006). Expression of LAG-3 by tumor-infiltrating lymphocytes is coincident with the suppression of latent membrane antigen-specific CD8+ T-cell function in Hodgkin lymphoma patients. Blood 108, 2280-2289.

Gao, X., Zhu, Y., Li, G., Huang, H., Zhang, G., Wang, F., Sun, J., Yang, Q., Zhang, X., and Lu, B. (2012). TIM-3 expression characterizes regulatory T cells in tumor tissues and is associated with lung cancer progression. PLoS One 7, e30676.

Germar, K., Dose, M., Konstantinou, T., Zhang, J., Wang, H., Lobry, C., Arnett, K.L., Blacklow, S.C., Aifantis, I., Aster, J.C., et al. (2011). T-cell factor 1 is a gatekeeper for T-cell specification in response to Notch signaling. Proc Natl Acad Sci U S A 108, 20060-20065.

Giordano, M., Henin, C., Maurizio, J., Imbratta, C., Bourdely, P., Buferne, M., Baitsch, L., Vanhille, L., Sieweke, M.H., Speiser, D.E., et al. (2015). Molecular profiling of CD8 T cells in autochthonous melanoma identifies Maf as driver of exhaustion. EMBO J 34, 2042-2058.

Goepfert, P.A., Bansal, A., Edwards, B.H., Ritter, G.D., Jr., Tellez, I., McPherson, S.A., Sabbaj, S., and Mulligan, M.J. (2000). A significant number of human immunodeficiency virus epitope-specific cytotoxic T lymphocytes detected by tetramer binding do not produce gamma interferon. J Virol 74, 10249-10255.

Graf, D., Muller, S., Korthauer, U., van Kooten, C., Weise, C., and Kroczek, R.A. (1995). A soluble form of TRAP (CD40 ligand) is rapidly released after T cell activation. Eur J Immunol 25, 1749-1754.

Grewal, I.S., and Flavell, R.A. (1998). CD40 and CD154 in cell-mediated immunity. Annu Rev Immunol 16, 111-135.

Gruener, N.H., Lechner, F., Jung, M.C., Diepolder, H., Gerlach, T., Lauer, G., Walker, B., Sullivan, J., Phillips, R., Pape, G.R., et al. (2001). Sustained dysfunction of antiviral CD8+ T lymphocytes after infection with hepatitis C virus. J Virol 75, 5550-5558.

Hale, J.S., Youngblood, B., Latner, D.R., Mohammed, A.U., Ye, L., Akondy, R.S., Wu, T., Iyer, S.S., and Ahmed, R. (2013). Distinct memory CD4+ T cells with commitment to T follicular helper- and T helper 1-cell lineages are generated after acute viral infection. Immunity 38, 805-817.

Han, S., Asoyan, A., Rabenstein, H., Nakano, N., and Obst, R. (2010). Role of antigen persistence and dose for CD4+ T-cell exhaustion and recovery. Proc Natl Acad Sci U S A 107, 20453-20458.

Hannier, S., Tournier, M., Bismuth, G., and Triebel, F. (1998). CD3/TCR complex-associated lymphocyte activation gene-3 molecules inhibit CD3/TCR signaling. J Immunol 161, 4058-4065.

Hanninen, A., Maksimow, M., Alam, C., Morgan, D.J., and Jalkanen, S. (2011). Ly6C supports preferential homing of central memory CD8+ T cells into lymph nodes. Eur J Immunol 41, 634-644.

Hataye, J., Moon, J.J., Khoruts, A., Reilly, C., and Jenkins, M.K. (2006). Naive and memory CD4+ T cell survival controlled by clonal abundance. Science 312, 114-116.

Hawiger, D., Inaba, K., Dorsett, Y., Guo, M., Mahnke, K., Rivera, M., Ravetch, J.V., Steinman, R.M., and Nussenzweig, M.C. (2001). Dendritic cells induce peripheral T cell unresponsiveness under steady state conditions in vivo. J Exp Med 194, 769-779.

Hegazy, A.N., Peine, M., Helmstetter, C., Panse, I., Frohlich, A., Bergthaler, A., Flatz, L., Pinschewer, D.D., Radbruch, A., and Lohning, M. (2010). Interferons direct Th2 cell reprogramming to generate a stable GATA-3+T-bet+ cell subset with combined Th2 and Th1 cell functions. Immunity 32, 116-128.

Ho, I.C., Lo, D., and Glimcher, L.H. (1998). c-maf promotes T helper cell type 2 (Th2) and attenuates Th1 differentiation by both interleukin 4-dependent and -independent mechanisms. J Exp Med 188, 1859-1866.

Hogan, P.G., Lewis, R.S., and Rao, A. (2010). Molecular basis of calcium signaling in lymphocytes: STIM and ORAI. Annu Rev Immunol 28, 491-533.

Hogquist, K.A., Jameson, S.C., Heath, W.R., Howard, J.L., Bevan, M.J., and Carbone, F.R. (1994). T cell receptor antagonist peptides induce positive selection. Cell 76, 17-27.

Hogquist, K.A., Jameson, S.C., Heath, W.R., Howard, J.L., Bevan, M.J., and Carbone, F.R. (2012). Pillars article: T cell receptor antagonist peptides induce positive selection. J Immunol 188, 2046-2056.

Huang, A.C., Postow, M.A., Orlowski, R.J., Mick, R., Bengsch, B., Manne, S., Xu, W., Harmon, S., Giles, J.R., Wenz, B., et al. (2017). T-cell invigoration to tumour burden ratio associated with anti-PD-1 response. Nature 545, 60-65.

Huang, Y., Litvinov, I.V., Wang, Y., Su, M.W., Tu, P., Jiang, X., Kupper, T.S., Dutz, J.P., Sasseville, D., and Zhou, Y. (2014). Thymocyte selection-associated high mobility group box gene (TOX) is aberrantly over-expressed in mycosis fungoides and correlates with poor prognosis. Oncotarget 5, 4418-4425.

Huard, B., Gaulard, P., Faure, F., Hercend, T., and Triebel, F. (1994a). Cellular expression and tissue distribution of the human LAG-3-encoded protein, an MHC class II ligand. Immunogenetics 39, 213-217.

Huard, B., Prigent, P., Tournier, M., Bruniquel, D., and Triebel, F. (1995). CD4/major histocompatibility complex class II interaction analyzed with CD4- and lymphocyte activation gene-3 (LAG-3)-Ig fusion proteins. Eur J Immunol 25, 2718-2721.

Huard, B., Tournier, M., Hercend, T., Triebel, F., and Faure, F. (1994b). Lymphocyte-activation gene 3/major histocompatibility complex class II interaction modulates the antigenic response of CD4+ T lymphocytes. Eur J Immunol 24, 3216-3221.

Hui, E., Cheung, J., Zhu, J., Su, X., Taylor, M.J., Wallweber, H.A., Sasmal, D.K., Huang, J., Kim, J.M., Mellman, I., et al. (2017). T cell costimulatory receptor CD28 is a primary target for PD-1-mediated inhibition. Science 355, 1428-1433.

Huster, K.M., Busch, V., Schiemann, M., Linkemann, K., Kerksiek, K.M., Wagner, H., and Busch, D.H. (2004). Selective expression of IL-7 receptor on memory T cells identifies early CD40L-dependent generation of distinct CD8+ memory T cell subsets. Proc Natl Acad Sci U S A 101, 5610-5615.

Ip, Y.T., and Davis, R.J. (1998). Signal transduction by the c-Jun N-terminal kinase (JNK)--from inflammation to development. Curr Opin Cell Biol 10, 205-219.

Iwai, Y., Ishida, M., Tanaka, Y., Okazaki, T., Honjo, T., and Minato, N. (2002). Involvement of PD-L1 on tumor cells in the escape from host immune system and tumor immunotherapy by PD-L1 blockade. Proc Natl Acad Sci U S A 99, 12293-12297.

Jain, J., Loh, C., and Rao, A. (1995). Transcriptional regulation of the IL-2 gene. Curr Opin Immunol 7, 333-342.

Jain, J., McCaffrey, P.G., Miner, Z., Kerppola, T.K., Lambert, J.N., Verdine, G.L., Curran, T., and Rao, A. (1993). The T-cell transcription factor NFATp is a substrate for calcineurin and interacts with Fos and Jun. Nature 365, 352-355.

Jenkins, M.K., and Johnson, J.G. (1993). Molecules involved in T-cell costimulation. Curr Opin Immunol 5, 361-367.

Jenkins, M.K., and Schwartz, R.H. (1987). Antigen presentation by chemically modified splenocytes induces antigen-specific T cell unresponsiveness in vitro and in vivo. J Exp Med 165, 302-319.

Jin, H.T., Anderson, A.C., Tan, W.G., West, E.E., Ha, S.J., Araki, K., Freeman, G.J., Kuchroo, V.K., and Ahmed, R. (2010). Cooperation of Tim-3 and PD-1 in CD8 T-cell exhaustion during chronic viral infection. Proc Natl Acad Sci U S A 107, 14733-14738.

Kaech, S.M., Tan, J.T., Wherry, E.J., Konieczny, B.T., Surh, C.D., and Ahmed, R. (2003). Selective expression of the interleukin 7 receptor identifies effector CD8 T cells that give rise to long-lived memory cells. Nat Immunol 4, 1191-1198.

Kalekar, L.A., and Mueller, D.L. (2017). Relationship between CD4 regulatory T cells and anergy in vivo. J Immunol 198, 2527-2533.

Kalekar, L.A., Schmiel, S.E., Nandiwada, S.L., Lam, W.Y., Barsness, L.O., Zhang, N., Stritesky, G.L., Malhotra, D., Pauken, K.E., Linehan, J.L., et al. (2016). CD4+ T cell anergy prevents autoimmunity and generates regulatory T cell precursors. Nat Immunol 17, 304-314.

Kamphorst, A.O., Pillai, R.N., Yang, S., Nasti, T.H., Akondy, R.S., Wieland, A., Sica, G.L., Yu, K., Koenig, L., Patel, N.T., et al. (2017). Proliferation of PD-1+ CD8 T cells in peripheral blood after PD-1-targeted therapy in lung cancer patients. Proc Natl Acad Sci U S A 114, 4993-4998.

Kaufmann, D.E., Kavanagh, D.G., Pereyra, F., Zaunders, J.J., Mackey, E.W., Miura, T., Palmer, S., Brockman, M., Rathod, A., Piechocka-Trocha, A., et al. (2007). Upregulation of CTLA-4 by HIV-specific CD4+ T cells correlates with disease progression and defines a reversible immune dysfunction. Nat Immunol 8, 1246-1254.

Kawabe, T., Naka, T., Yoshida, K., Tanaka, T., Fujiwara, H., Suematsu, S., Yoshida, N., Kishimoto, T., and Kikutani, H. (1994). The immune responses in CD40-deficient mice: impaired immunoglobulin class switching and germinal center formation. Immunity 1, 167-178.

Kaye, J., Hsu, M.L., Sauron, M.E., Jameson, S.C., Gascoigne, N.R., and Hedrick, S.M. (1989). Selective development of CD4+ T cells in transgenic mice expressing a class II MHC-restricted antigen receptor. Nature 341, 746-749.

Keir, M.E., Butte, M.J., Freeman, G.J., and Sharpe, A.H. (2008). PD-1 and its ligands in tolerance and immunity. Annu Rev Immunol 26, 677-704.

Kennedy, M.K., Mohler, K.M., Shanebeck, K.D., Baum, P.R., Picha, K.S., Otten-Evans, C.A., Janeway, C.A., Jr., and Grabstein, K.H. (1994). Induction of B cell costimulatory function by recombinant murine CD40 ligand. Eur J Immunol 24, 116-123.

Kerksiek, K.M., Niedergang, F., Chavrier, P., Busch, D.H., and Brocker, T. (2005). Selective Rac1 inhibition in dendritic cells diminishes apoptotic cell uptake and cross-presentation in vivo. Blood 105, 742-749.

Khan, O., Giles, J.R., McDonald, S., Manne, S., Ngiow, S.F., Patel, K.P., Werner, M.T., Huang, A.C., Alexander, K.A., Wu, J.E., et al. (2019). TOX transcriptionally and epigenetically programs $CD8^+$ T cell exhaustion. Nature 571, 211-218.

King, C., Tangye, S.G., and Mackay, C.R. (2008). T follicular helper (TFH) cells in normal and dysregulated immune responses. Annu Rev Immunol 26, 741-766.

Kirchhoff, D., Frentsch, M., Leclerk, P., Bumann, D., Rausch, S., Hartmann, S., Thiel, A., and Scheffold, A. (2007). Identification and isolation of murine antigen-reactive T cells according to CD154 expression. Eur J Immunol 37, 2370-2377.

Klee, C.B., Ren, H., and Wang, X. (1998). Regulation of the calmodulin-stimulated protein phosphatase, calcineurin. J Biol Chem 273, 13367-13370.

Klein, L., Kyewski, B., Allen, P.M., and Hogquist, K.A. (2014). Positive and negative selection of the T cell repertoire: what thymocytes see (and don't see). Nat Rev Immunol 14, 377-391.

Knoechel, B., Lohr, J., Kahn, E., and Abbas, A.K. (2005). The link between lymphocyte deficiency and autoimmunity: roles of endogenous T and B lymphocytes in tolerance. J Immunol 175, 21-26.

Kretschmer, K., Apostolou, I., Hawiger, D., Khazaie, K., Nussenzweig, M.C., and von Boehmer, H. (2005). Inducing and expanding regulatory T cell populations by foreign antigen. Nat Immunol 6, 1219-1227.

Kroenke, M.A., Eto, D., Locci, M., Cho, M., Davidson, T., Haddad, E.K., and Crotty, S. (2012). Bcl6 and Maf cooperate to instruct human follicular helper CD4 T cell differentiation. J Immunol 188, 3734-3744.

Lechner, F., Wong, D.K., Dunbar, P.R., Chapman, R., Chung, R.T., Dohrenwend, P., Robbins, G., Phillips, R., Klenerman, P., and Walker, B.D. (2000). Analysis of successful immune responses in persons infected with hepatitis C virus. J Exp Med 191, 1499-1512.

Lee, J., Su, E.W., Zhu, C., Hainline, S., Phuah, J., Moroco, J.A., Smithgall, T.E., Kuchroo, V.K., and Kane, L.P. (2011). Phosphotyrosine-dependent coupling of Tim-3 to T-cell receptor signaling pathways. Mol Cell Biol 31, 3963-3974.

Lee, P.P., Yee, C., Savage, P.A., Fong, L., Brockstedt, D., Weber, J.S., Johnson, D., Swetter, S., Thompson, J., Greenberg, P.D., et al. (1999). Characterization of circulating T cells specific for tumor-associated antigens in melanoma patients. Nat Med 5, 677-685.

Li, M.O., Wan, Y.Y., Sanjabi, S., Robertson, A.K., and Flavell, R.A. (2006). Transforming growth factor-beta regulation of immune responses. Annu Rev Immunol 24, 99-146.

Li, Q.J., Dinner, A.R., Qi, S., Irvine, D.J., Huppa, J.B., Davis, M.M., and Chakraborty, A.K. (2004). CD4 enhances T cell sensitivity to antigen by coordinating Lck accumulation at the immunological synapse. Nat Immunol 5, 791-799.

Liang, S.C., Latchman, Y.E., Buhlmann, J.E., Tomczak, M.F., Horwitz, B.H., Freeman, G.J., and Sharpe, A.H. (2003). Regulation of PD-1, PD-L1, and PD-L2 expression during normal and autoimmune responses. Eur J Immunol 33, 2706-2716.

Lin, W.W., Nish, S.A., Yen, B., Chen, Y.H., Adams, W.C., Kratchmarov, R., Rothman, N.J., Bhandoola, A., Xue, H.H., and Reiner, S.L. (2016). $CD8^+$ T lymphocyte Self-renewal during effector cell determination. Cell Rep 17, 1773-1782.

Lu, X., Yang, L., Yao, D., Wu, X., Li, J., Liu, X., Deng, L., Huang, C., Wang, Y., Li, D., et al. (2017). Tumor antigen-specific $CD8^+$ T cells are negatively regulated by PD-1 and Tim-3 in human gastric cancer. Cell Immunol 313, 43-51.

Macian, F., Garcia-Cozar, F., Im, S.H., Horton, H.F., Byrne, M.C., and Rao, A. (2002). Transcriptional mechanisms underlying lymphocyte tolerance. Cell 109, 719-731.

Macian, F., Garcia-Rodriguez, C., and Rao, A. (2000). Gene expression elicited by NFAT in the presence or absence of cooperative recruitment of Fos and Jun. EMBO J 19, 4783-4795.

Mackerness, K.J., Cox, M.A., Lilly, L.M., Weaver, C.T., Harrington, L.E., and Zajac, A.J. (2010). Pronounced virus-dependent activation drives exhaustion but sustains IFN-gamma transcript levels. J Immunol 185, 3643-3651.

Man, K., Gabriel, S.S., Liao, Y., Gloury, R., Preston, S., Henstridge, D.C., Pellegrini, M., Zehn, D., Berberich-Siebelt, F., Febbraio, M.A., et al. (2017). Transcription factor IRF4 promotes $CD8^+$ T cell exhaustion and limits the development of memory-like T cells during chronic infection. Immunity 47, 1129-1141 e1125.

Martinez, G.J., Pereira, R.M., Aijo, T., Kim, E.Y., Marangoni, F., Pipkin, M.E., Togher, S., Heissmeyer, V., Zhang, Y.C., Crotty, S., et al. (2015). The transcription factor NFAT promotes exhaustion of activated $CD8^+$ T cells. Immunity 42, 265-278.

Martinez, R.J., Zhang, N., Thomas, S.R., Nandiwada, S.L., Jenkins, M.K., Binstadt, B.A., and Mueller, D.L. (2012). Arthritogenic self-reactive $CD4^+$ T cells acquire an $FR4^{hi}CD73^{hi}$ anergic state in the presence of $Foxp3^+$ regulatory T cells. J Immunol 188, 170-181.

Matloubian, M., Concepcion, R.J., and Ahmed, R. (1994). $CD4^+$ T cells are required to sustain $CD8^+$ cytotoxic T-cell responses during chronic viral infection. J Virol 68, 8056-8063.

Matsuzaki, J., Gnjatic, S., Mhawech-Fauceglia, P., Beck, A., Miller, A., Tsuji, T., Eppolito, C., Qian, F., Lele, S., Shrikant, P., et al. (2010). Tumor-infiltrating NY-ESO-1-specific $CD8^+$ T cells are negatively regulated by LAG-3 and PD-1 in human ovarian cancer. Proc Natl Acad Sci U S A 107, 7875-7880.

McHenry, C.R., Stenger, D.B., and Kunze, D.L. (1998). Inwardly rectifying K^+ channels in dispersed bovine parathyroid cells. J Surg Res 76, 37-40.

McLane, L.M., Abdel-Hakeem, M.S., and Wherry, E.J. (2019). CD8 T cell exhaustion during chronic viral infection and cancer. Annu Rev Immunol 37, 457-495.

Moir, S., and Fauci, A.S. (2014). B-cell exhaustion in HIV infection: the role of immune activation. Curr Opin HIV AIDS 9, 472-477.

Monks, C.R., Freiberg, B.A., Kupfer, H., Sciaky, N., and Kupfer, A. (1998). Three-dimensional segregation of supramolecular activation clusters in T cells. Nature 395, 82-86.

Monney, L., Sabatos, C.A., Gaglia, J.L., Ryu, A., Waldner, H., Chernova, T., Manning, S., Greenfield, E.A., Coyle, A.J., Sobel, R.A., et al. (2002). Th1-specific cell surface protein Tim-3 regulates macrophage activation and severity of an autoimmune disease. Nature 415, 536-541.

Moran, A.E., Holzapfel, K.L., Xing, Y., Cunningham, N.R., Maltzman, J.S., Punt, J., and Hogquist, K.A. (2011). T cell receptor signal strength in Treg and iNKT cell development demonstrated by a novel fluorescent reporter mouse. J Exp Med 208, 1279-1289.

Moskophidis, D., Lechner, F., Pircher, H., and Zinkernagel, R.M. (1993). Virus persistence in acutely infected immunocompetent mice by exhaustion of antiviral cytotoxic effector T cells. Nature 362, 758-761.

Moskophidis, D., and Zinkernagel, R.M. (1995). Immunobiology of cytotoxic T-cell escape mutants of lymphocytic choriomeningitis virus. J Virol 69, 2187-2193.

Mothe, B.R., Stewart, B.S., Oseroff, C., Bui, H.H., Stogiera, S., Garcia, Z., Dow, C., Rodriguez-Carreno, M.P., Kotturi, M., Pasquetto, V., et al. (2007). Chronic lymphocytic choriomeningitis virus infection actively down-regulates $CD4^+$ T cell responses directed against a broad range of epitopes. J Immunol 179, 1058-1067.

Mueller, S.N., and Ahmed, R. (2009). High antigen levels are the cause of T cell exhaustion during chronic viral infection. Proc Natl Acad Sci U S A 106, 8623-8628.

Mumprecht, S., Schurch, C., Schwaller, J., Solenthaler, M., and Ochsenbein, A.F. (2009). Programmed death 1 signaling on chronic myeloid leukemia-specific T cells results in T-cell exhaustion and disease progression. Blood 114, 1528-1536.

Nakabeppu, Y., Ryder, K., and Nathans, D. (1988). DNA binding activities of three murine Jun proteins: stimulation by Fos. Cell 55, 907-915.

Ni, G., Wang, T., Walton, S., Zhu, B., Chen, S., Wu, X., Wang, Y., Wei, M.Q., and Liu, X. (2015). Manipulating IL-10 signalling blockade for better immunotherapy. Cell Immunol 293, 126-129.

Nika, K., Soldani, C., Salek, M., Paster, W., Gray, A., Etzensperger, R., Fugger, L., Polzella, P., Cerundolo, V., Dushek, O., et al. (2010). Constitutively active Lck kinase in T cells drives antigen receptor signal transduction. Immunity 32, 766-777.

Nossal, G.J. (1994). Negative selection of lymphocytes. Cell 76, 229-239.

O'Shea, J.J., and Paul, W.E. (2010). Mechanisms underlying lineage commitment and plasticity of helper CD4+ T cells. Science 327, 1098-1102.

Obst, R., van Santen, H.M., Mathis, D., and Benoist, C. (2005). Antigen persistence is required throughout the expansion phase of a CD4+ T cell response. J Exp Med 201, 1555-1565.

Obst, R., van Santen, H.M., Melamed, R., Kamphorst, A.O., Benoist, C., and Mathis, D. (2007). Sustained antigen presentation can promote an immunogenic T cell response, like dendritic cell activation. Proc Natl Acad Sci U S A 104, 15460-15465.

Odorizzi, P.M., Pauken, K.E., Paley, M.A., Sharpe, A., and Wherry, E.J. (2015). Genetic absence of PD-1 promotes accumulation of terminally differentiated exhausted CD8+ T cells. J Exp Med 212, 1125-1137.

Odorizzi, P.M., and Wherry, E.J. (2012). Inhibitory receptors on lymphocytes: insights from infections. J Immunol 188, 2957-2965.

Oestreich, K.J., Yoon, H., Ahmed, R., and Boss, J.M. (2008). NFATc1 regulates PD-1 expression upon T cell activation. J Immunol 181, 4832-4839.

Okazaki, T., Chikuma, S., Iwai, Y., Fagarasan, S., and Honjo, T. (2013). A rheostat for immune responses: the unique properties of PD-1 and their advantages for clinical application. Nat Immunol 14, 1212-1218.

Paley, M.A., Kroy, D.C., Odorizzi, P.M., Johnnidis, J.B., Dolfi, D.V., Barnett, B.E., Bikoff, E.K., Robertson, E.J., Lauer, G.M., Reiner, S.L., et al. (2012). Progenitor and terminal subsets of CD8+ T cells cooperate to contain chronic viral infection. Science 338, 1220-1225.

Pardoll, D.M. (2012). The blockade of immune checkpoints in cancer immunotherapy. Nat Rev Cancer 12, 252-264.

Patsoukis, N., Sari, D., and Boussiotis, V.A. (2012). PD-1 inhibits T cell proliferation by upregulating p27 and p15 and suppressing Cdc25A. Cell Cycle 11, 4305-4309.

Pauken, K.E., Sammons, M.A., Odorizzi, P.M., Manne, S., Godec, J., Khan, O., Drake, A.M., Chen, Z., Sen, D.R., Kurachi, M., et al. (2016). Epigenetic stability of exhausted T cells limits durability of reinvigoration by PD-1 blockade. Science 354, 1160-1165.

Paz, P.E., Wang, S., Clarke, H., Lu, X., Stokoe, D., and Abo, A. (2001). Mapping the Zap-70 phosphorylation sites on LAT (linker for activation of T cells) required for recruitment and activation of signalling proteins in T cells. Biochem J 356, 461-471.

Pentcheva-Hoang, T., Egen, J.G., Wojnoonski, K., and Allison, J.P. (2004). B7-1 and B7-2 selectively recruit CTLA-4 and CD28 to the immunological synapse. Immunity 21, 401-413.

Petrovas, C., Casazza, J.P., Brenchley, J.M., Price, D.A., Gostick, E., Adams, W.C., Precopio, M.L., Schacker, T., Roederer, M., Douek, D.C., et al. (2006). PD-1 is a regulator of virus-specific CD8+ T cell survival in HIV infection. J Exp Med 203, 2281-2292.

Philip, M., Fairchild, L., Sun, L., Horste, E.L., Camara, S., Shakiba, M., Scott, A.C., Viale, A., Lauer, P., Merghoub, T., et al. (2017). Chromatin states define tumour-specific T cell dysfunction and reprogramming. Nature 545, 452-456.

Pirquet, C. (1908). Das Verhalten der kutanen Tuberkulinreaktion während der Masern. DMW - Deutsche Medizinische Wochenschrift.

Pot, C., Jin, H., Awasthi, A., Liu, S.M., Lai, C.Y., Madan, R., Sharpe, A.H., Karp, C.L., Miaw, S.C., Ho, I.C., et al. (2009). Cutting edge: IL-27 induces the transcription factor c-Maf, cytokine IL-21, and the costimulatory receptor ICOS that coordinately act together to promote differentiation of IL-10-producing Tr1 cells. J Immunol 183, 797-801.

Quah, B.J., and Parish, C.R. (2012). New and improved methods for measuring lymphocyte proliferation in vitro and in vivo using CFSE-like fluorescent dyes. J Immunol Methods 379, 1-14.

Quigley, M., Pereyra, F., Nilsson, B., Porichis, F., Fonseca, C., Eichbaum, Q., Julg, B., Jesneck, J.L., Brosnahan, K., Imam, S., et al. (2010). Transcriptional analysis of HIV-specific CD8+ T cells shows that PD-1 inhibits T cell function by upregulating BATF. Nat Med 16, 1147-1151.

Qureshi, O.S., Zheng, Y., Nakamura, K., Attridge, K., Manzotti, C., Schmidt, E.M., Baker, J., Jeffery, L.E., Kaur, S., Briggs, Z., et al. (2011). Trans-endocytosis of CD80 and CD86: a molecular basis for the cell-extrinsic function of CTLA-4. Science 332, 600-603.

Rabenstein, H., Behrendt, A.C., Ellwart, J.W., Naumann, R., Horsch, M., Beckers, J., and Obst, R. (2014). Differential kinetics of antigen dependency of CD4+ and CD8+ T cells. J Immunol 192, 3507-3517.

Radoja, S., Saio, M., Schaer, D., Koneru, M., Vukmanovic, S., and Frey, A.B. (2001). CD8+ tumor-infiltrating T cells are deficient in perforin-mediated cytolytic activity due to defective microtubule-organizing center mobilization and lytic granule exocytosis. J Immunol 167, 5042-5051.

Radziewicz, H., Ibegbu, C.C., Fernandez, M.L., Workowski, K.A., Obideen, K., Wehbi, M., Hanson, H.L., Steinberg, J.P., Masopust, D., Wherry, E.J., et al. (2007). Liver-infiltrating lymphocytes in chronic human hepatitis C virus infection display an exhausted phenotype with high levels of PD-1 and low levels of CD127 expression. J Virol 81, 2545-2553.

Ranheim, E.A., and Kipps, T.J. (1993). Activated T cells induce expression of B7/BB1 on normal or leukemic B cells through a CD40-dependent signal. J Exp Med 177, 925-935.

Rao, A., Luo, C., and Hogan, P.G. (1997). Transcription factors of the NFAT family: regulation and function. Annu Rev Immunol 15, 707-747.

Reignat, S., Webster, G.J., Brown, D., Ogg, G.S., King, A., Seneviratne, S.L., Dusheiko, G., Williams, R., Maini, M.K., and Bertoletti, A. (2002). Escaping high viral load exhaustion: CD8 cells with altered tetramer binding in chronic hepatitis B virus infection. J Exp Med 195, 1089-1101.

Rellahan, B.L., Jones, L.A., Kruisbeek, A.M., Fry, A.M., and Matis, L.A. (1990). In vivo induction of anergy in peripheral V beta 8+ T cells by staphylococcal enterotoxin B. J Exp Med 172, 1091-1100.

Ribas, A., and Wolchok, J.D. (2018). Cancer immunotherapy using checkpoint blockade. Science 359, 1350-1355.

Riches, J.C., Davies, J.K., McClanahan, F., Fatah, R., Iqbal, S., Agrawal, S., Ramsay, A.G., and Gribben, J.G. (2013). T cells from CLL patients exhibit features of T-cell exhaustion but retain capacity for cytokine production. Blood 121, 1612-1621.

Richter, K., Agnellini, P., and Oxenius, A. (2010). On the role of the inhibitory receptor LAG-3 in acute and chronic LCMV infection. Int Immunol 22, 13-23.

Riley, J.L. (2009). PD-1 signaling in primary T cells. Immunol Rev 229, 114-125.

Rincon, M., and Flavell, R.A. (1994). AP-1 transcriptional activity requires both T-cell receptor-mediated and co-stimulatory signals in primary T lymphocytes. EMBO J 13, 4370-4381.

Rocha, B., Tanchot, C., and Von Boehmer, H. (1993). Clonal anergy blocks in vivo growth of mature T cells and can be reversed in the absence of antigen. J Exp Med 177, 1517-1521.

Roncarolo, M.G., Gregori, S., Bacchetta, R., Battaglia, M., and Gagliani, N. (2018). The biology of T regulatory type 1 cells and their therapeutic application in immune-mediated diseases. Immunity 49, 1004-1019.

Rooney, J.W., Sun, Y.L., Glimcher, L.H., and Hoey, T. (1995). Novel NFAT sites that mediate activation of the interleukin-2 promoter in response to T-cell receptor stimulation. Mol Cell Biol 15, 6299-6310.

Rothenberg, E.V. (1996). How T cells count. Science 273, 78-79.

Salio, M., Valitutti, S., and Lanzavecchia, A. (1997). Agonist-induced T cell receptor down-regulation: molecular requirements and dissociation from T cell activation. Eur J Immunol 27, 1769-1773.

Sallusto, F. (2016). Heterogeneity of human CD4+ T cells against microbes. Annu Rev Immunol 34, 317-334.

Saveanu, L., Zucchetti, A.E., Evnouchidou, I., Ardouin, L., and Hivroz, C. (2019). Is there a place and role for endocytic TCR signaling? Immunol Rev 291, 57-74.

Schietinger, A., and Greenberg, P.D. (2014). Tolerance and exhaustion: defining mechanisms of T cell dysfunction. Trends Immunol 35, 51-60.

Schietinger, A., Philip, M., Krisnawan, V.E., Chiu, E.Y., Delrow, J.J., Basom, R.S., Lauer, P., Brockstedt, D.G., Knoblaugh, S.E., Hammerling, G.J., et al. (2016). Tumor-specific T cell dysfunction Is a dynamic antigen-driven differentiation program initiated early during tumorigenesis. Immunity 45, 389-401.

Schmitt, N., and Ueno, H. (2013). Blood Tfh cells come with colors. Immunity 39, 629-630.

Schrader, C.E., Stavnezer, J., Kikutani, H., and Parker, D.C. (1997). Cognate T cell help for CD40-deficient B cells induces c-myc RNA expression, but DNA synthesis requires an additional signal through surface Ig. J Immunol 158, 153-162.

Schraml, B.U., Hildner, K., Ise, W., Lee, W.-L., Smith, W.A.E., Solomon, B., Sahota, G., Sim, J., Mukasa, R., Cemerski, S., et al. (2009). The AP-1 transcription factor Batf controls TH17 differentiation. Nature 460, 405-409.

Schwartz, R.H. (1990). A cell culture model for T lymphocyte clonal anergy. Science 248, 1349-1356.

Schwartz, R.H. (2003). T cell anergy. Annu Rev Immunol 21, 305-334.

Schwartz, R.H., Mueller, D.L., Jenkins, M.K., and Quill, H. (1989). T-cell clonal anergy. Cold Spring Harb Symp Quant Biol 54 Pt 2, 605-610.

Scott, A.C., Dundar, F., Zumbo, P., Chandran, S.S., Klebanoff, C.A., Shakiba, M., Trivedi, P., Menocal, L., Appleby, H., Camara, S., et al. (2019). TOX is a critical regulator of tumour-specific T cell differentiation. Nature 571, 270-274.

Scott-Browne, J.P., Lopez-Moyado, I.F., Trifari, S., Wong, V., Chavez, L., Rao, A., and Pereira, R.M. (2016). Dynamic Changes in Chromatin Accessibility Occur in CD8+ T Cells Responding to Viral Infection. Immunity 45, 1327-1340.

Sen, D.R., Kaminski, J., Barnitz, R.A., Kurachi, M., Gerdemann, U., Yates, K.B., Tsao, H.W., Godec, J., LaFleur, M.W., Brown, F.D., et al. (2016). The epigenetic landscape of T cell exhaustion. Science 354, 1165-1169.

Shakhar, G., Lindquist, R.L., Skokos, D., Dudziak, D., Huang, J.H., Nussenzweig, M.C., and Dustin, M.L. (2005). Stable T cell-dendritic cell interactions precede the development of both tolerance and immunity in vivo. Nat Immunol 6, 707-714.

Shankar, P., Russo, M., Harnisch, B., Patterson, M., Skolnik, P., and Lieberman, J. (2000). Impaired function of circulating HIV-specific CD8+ T cells in chronic human immunodeficiency virus infection. Blood 96, 3094-3101.

Sharma, P., and Allison, J.P. (2015). The future of immune checkpoint therapy. Science 348, 56-61.

Shayan, G., Srivastava, R., Li, J., Schmitt, N., Kane, L.P., and Ferris, R.L. (2017). Adaptive resistance to anti-PD1 therapy by Tim-3 upregulation is mediated by the PI3K-Akt pathway in head and neck cancer. Oncoimmunology 6, e1261779.

Shin, H., Blackburn, S.D., Intlekofer, A.M., Kao, C., Angelosanto, J.M., Reiner, S.L., and Wherry, E.J. (2009). A role for the transcriptional repressor Blimp-1 in CD8+ T cell exhaustion during chronic viral infection. Immunity 31, 309-320.

Smalley, D.M., and Ley, K. (2005). L-selectin: mechanisms and physiological significance of ectodomain cleavage. J Cell Mol Med 9, 255-266.

Soto-Nieves, N., Puga, I., Abe, B.T., Bandyopadhyay, S., Baine, I., Rao, A., and Macian, F. (2009). Transcriptional complexes formed by NFAT dimers regulate the induction of T cell tolerance. J Exp Med 206, 867-876.

Soyer, O.U., Akdis, M., Ring, J., Behrendt, H., Crameri, R., Lauener, R., and Akdis, C.A. (2013). Mechanisms of peripheral tolerance to allergens. Allergy 68, 161-170.

Starr, T.K., Jameson, S.C., and Hogquist, K.A. (2003). Positive and negative selection of T cells. Annu Rev Immunol 21, 139-176.

Stelekati, E., Shin, H., Doering, T.A., Dolfi, D.V., Ziegler, C.G., Beiting, D.P., Dawson, L., Liboon, J., Wolski, D., Ali, M.A., et al. (2014). Bystander chronic infection negatively impacts development of CD8+ T cell memory. Immunity 40, 801-813.

Streeck, H., Brumme, Z.L., Anastario, M., Cohen, K.W., Jolin, J.S., Meier, A., Brumme, C.J., Rosenberg, E.S., Alter, G., Allen, T.M., et al. (2008). Antigen load and viral sequence diversification determine the functional profile of HIV-1-specific CD8+ T cells. PLoS Med 5, e100.

Strohl, W.R. (2018). Current progress in innovative engineered antibodies. Protein Cell 9, 86-120.

Swain, S.L., McKinstry, K.K., and Strutt, T.M. (2012). Expanding roles for CD4+ T cells in immunity to viruses. Nat Rev Immunol 12, 136-148.

Szymczak-Workman, A.L., Workman, C.J., and Vignali, D.A. (2009). Cutting edge: regulatory T cells do not require stimulation through their TCR to suppress. J Immunol 182, 5188-5192.

Taams, L.S., van Eden, W., and Wauben, M.H. (1999). Dose-dependent induction of distinct anergic phenotypes: multiple levels of T cell anergy. J Immunol 162, 1974-1981.

Tinoco, R., Alcalde, V., Yang, Y., Sauer, K., and Zuniga, E.I. (2009). Cell-intrinsic transforming growth factor-beta signaling mediates virus-specific CD8+ T cell deletion and viral persistence in vivo. Immunity 31, 145-157.

Tivol, E.A., Borriello, F., Schweitzer, A.N., Lynch, W.P., Bluestone, J.A., and Sharpe, A.H. (1995). Loss of CTLA-4 leads to massive lymphoproliferation and fatal multiorgan tissue destruction, revealing a critical negative regulatory role of CTLA-4. Immunity 3, 541-547.

Tokoyoda, K., Zehentmeier, S., Hegazy, A.N., Albrecht, I., Grun, J.R., Lohning, M., and Radbruch, A. (2009). Professional memory CD4+ T lymphocytes preferentially reside and rest in the bone marrow. Immunity 30, 721-730.

Tomkowicz, B., Walsh, E., Cotty, A., Verona, R., Sabins, N., Kaplan, F., Santulli-Marotto, S., Chin, C.N., Mooney, J., Lingham, R.B., et al. (2015). TIM-3 suppresses anti-CD3/CD28-Induced TCR activation and IL-2 expression through the NFAT signaling pathway. PLoS One 10, e0140694.

Topalian, S.L., Drake, C.G., and Pardoll, D.M. (2012). Targeting the PD-1/B7-H1(PD-L1) pathway to activate anti-tumor immunity. Curr Opin Immunol 24, 207-212.

Topalian, S.L., Drake, C.G., and Pardoll, D.M. (2015). Immune checkpoint blockade: a common denominator approach to cancer therapy. Cancer Cell 27, 450-461.

Trautmann, L., Janbazian, L., Chomont, N., Said, E.A., Gimmig, S., Bessette, B., Boulassel, M.R., Delwart, E., Sepulveda, H., Balderas, R.S., et al. (2006). Upregulation of PD-1 expression on HIV-specific CD8+ T cells leads to reversible immune dysfunction. Nat Med 12, 1198-1202.

Truneh, A., Albert, F., Golstein, P., and Schmitt-Verhulst, A.M. (1985). Calcium ionophore plus phorbol ester can substitute for antigen in the induction of cytolytic T lymphocytes from specifically primed precursors. J Immunol 135, 2262-2267.

Turner, J.M., Brodsky, M.H., Irving, B.A., Levin, S.D., Perlmutter, R.M., and Littman, D.R. (1990). Interaction of the unique N-terminal region of tyrosine kinase p56lck with cytoplasmic domains of CD4 and CD8 is mediated by cysteine motifs. Cell 60, 755-765.

Twyman-Saint Victor, C., Rech, A.J., Maity, A., Rengan, R., Pauken, K.E., Stelekati, E., Benci, J.L., Xu, B., Dada, H., Odorizzi, P.M., et al. (2015). Radiation and dual checkpoint blockade activate non-redundant immune mechanisms in cancer. Nature 520, 373-377.

Urbani, S., Amadei, B., Tola, D., Massari, M., Schivazappa, S., Missale, G., and Ferrari, C. (2006). PD-1 expression in acute hepatitis C virus (HCV) infection is associated with HCV-specific CD8 exhaustion. J Virol 80, 11398-11403.

Utzschneider, D.T., Alfei, F., Roelli, P., Barras, D., Chennupati, V., Darbre, S., Delorenzi, M., Pinschewer, D.D., and Zehn, D. (2016a). High antigen levels induce an exhausted phenotype in a chronic infection without impairing T cell expansion and survival. J Exp Med 213, 1819-1834.

Utzschneider, D.T., Charmoy, M., Chennupati, V., Pousse, L., Ferreira, D.P., Calderon-Copete, S., Danilo, M., Alfei, F., Hofmann, M., Wieland, D., et al. (2016b). T cell factor 1-expressing memory-like CD8+ T cells sustain the immune response to chronic viral infections. Immunity 45, 415-427.

Valitutti, S. (2012). The serial engagement model 17 years after: from TCR triggering to immunotherapy. Front Immunol 3, 272.

Valitutti, S., Dessing, M., Aktories, K., Gallati, H., and Lanzavecchia, A. (1995a). Sustained signaling leading to T cell activation results from prolonged T cell receptor occupancy. Role of T cell actin cytoskeleton. J Exp Med 181, 577-584.

Valitutti, S., Muller, S., Cella, M., Padovan, E., and Lanzavecchia, A. (1995b). Serial triggering of many T-cell receptors by a few peptide-MHC complexes. Nature 375, 148-151.

Valitutti, S., Muller, S., Dessing, M., and Lanzavecchia, A. (1996). Different responses are elicited in cytotoxic T lymphocytes by different levels of T cell receptor occupancy. J Exp Med 183, 1917-1921.

van de Weyer, P.S., Muehlfeit, M., Klose, C., Bonventre, J.V., Walz, G., and Kuehn, E.W. (2006). A highly conserved tyrosine of Tim-3 is phosphorylated upon stimulation by its ligand galectin-9. Biochem Biophys Res Commun 351, 571-576.

Van den Broeck, W., Derore, A., and Simoens, P. (2006). Anatomy and nomenclature of murine lymph nodes: Descriptive study and nomenclatory standardization in BALB/cAnNCrl mice. J Immunol Methods 312, 12-19.

van Santen, H., Benoist, C., and Mathis, D. (2000). A cassette vector for high-level reporter expression driven by a hybrid invariant chain promoter in transgenic mice. J Immunol Methods 245, 133-137.

van Santen, H.M., Benoist, C., and Mathis, D. (2004). Number of T reg cells that differentiate does not increase upon encounter of agonist ligand on thymic epithelial cells. J Exp Med 200, 1221-1230.

Veiga-Parga, T., Sehrawat, S., and Rouse, B.T. (2013). Role of regulatory T cells during virus infection. Immunol Rev 255, 182-196.

Vella, A.T., Dow, S., Potter, T.A., Kappler, J., and Marrack, P. (1998). Cytokine-induced survival of activated T cells in vitro and in vivo. Proc Natl Acad Sci U S A 95, 3810-3815.

Vella, L.A., Herati, R.S., and Wherry, E.J. (2017). CD4+ T cell Ddifferentiation in chronic viral infections: The Tfh perspective. Trends Mol Med 23, 1072-1087.

Verbeek, S., Izon, D., Hofhuis, F., Robanus-Maandag, E., te Riele, H., van de Wetering, M., Oosterwegel, M., Wilson, A., MacDonald, H.R., and Clevers, H. (1995). An HMG-box-containing T-cell factor required for thymocyte differentiation. Nature 374, 70-74.

Verdeil, G. (2016). MAF drives CD8+ T-cell exhaustion. Oncoimmunology 5, e1082707.

Verginis, P., McLaughlin, K.A., Wucherpfennig, K.W., von Boehmer, H., and Apostolou, I. (2008). Induction of antigen-specific regulatory T cells in wild-type mice: visualization and targets of suppression. Proc Natl Acad Sci U S A 105, 3479-3484.

Viola, A., and Lanzavecchia, A. (1996). T cell activation determined by T cell receptor number and tunable thresholds. Science 273, 104-106.

Virgin, H.W., Wherry, E.J., and Ahmed, R. (2009). Redefining chronic viral infection. Cell 138, 30-50.

Wada, J., and Kanwar, Y.S. (1997). Identification and characterization of galectin-9, a novel beta-galactoside-binding mammalian lectin. J Biol Chem 272, 6078-6086.

Wang, J., Hu, Y., and Huang, H. (2017). Acute lymphoblastic leukemia relapse after CD19-targeted chimeric antigen receptor T cell therapy. J Leukoc Biol 102, 1347-1356.

Wells, A.D. (2009). New insights into the molecular basis of T cell anergy: anergy factors, avoidance sensors, and epigenetic imprinting. J Immunol 182, 7331-7341.

West, E.E., Jin, H.T., Rasheed, A.U., Penaloza-Macmaster, P., Ha, S.J., Tan, W.G., Youngblood, B., Freeman, G.J., Smith, K.A., and Ahmed, R. (2013). PD-L1 blockade synergizes with IL-2 therapy in reinvigorating exhausted T cells. J Clin Invest 123, 2604-2615.

Wherry, E.J. (2011). T cell exhaustion. Nat Immunol 12, 492-499.

Wherry, E.J., Blattman, J.N., Murali-Krishna, K., van der Most, R., and Ahmed, R. (2003a). Viral persistence alters CD8 T-cell immunodominance and tissue distribution and results in distinct stages of functional impairment. J Virol 77, 4911-4927.

Wherry, E.J., Ha, S.J., Kaech, S.M., Haining, W.N., Sarkar, S., Kalia, V., Subramaniam, S., Blattman, J.N., Barber, D.L., and Ahmed, R. (2007). Molecular signature of $CD8^+$ T cell exhaustion during chronic viral infection. Immunity 27, 670-684.

Wherry, E.J., and Kurachi, M. (2015). Molecular and cellular insights into T cell exhaustion. Nat Rev Immunol 15, 486-499.

Wherry, E.J., Teichgraber, V., Becker, T.C., Masopust, D., Kaech, S.M., Antia, R., von Andrian, U.H., and Ahmed, R. (2003b). Lineage relationship and protective immunity of memory CD8 T cell subsets. Nat Immunol 4, 225-234.

Whitmarsh, A.J., and Davis, R.J. (1996). Transcription factor AP-1 regulation by mitogen-activated protein kinase signal transduction pathways. J Mol Med (Berl) 74, 589-607.

Wilkinson, B., Chen, J.Y., Han, P., Rufner, K.M., Goularte, O.D., and Kaye, J. (2002). TOX: an HMG box protein implicated in the regulation of thymocyte selection. Nat Immunol 3, 272-280.

Wilson, E.B., and Brooks, D.G. (2011). The role of IL-10 in regulating immunity to persistent viral infections. Curr Top Microbiol Immunol 350, 39-65.

Wolchinsky, R., Hod-Marco, M., Oved, K., Shen-Orr, S.S., Bendall, S.C., Nolan, G.P., and Reiter, Y. (2014). Antigen-dependent integration of opposing proximal TCR-signaling cascades determines the functional fate of T lymphocytes. J Immunol 192, 2109-2119.

Wolchok, J.D., Kluger, H., Callahan, M.K., Postow, M.A., Rizvi, N.A., Lesokhin, A.M., Segal, N.H., Ariyan, C.E., Gordon, R.A., Reed, K., et al. (2013). Nivolumab plus ipilimumab in advanced melanoma. N Engl J Med 369, 122-133.

Workman, C.J., and Vignali, D.A. (2003). The CD4-related molecule, LAG-3 (CD223), regulates the expansion of activated T cells. Eur J Immunol 33, 970-979.

Wu, T., Ji, Y., Moseman, E.A., Xu, H.C., Manglani, M., Kirby, M., Anderson, S.M., Handon, R., Kenyon, E., Elkahloun, A., et al. (2016). The TCF1-Bcl6 axis counteracts type I interferon to repress exhaustion and maintain T cell stemness. Sci Immunol 1.

Xu, C., Gagnon, E., Call, M.E., Schnell, J.R., Schwieters, C.D., Carman, C.V., Chou, J.J., and Wucherpfennig, K.W. (2008). Regulation of T cell receptor activation by dynamic membrane binding of the CD3epsilon cytoplasmic tyrosine-based motif. Cell 135, 702-713.

Xu, F., Liu, J., Liu, D., Liu, B., Wang, M., Hu, Z., Du, X., Tang, L., and He, F. (2014). LSECtin expressed on melanoma cells promotes tumor progression by inhibiting antitumor T-cell responses. Cancer Res 74, 3418-3428.

Xu, J., Yang, Y., Qiu, G., Lal, G., Wu, Z., Levy, D.E., Ochando, J.C., Bromberg, J.S., and Ding, Y. (2009). c-Maf regulates IL-10 expression during Th17 polarization. J Immunol 182, 6226-6236.

Yang, D.D., Conze, D., Whitmarsh, A.J., Barrett, T., Davis, R.J., Rincon, M., and Flavell, R.A. (1998). Differentiation of $CD4^+$ T cells to Th1 cells requires MAP kinase JNK2. Immunity 9, 575-585.

Yang, Z.Z., Grote, D.M., Ziesmer, S.C., Niki, T., Hirashima, M., Novak, A.J., Witzig, T.E., and Ansell, S.M. (2012). IL-12 upregulates TIM-3 expression and induces T cell exhaustion in patients with follicular B cell non-Hodgkin lymphoma. J Clin Invest 122, 1271-1282.

Ye, B., Liu, X., Li, X., Kong, H., Tian, L., and Chen, Y. (2015). T-cell exhaustion in chronic hepatitis B infection: current knowledge and clinical significance. Cell Death Dis 6, e1694.

Yi, J.S., Cox, M.A., and Zajac, A.J. (2010). T-cell exhaustion: characteristics, causes and conversion. Immunology 129, 474-481.

Yokosuka, T., Takamatsu, M., Kobayashi-Imanishi, W., Hashimoto-Tane, A., Azuma, M., and Saito, T. (2012). Programmed cell death 1 forms negative costimulatory microclusters that directly inhibit T cell receptor signaling by recruiting phosphatase SHP2. J Exp Med 209, 1201-1217.

Yu, Q., Sharma, A., Oh, S.Y., Moon, H.G., Hossain, M.Z., Salay, T.M., Leeds, K.E., Du, H., Wu, B., Waterman, M.L., et al. (2009a). T cell factor 1 initiates the T helper type 2 fate by inducing the transcription factor GATA-3 and repressing interferon-gamma. Nat Immunol 10, 992-999.

Yu, X., Harden, K., Gonzalez, L.C., Francesco, M., Chiang, E., Irving, B., Tom, I., Ivelja, S., Refino, C.J., Clark, H., et al. (2009b). The surface protein TIGIT suppresses T cell activation by promoting the generation of mature immunoregulatory dendritic cells. Nat Immunol 10, 48-57.

Yu, X., and Li, Z. (2015). TOX gene: a novel target for human cancer gene therapy. Am J Cancer Res 5, 3516-3524.

Zajac, A.J., Blattman, J.N., Murali-Krishna, K., Sourdive, D.J., Suresh, M., Altman, J.D., and Ahmed, R. (1998). Viral immune evasion due to persistence of activated T cells without effector function. J Exp Med 188, 2205-2213.

Zanders, E.D., Lamb, J.R., Feldmann, M., Green, N., and Beverley, P.C. (1983). Tolerance of T-cell clones is associated with membrane antigen changes. Nature 303, 625-627.

Zanussi, S., Simonelli, C., D'Andrea, M., Caffau, C., Clerici, M., Tirelli, U., and DePaoli, P. (1996). $CD8^+$ lymphocyte phenotype and cytokine production in long-term non-progressor and in progressor patients with HIV-1 infection. Clin Exp Immunol 105, 220-224.

Zarour, H.M. (2016). Reversing T-cell dysfunction and exhaustion in cancer. Clin Cancer Res 22, 1856-1864.

Zhang, S.L., Yu, Y., Roos, J., Kozak, J.A., Deerinck, T.J., Ellisman, M.H., Stauderman, K.A., and Cahalan, M.D. (2005). STIM1 is a Ca^{2+} sensor that activates CRAC channels and migrates from the Ca^{2+} store to the plasma membrane. Nature 437, 902-905.

Zhang, Y., Huang, S., Gong, D., Qin, Y., and Shen, Q. (2010). Programmed death-1 upregulation is correlated with dysfunction of tumor-infiltrating $CD8^+$ T lymphocytes in human non-small cell lung cancer. Cell Mol Immunol 7, 389-395.

Zheng, Y., Zha, Y., Driessens, G., Locke, F., and Gajewski, T.F. (2012). Transcriptional regulator early growth response gene 2 (Egr2) is required for T cell anergy in vitro and in vivo. J Exp Med 209, 2157-2163.

Zhou, L., Chong, M.M., and Littman, D.R. (2009). Plasticity of $CD4^+$ T cell lineage differentiation. Immunity 30, 646-655.

Zhou, X., Yu, S., Zhao, D.M., Harty, J.T., Badovinac, V.P., and Xue, H.H. (2010). Differentiation and persistence of memory $CD8^+$ T cells depend on T cell factor 1. Immunity 33, 229-240.

Zhu, C., Anderson, A.C., Schubart, A., Xiong, H., Imitola, J., Khoury, S.J., Zheng, X.X., Strom, T.B., and Kuchroo, V.K. (2005). The Tim-3 ligand galectin-9 negatively regulates T helper type 1 immunity. Nat Immunol 6, 1245-1252.

Zinkernagel, R.M. (1996). Immunology taught by viruses. Science 271, 173-178.

Zou, W., and Chen, L. (2008). Inhibitory B7-family molecules in the tumour microenvironment. Nat Rev Immunol 8, 467-477.

7. Acknowledgements

First and foremost, I would like to thank my advisor PD Dr. rer. nat. Reinhard Obst for the constant support and great supervision during my doctoral study and related research, for his guidance, motivation, and immense knowledge. As well together with Prof. Dr. rer. nat. Thomas Brocker, for giving me the great opportunity to work on this highly relevant and fascinating project at the Institute for Immunology.

Furthermore, I would like to thank the members of my thesis advisory committee: Dr. Dirk Baumjohann, Prof. Dr. Ludger Klein and Dr. rer. nat. Jan Kranich, for their encouragement, advice, and hard question which inspired me to broaden my research from various perspectives.

I am grateful for the constant support and help from my cooperation partners. Thank you very much Lynette Henckel and Dr. rer. nat. Matthias Schiemann (TU, Munich) for reliable cell sorting, thank you Dr. Martin Irmler and Prof. Dr. Johannes Beckers (Helmholtz, Munich) for your diligent microarray generation and thank you Dr. Tobias Straub (LMU, Munich) for plenty statistical discussions even on the phone and your kind support with statistical analysis of the microarray data.

I would like to take the opportunity to appreciate the SFB 1054 as well as the associated IRGT for professional training activities, excellent lecture series, and financial support.

Many thanks go to the whole AG Obst, all current and former fellows, for creative input, stimulating discussions of the project, for enjoyable café breaks, and many, many other things – I will miss you all! Particularly, I want to express my appreciation to the technicians of the laboratory, Anna Kollar and Simone Pentz, I am grateful for all their help at the bench, for their kind support, and especially for managing our mouse lines. In this respect, I also would like to thank Andrea Bol, Wolfgang Mertl, and the whole rest of the Mouse Facility team, for great animal husbandry.

I thank all members at the Institute for Immunology for an innovative and throughout positive working atmosphere. In particular, Jan Kranich, Ina Kugler, Lisa Rausch, and Teresa Scheibenzuber for the countless and fruitful discussions and for all the fun we have had in the last few years.

Last but not the least, I would like to thank my family and Felix Kuhne for supporting me emotionally and spiritually during this exciting phase of my life. A special thanks goes to Felix, who has always believed in me. Thank you for your patience, your faith, all the productive suggestions and inspirations, thank you for being my Lighthouse.

8. Affidavit

Trefzer, Anne

.....
Surname, first name

I hereby declare, that the submitted thesis entitled

Antigen-exhausted CD4^{+} T cells deviate towards multiple states of anergy

is my own work. I have only used the sources indicated and have not made unauthorized use of services of a third party. Where the work of others has been quoted or reproduced, the source is always given.

I further declare, that the submitted thesis or parts thereof have not been presented as part of an examination degree to any other university.

Martinsried, 25.09.2019

.....
Ort, Datum

Anne Trefzer

.....
Unterschrift, Doktorandin